



**UNIVERSIDADE FEDERAL DO CEARÁ**  
**CENTRO DE CIÊNCIAS**  
**DEPARTAMENTO DE BIOQUÍMICA E BIOLOGIA MOLECULAR**  
**PROGRAMA DE PÓS-GRADUAÇÃO EM BIOQUÍMICA**

**LEANDRO DE PAULA BEZERRA**

**ATIVIDADE ANTIBIOFILME DE PEPTÍDEOS SINTÉTICOS: MECANISMOS DE  
AÇÃO E APLICAÇÕES NA SAÚDE**

**FORTALEZA**

**2022**

LEANDRO DE PAULA BEZERRA

ATIVIDADE ANTIBIOFILME DE PEPTÍDEOS SINTÉTICOS: MECANISMOS DE AÇÃO E  
APLICAÇÕES NA SAÚDE

Dissertação apresentada à coordenação do Programa de Pós-graduação em Bioquímica da Universidade Federal do Ceará – UFC como requisito parcial para a obtenção do título de Mestre em Bioquímica. Área de concentração: Bioquímica Vegetal.

Orientador: Prof<sup>o</sup>. Dr. Cléverson Diniz Teixeira de Freitas.

Coorientador: Prof<sup>o</sup>. Dr. Pedro Filho Noronha de Souza.

FORTALEZA

2022

Dados Internacionais de Catalogação na Publicação  
Universidade Federal do Ceará  
Biblioteca Universitária

Gerada automaticamente pelo módulo Catalog, mediante os dados fornecidos pelo(a) autor(a)

---

- B469a Bezerra, Leandro de Paula.  
Atividade antibiofilme de peptídeos sintéticos: mecanismos de ação e aplicações na saúde / Leandro de Paula Bezerra. – 2022.  
112 f. : il. color.
- Dissertação (mestrado) – Universidade Federal do Ceará, Centro de Ciências, Programa de Pós-Graduação em Bioquímica, Fortaleza, 2022.  
Orientação: Prof. Dr. Cléverson Diniz Teixeira de Freitas.  
Coorientação: Prof. Dr. Pedro Filho Noronha de Souza.
1. Peptídeos. I. Título.

CDD 572

---

LEANDRO DE PAULA BEZERRA

ATIVIDADE ANTIBIOFILME DE PEPTÍDEOS SINTÉTICOS: MECANISMOS DE AÇÃO E  
APLICAÇÕES NA SAÚDE

Dissertação apresentada à coordenação do Programa de Pós-graduação em Bioquímica da Universidade Federal do Ceará – UFC como requisito parcial para a obtenção do título de Mestre em Bioquímica. Área de concentração: Bioquímica Vegetal.

Aprovada em: \_\_/\_\_/\_\_\_\_

BANCA EXAMINADORA

---

Prof. Dr. Cléverson Diniz Teixeira de Freitas  
Universidade Federal do Ceará (UFC)

---

Prof.<sup>a</sup> Dra. Luciana Magalhães Rabêlo Alencar  
Universidade Federal do Maranhão (UFMA)

---

Prof. Dr. Ralph Santos-Oliveira  
Universidade Federal do Rio de Janeiro (UFRJ)

---

Prof. Dr. Pedro Filho Noronha de Souza  
Universidade Federal do Ceará (UFC)

## **AGRADECIMENTOS**

Aos meus orientadores, Prof. Dr. Cléverson Diniz Teixeira de Freitas e o Prof. Dr. Pedro Filho Noronha de Souza pelos ensinamentos, conselhos, troca de conhecimentos e por todo o auxílio prestado ao longo dessa trajetória. Aos membros da banca examinadora por aceitarem o convite para colaborar com este trabalho.

À FUNCAP e ao governo do estado do Ceará por financiarem a minha pesquisa e permitido a minha permanência neste Programa de Pós-graduação.

A todos que, de alguma forma, contribuíram para a realização deste trabalho. Meu muito obrigado!

## RESUMO

Biofilmes formados por leveduras do gênero *Candida* são um grande problema de saúde pública devido à sua alta resistência aos agentes antimicrobianos. Dentre estes, *Candida albicans*, *C. krusei* e *C. parapsilosis* são fungos resistentes a agentes antimicrobianos que são responsáveis por causar graves infecções da corrente sanguínea podendo levar os pacientes à morte. Para superar esse cenário, peptídeos antimicrobianos sintéticos (PAMs) são considerados novas ferramentas para combater infecções, tendo em vista que seu principal mecanismo de ação está relacionado com o ataque e desestabilização da membrana celular do patógeno. Estas moléculas podem ser usadas tanto isoladamente quanto em sinergismo com drogas que já apresentam tolerância pelos microrganismos. Neste trabalho, cinco PAMs sintéticos denominados *Mo*-CBP3-PepI, *Mo*-CBP3-PepII, *Mo*-CBP3-PepIII obtidos da sequência proteica de *Mo*-CBP3, uma proteína ligante à quitina purificada de sementes de *Moringa oleífera* e PepGAT e PepKAA, obtidos com base na sequência de uma quitinase de *Arabidopsis thaliana* foram testados sozinhos e em combinação com Nistatina (NYS) e Itraconazol (ITR) contra biofilmes formados por *C. albicans*, *C. krusei* e *C. parapsilosis*. Além disso, os mecanismos por trás da atividade tal atividade foram avaliados por microscopia de fluorescência e microscopia eletrônica de varredura (MEV). Os resultados revelaram uma melhora de 2 a 4 vezes na atividade antibiofilme dos fármacos NYS e ITR quando combinado com peptídeos. Análises microscópicas mostraram que os mecanismos de ação são baseados na degradação da parede celular, superprodução de espécies reativas de oxigênio (ROS) e formação de poros da membrana causando extravasamento de conteúdo celular e levando as células do biofilme à morte. Ao aumentar a atividade de NYS e ITR, os peptídeos apresentaram grande potencial como adjuvantes. Em conjunto, os resultados sugerem o potencial de *Mo*-CBP3-PepI, *Mo*-CBP3-PepII *Mo*-CBP3-PepIII, PepGAT e PepKAA como novas drogas e/ou adjuvantes para aumentar a atividade de drogas convencionais para o tratamento de infecções clínicas causada por biofilmes resistentes do gênero *Candida*.

**Palavras-chave:** atividade antibiofilme; sinergismo; *Candida*; peptídeos sintéticos; aplicação clínica.

## ABSTRACT

Biofilm-forming yeasts are major public health problem because its high resistance to microbial agents. Among those, *Candida albicans*, *C. krusei* and *C. parapsilosis* are drug-resistant yeasts responsible for bloodstream infections leading individuals to death. To overcome this scenario, synthetic antimicrobial peptides (SAMPs) are considered new weapons to combat infections either alone or conjugated with drugs that are losing their activity because its capacity to cause a disruption of pathogen cell membrane. Here, five SAMPs named *Mo*-CBP3-PepI, *Mo*-CBP3-PepII, *Mo*-CBP3-PepIII, were designed based in the protein sequence of a chitin-binding protein from *Moringa oleifera* seeds and PepGAT and PepKAA, obtained by a protein sequence from a *Arabidopsis thaliana* chitinase were tested alone or in combination with Nystatin (NYS) and Itraconazole (ITR) against biofilms formed by *C. albicans*, *C. krusei* and *C. parapsilosis*. Furthermore, the mechanisms behind the antibiofilm activity was evaluated by fluorescence and scanning electron microscopies. The results revealed an improvement of 2 up to 4-fold in NYS and ITR antibiofilm activity when combined with peptides. Microscopic analyses showed that mechanisms of action is based on cell wall degradation, overproduction of reactive oxygen species (ROS) and membrane pore formation causing leakage of internal content and leading biofilm cells to death. By increasing the activity of NYS and ITR, peptides exhibited a great potential as adjuvants. Altogether, results suggest the potential of *Mo*-CBP<sub>3</sub>-PepI, *Mo*-CBP<sub>3</sub>-PepIII, PepGAT and PepKAA as new drugs and/or adjuvants to increase the activity of conventional drugs for treatment of clinical infection caused by resistant biofilms of *Candida* specie.

**Keywords:** antibiofilm activity; synergism; *Candida*; synthetic peptides; clinical application.

## SUMÁRIO

<b>1</b>	<b>INTRODUÇÃO</b> .....	8
<b>2</b>	<b>CAPÍTULO I - REVISÃO DE LITERATURA</b> .....	9
<b>2.1</b>	<b>Histórico dos agentes antimicrobianos</b> .....	9
<b>2.2</b>	<b>Evolução dos mecanismos de resistência</b> .....	10
<b>2.3</b>	<b>Resistência às drogas antifúngicas e saúde humana</b> .....	13
<b>2.4</b>	<b>Biofilmes</b> .....	14
<b>2.5</b>	<b>Peptídeos antimicrobianos (PAMs) naturais e suas características</b> .....	16
<b>2.6</b>	<b>Mecanismos de ação dos PAMs</b> .....	17
<b>2.7</b>	<b>Peptídeos antimicrobianos sintéticos</b> .....	19
<b>2.8</b>	<b>Peptídeos inspirados em <i>Mo</i>-CBP3 e uma quitinase de <i>A. thaliana</i></b> .....	20
<b>2.9</b>	<b>Sinergismo</b> .....	23
<b>3</b>	<b>HIPÓTESE</b> .....	24
<b>4</b>	<b>OBJETIVOS</b> .....	24
<b>5</b>	<b>CAPÍTULO II - ARTIGO CIENTÍFICO 1</b> .....	25
<b>6</b>	<b>CAPÍTULO III - ARTIGO CIENTÍFICO 2</b> .....	66
<b>7</b>	<b>CONCLUSÃO</b> .....	105
	<b>REFERENCIAS</b> .....	106
	<b>APÊNDICE A - (ARTIGO CIENTÍFICO 3)</b> .....	112
	<b>APÊNDICE B - (ARTIGO CIENTÍFICO 4)</b> .....	113
	<b>ANEXO A - (ARTIGO CIENTÍFICO 5)</b> .....	114



## 1. INTRODUÇÃO

Um dos principais problemas de saúde pública mundial no século XXI tem sido a ascensão da microrganismos resistentes às drogas antimicrobianas (HILLER et al, 2019). Estudos estimam que o número de mortes causadas pela resistência microbiana ultrapasse os 10 milhões até 2050 (DODDS, 2017) onde mais de 2,7 milhões de pessoas poderão entrar em óbito a cada ano devido às infecções causadas por microrganismos em todos os continentes do globo (STROLLO et al, 2016).

Muito dessa problemática está relacionada com a resistência às drogas antifúngicas, onde espécies do gênero *Candida* tem se destacado nos últimos anos, sendo responsáveis pelos infecções mais recorrentes, levando ao quadro clínico de infecção na corrente sanguínea, conhecido como candidíase invasiva (PAPPAS et al, 2018). Mais de 700.000 casos de candidíase são relatados anualmente, sendo a taxa de mortalidade superior a 40%, gerando despesas aos cofres públicos de mais de US\$ 50.000 por paciente (DHINGRA et al, 2020). Aliado a isso, está a capacidade de tais microrganismos se associarem em comunidades mais estáveis conhecidas como biofilmes, o que garante uma maior resistência à administração de drogas no combate à patogénia (RIVIE et al, 2018).

Com o aumento da resistência a muitas drogas já disponíveis no mercado, os peptídeos antimicrobianos (PAMs) surgem como uma alternativa promissora na prevenção e combate a biofilmes de alto potencial patológico. PAMs são pequenas sequências de aminoácidos que compõem o sistema imune inato de quase todos os organismos vivos, desde microrganismos até plantas, insetos e animais, incluindo o ser humano (BORARAI et al, 2020). O amplo espectro de atividade antimicrobiana demonstrado pelos PAMs desfavorecem o desenvolvimento de mecanismos de resistência pelos microrganismos, tendo em vista que o seu principal mecanismo de ação envolve o ataque a membrana celular do patógeno (LIMA et al, 2021), inviabilizando o reparo de tal estrutura celular pelas células afetadas. Entretanto, algumas desvantagens são encontradas em PAMs naturais como instabilidade físico-química, elevados níveis de toxicidade bem como elevada possibilidade de proteólise, o que dificulta o seu uso (OLIVEIRA et al, 2019). Felizmente, estes problemas podem ser contornados com o desenho racional de peptídeos sintéticos cujas sequências selecionadas apresentam o menor grau de toxicidade e podem ser mais promissoras.

Nosso grupo de pesquisa já tem purificado inúmeras proteínas com potencial antimicrobiano comprovado, dentre as quais podem ser destacas *Mo-CBP3*, uma proteína

ligante à quitina purificada de sementes de *Moringa oleífera* e Rc-2S-Alb, purificada da torta de mamona de *Ricinus communis*, ambas pertencentes à família das albuminas 2S. No entanto, o baixo rendimento após o processo de purificação torna o trabalho com tais moléculas inviável. Com isso, tem-se empenhado esforços no desenho de peptídeos sintéticos bioinspirados nas sequências de proteínas anteriormente identificadas, gerando peptídeos biologicamente ativos denominados *Mo*-CBP3-PepI, *Mo*-CBP3-PepII e *Mo*-CBP3-PepIII os quais apresentam baixa ou nenhuma toxicidade às células humanas (OLIVEIRA et al, 2019). Um outro trabalho também desenvolvido pelo nosso grupo focou no desenho de dois peptídeos sintéticos baseados na sequência proteica de uma quitinase identificada em *Arabidopsis thaliana*, gerando PepGAT e PepKAA (SOUZA et al, 2020). Tais peptídeos tem demonstrado atividade contra células planctônicas de algumas espécies de bactérias e leveduras. Faz-se necessário, no entanto, a realização de estudos no tocante ao potencial de inibição e redução da biomassa de biofilmes antimicrobianos de interesse clínico (tendo em vista que a associação de microrganismos em biofilmes aumenta a resistência contra as drogas utilizadas), a elucidação dos mecanismos de ação por trás de tais atividades e, ainda, explorar os efeitos de sinergismo de tais moléculas com drogas antifúngicas convencionais.

## **2. CAPITULO 1 - REVISÃO DE LITERATURA**

### **2.1 Histórico dos agentes antimicrobianos**

Em 1928, com a descoberta da penicilina e posteriormente o seu uso como antibiótico em 1942 deram início a uma fase progressista no campo da medicina (STEKEL, 2018). A década seguinte ficou conhecida como aquela responsável por iniciar a chamada era dos antibióticos (1950 – 1970), a qual foi marcada pela descoberta de muitos fármacos com atividade antimicrobiana como tetraciclina (1950), eritromicina (1953), gentamicina (1967) e vancomicina (1972) (RIBEIRO DA CUNHA et al, 2019). Com isso, houve uma drástica redução no número de mortes causadas por infecções bacterianas, cuja expectativa de vida humana à época foi elevada para até 79 anos (BARREIRO et al, 2021).

Por outro lado, a descoberta e desenvolvimento de agentes antifúngicos não ocorria na mesma velocidade que àqueles fármacos antibacterianos, sendo estes últimos mais rapidamente desenvolvidos tendo em vista o grande número de infecções bacterianas registradas, quando comparadas àquelas causadas por fungos (BARTELL et al, 2019). Desta forma, o primeiro agente antifúngico, anfotericina B, apenas foi introduzido em 1958, após

aumento da taxa de crescimento no número de infecções e mortes causadas por fungos patogênicos (KEANE et al, 2018).

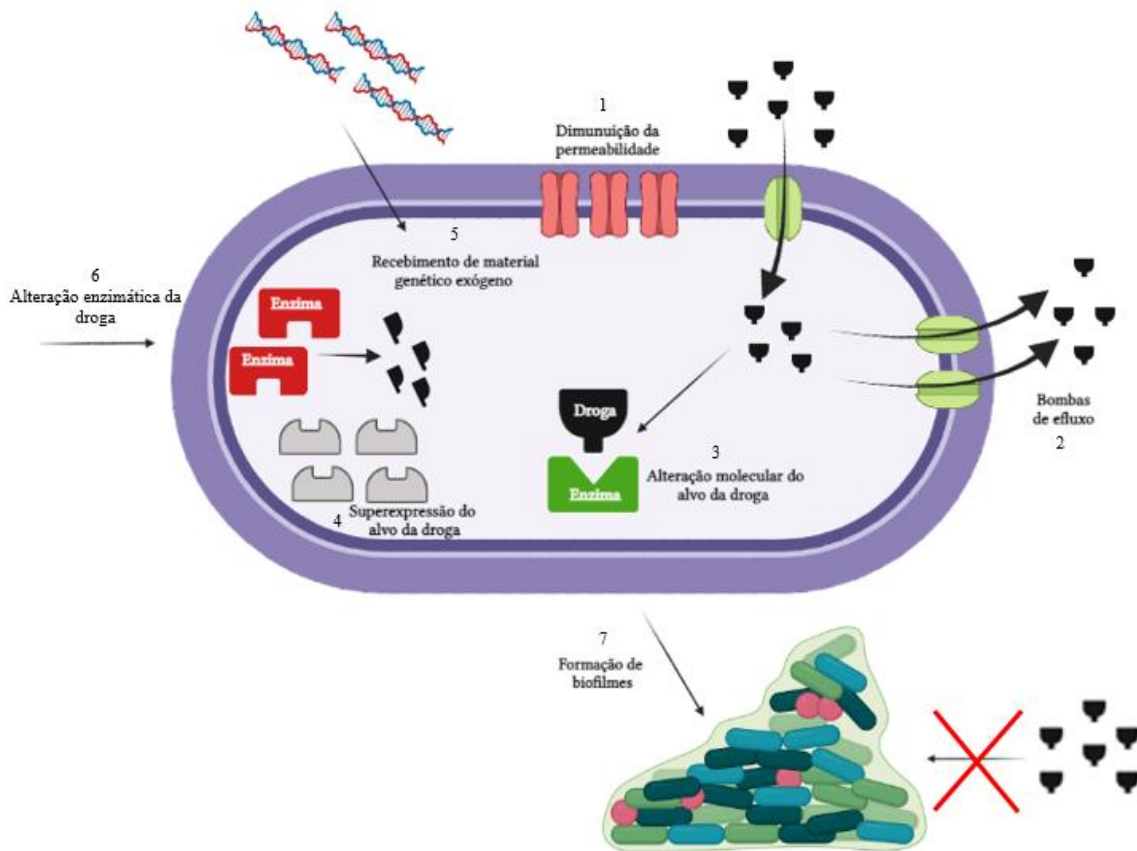
Apesar de todos os esforços, a eficiência dessas drogas não permaneceu a longo prazo. Microrganismos encontraram formas de driblar os mecanismos de ação dos antibióticos e se proliferarem continuamente, sem danos aparentes. Um fato interessante é que a resistência à penicilina (1940) foi observada antes mesmo desta droga ser disponibilizada comercialmente em 1942, o que vem se estendendo até os dias atuais (CHAN, 2020). Desde então, inúmeros microrganismos desenvolveram mecanismos de resistência e, inclusive, multirresistência a drogas, tal como *Staphylococcus aureus*, uma das bactérias mais estudadas e que apresenta resistência à vancomicina (classe dos glicopeptídeos) e meticilina, pertencente ao grupo das penicilinas (GUO et al, 2020). Outra espécie que tem recebido atenção é a *Pseudomonas aeruginosa*, na qual já existem dados na literatura relatando sua resistência a antibióticos da classe dos aminoglicosídicos, quinolonas e  $\beta$ -lactâmicos (PANG et al, 2019). Associado a isso, algumas espécies de fungos filamentosos e leveduriformes têm apresentado mecanismos de resistência às drogas antifúngicas disponíveis, incluindo espécies do gênero *Candida*, muitas delas com mecanismos de resposta aos antifúngicos da classe dos azóis (PRISTOV et al, 2019).

## **2.2 Evolução dos mecanismos de resistência**

Considerado um processo evolutivo natural, o desenvolvimento de mecanismos de resistência tem sido acelerado pela pressão seletiva ocasionada pelo uso indiscriminado de fármacos antimicrobianos, como mostrados na Figura 1 (KLUMPER et al, 2019). Tal uso não se dá apenas pela má utilização ou interrupção antecipada dos tratamentos pela população, mas também pela prescrição inadequada desses medicamentos por parte de profissionais da saúde. Outrossim, está a aplicação de antimicrobianos em setores não convencionais como a agricultura, o que também contribui para o desenvolvimento da resistência microbiana (TAYLOR et al, 2020).

Com a fundamentação de que a aquisição dos mecanismos de resistência têm caráter natural e evolutivo, tais mecanismos são desenvolvidos levando em conta um conjunto de características próprias de cada microrganismo associado a fatores mutagênicos e/ou de transferência de genes de resistência entre indivíduos numa determinada população. Além disso, muitos microrganismos conseguem desenvolver mecanismos de resistência muito rapidamente em pouco tempo após exposição à droga (HILLER et al, 2019).

Figura 1 – Mecanismos de resistência aos antimicrobianos



Fonte: elaborada pelo autor

Dentre os principais mecanismos de resistência conhecidos até o momento, a redução da concentração do droga dentro da célula tem sido um ponto chave no processo de resistência microbiana. As células microbianas se especializaram na expressão de genes responsáveis pela síntese de proteínas transmembrana denominadas bombas de efluxo, cuja atividade consiste em lançar a droga recém assimilada no espaço extracelular, impedindo não apenas o acúmulo da droga no citoplasma do microrganismo, mas também sua ação farmacológica intracelular no alvo desejado (LIMA et al, 2021). Um fato curioso é que essas estruturas foram desenvolvidas por fungos e bactérias para não serem específicas para apenas uma classe de antibióticos, mas para uma grande variedade de moléculas incluindo àquelas responsáveis pela inibição da síntese da parede celular (carbapenêmicos e  $\beta$ -lactâmicos), inibição da produção do ergosterol de membrana (azóis), desestabilização da parede celular (polimixinas), inibição da enzima topoisomerase [ocasionando problemas na replicação do DNA (fluoroquinolonas)], entre outros. Muitos patógenos não possuem apenas um mecanismo, mas vários destes, o que resulta no surgimento de microrganismos multirresistentes (RUSS, et al 2020, BHATNAGAR et al, 2019).

Além disso, a síntese de enzimas capazes de modificar o fármaco e impedir sua ação farmacológica se configura como um dos mecanismos de resistência mais sofisticados já identificados. Dentre estas, podem ser destacadas as  $\beta$ -lactamases cujo mecanismo consiste em desfazer a ligação amida do anel  $\beta$ -lactâmico, fazendo com que fármacos como penicilina, amoxicilina e ampicilina percam suas atividades farmacológicas (BEHZADI et al, 2020). A modificação do alvo celular chama a atenção dos pesquisadores devido a presença de mutações pontuais em determinadas regiões dos genes que codificam moléculas-alvo (YELIN et al, 2018). Nesse sentido, enzimas intracelulares podem ter os aminoácidos do seu sítio ativo modificado ou substituídos por outros que fazem o fármaco perder a sua afinidade pela enzima-alvo, resultando em pouca ou nenhuma atividade farmacológica. Como exemplo, o gene *ERG11* em *Candida albicans* possui 217 mutações, sendo 185 destas silenciosas (que não alteram o funcionamento ou função da proteína resultante) e outras 32 mutações ocasionadas por substituição dos aminoácidos (HEALEY et al, 2018). O resultado dessas mutações faz com que a enzima lanosterol 14 $\alpha$ -desmetilase não seja inibida pelas drogas antifúngicas da classe dos azóis e equinocandinas, garantindo que a enzima sintetize normalmente o ergosterol de membrana, tornando a cepa resistente. Ademais, o alvo farmacológico pode ser superexpresso, de modo que a concentração do fármaco disponível intracelularmente seja insuficiente para exercer uma atividade favorável (VILLASMIL et al, 2020).

A parede celular também é uma das estruturas celulares que possuem características de resistência já relatadas, destacando a redução da sua permeabilidade que culmina na redução da entrada do fármaco na célula (GHAI et al, 2018). Antimicrobianos cujas estruturas possuem um caráter hidrofílico têm como principal meio de acesso ao espaço intracelular proteínas canais responsáveis pela captação de água pelas células, as aquaporinas. Os mecanismos desenvolvidos pelos patógenos consistem em redução da expressão de aquaporinas na membrana celular, alteração da estrutura molecular ou nos índices de condutância das porinas e, inclusive, a cessação da síntese de tais canais (CHRISTAKI et al, 2020). Cepas clínicas de *Klebsiella pneumoniae* apresentam mutações no gene que codifica a aquaporina Ompk36, resultando na não passagem de fármacos hidrofílicos para o interior da célula (LIMA et al, 2021). A subunidade F da aquaporina OmpF de *Escherichia coli* também sofre mutações pontuais na sua sequência nucleotídica, implicando na redução de acesso do fármaco ao meio intracelular (LAUXEN et al, 2021).

A aquisição de genes de resistência por bactérias susceptíveis também tem se configurado um mecanismo de resistência importante (LERMINIAUX et al, 2019). Cepas mais resistentes acabam repassando (via conjugação, transformação ou transdução) genes com

capacidade para sintetizar moléculas resistentes em outras bactérias, reforçando a dificuldade de se combater bactérias que atuam em conjunto, como àquelas que se organizam em estruturas conhecidas como biofilmes (MCINNES et al, 2020).

### **2.3 Resistência às drogas antifúngicas e saúde humana**

Dentre os microrganismos causadores de doenças em humanos, os fungos são responsáveis por uma grande parcela nos índices de infecção relatados. De acordo com o Fundo de Ação Global para Doenças Fúngicas (GAFFI, da sigla em inglês) os efeitos da contaminação por alguns fungos patogênicos deixam sequelas irreparáveis até mesmo em indivíduos imunologicamente saudáveis (RODRIGUES et al, 2021). Além disso, com o aumento do número de infecções causadas por bactérias e vírus e consequente enfraquecimento do sistema imunológico na tentativa de superar as infecções, muitos fungos oportunistas tem ganhado espaço para colonizarem superfícies do corpo humano e instalarem doenças (SALEHI et al, 2020). Como exemplo, pacientes acometidos com a Síndrome da Imunodeficiência Adquirida (AIDS) são constantemente diagnosticados com infecções oportunistas envolvendo fungos. Além disso, pacientes sob tratamento oncológico, quimioterapia e terapias imunossupressoras são especialmente atacados por tais patógenos (ARMSTRONG et al, 2019). Devido a capacidade de muitos fungos aderirem às superfícies (além dos tecidos), indivíduos portadores de dispositivos médicos como marca-passos, cateteres e válvulas cardíacas frequentemente apresentam deposição de células nesses aparelhos (RAMSTEDT et al, 2022).

Diferentemente dos antibióticos, que desde 1942 vêm sendo produzidos em larga escala e são mais fáceis de serem sintetizados, os antifúngicos apresentam algumas limitações na sua síntese. Isso acontece pelo fato dos fungos terem uma maior proximidade filogenética com os humanos, compartilhando características como seres eucariotos (VAN DAELE et al, 2019). Essa semelhança dificulta o processo de descoberta de novos fármacos pois teme-se que os novos antifúngicos desenvolvidos afetem não apenas a célula patogênica, mas também os tecidos saudáveis do hospedeiro. Dessa forma, o número de alvos moleculares inerentes apenas aos fungos se torna mais escasso (LIU et al, 2018). Assim como os antibióticos, esperasse que os antifúngicos tenham uma alta especificidade molecular, amplo espectro de atuação, mecanismos de ação variados e, sobretudo, não favoreçam a resistência cruzada entre as drogas atualmente disponíveis (HASAN et al, 2020).

Desde a década de 2000 não são lançados novos fármacos com alvos moleculares específicos apenas para os fungos (PERFECT et al, 2017). Os antifúngicos disponíveis tem um espectro de atividade limitada, atuando sobre uma pequena parcela de alvos celulares

conhecidos diferentes daqueles compartilhados entre fungos e seres humanos. Por exemplo, antifúngicos da classe dos azóis e triazóis como fluconazol, cetoconazol e voriconazol atuam na inibição da enzima lanesterol 14 $\alpha$ -desmetilase (enzima chave na biossíntese do ergosterol) (VILLASMIL et al, 2020). Os polienos, por sua vez, atuam na desestabilização da membrana celular do microrganismo, como é o caso dos fármacos nistatina e anfotericina B via ligação com o ergosterol de membrana (ESCADÓN et al, 2019). A inibição da  $\beta$ -glucano sintase, por sua vez, é promovida por fármacos da classe das equinocandinas que atuam na interrupção da síntese e organização da parede celular (PRISTOV ET AL, 2019).

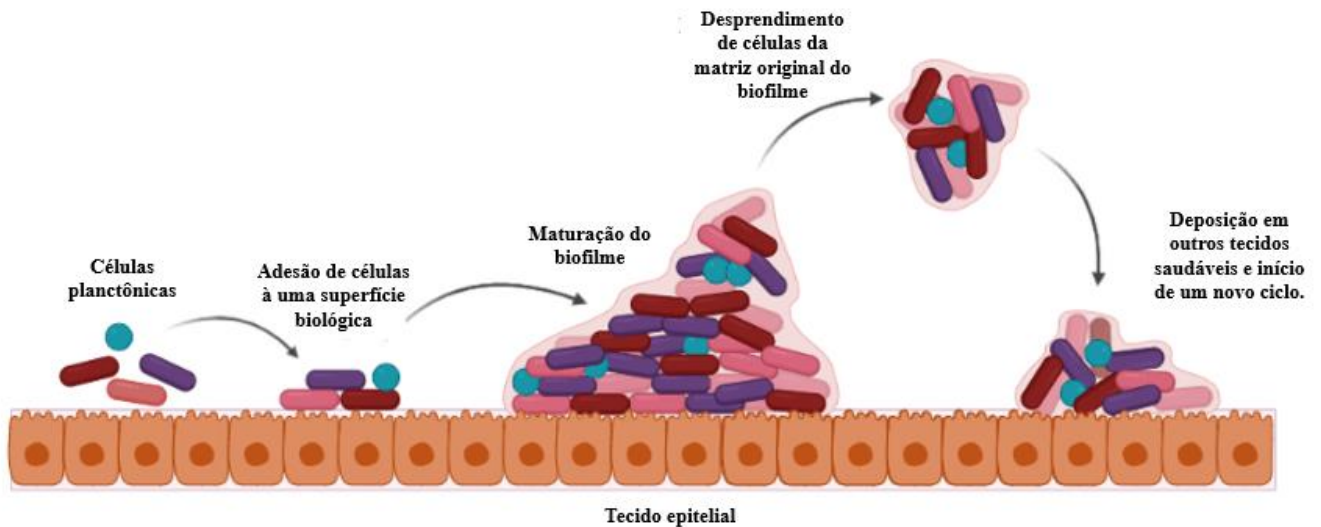
Tendo em vista essa limitação no número de alvos farmacológicos e a evolução natural dos mecanismos de resistência antimicrobianos, é urgente o desenvolvimento de alternativas que sejam capazes de interagir com alvos alternativos da maquinaria celular dos fungos e prevenir ou combater as infecções por estes causadas.

## **2.4 Biofilmes**

Os biofilmes são estruturas formadas pelo aglomerado de células com capacidade de se aderirem à uma superfície e se desenvolverem sobre esta. A estrutura de um biofilme é imersa em uma matriz complexa que é composta por polissacarídeos, lipídeos, proteínas e ácidos nucleicos que, juntos, conferem resistência à estrutura (KHATOON et al, 2018). Esta matriz pode ser modificada pelos microrganismos a depender dos estados do ambiente no qual estão inseridos levando em consideração fatores como o tipo de organismo invadido, forças mecânicas do tecido, disponibilidade de nutrientes e substratos e condições de temperatura do local infectado (DRAGOS et al, 2018).

A formação de uma estrutura complexa como o biofilme é dividida em três estágios: (1) deposição de células planctônicas, que pode ser reversível ou irreversível com o auxílio de proteínas conhecidas como adesinas que auxiliam na adesão à superfície, (2) maturação das micro colônias depositadas e (3) dispersão de células do aglomerado pela corrente sanguínea tendo acesso a outros órgãos e tecidos e iniciando um novo ciclo (KHATOON et al, 2018). A figura 2 exemplifica as fases da formação de um biofilme em uma superfície biológica.

Figura 2 – Fases da formação e desenvolvimento de biofilmes microbianos



Fonte: elaborada pelo autor

As células constituintes do biofilme trabalham de modo a garantir estratégias de sobrevivência e eficiência na invasão dos tecidos do hospedeiro, bem como resistir a uma gama de agentes antimicrobianos aos quais são submetidas (NETT et al, 2020). Ademais, a capacidade da estrutura de ser eficiente na produção de barreiras físicas e químicas dificulta a ação do sistema imunológico dos pacientes em controlar o crescimento e desenvolvimento de tais estruturas. Por exemplo, os exopolissacarídeos constituintes da matriz extracelular atuam como agentes quelantes de drogas antimicrobianas, impedindo sua ação. Outrossim, é a síntese de enzimas extracelulares com capacidade para degradar ligações específicas de fármacos e inviabilizar sua atividade farmacológica (KAVANAUGH et al, 2019).

Ao adentrar nos tecidos, os biofilmes podem causar lesão tecidual e levar a quadros de infecção aguda. Algumas células de um aglomerado inicial podem se desprender da estrutura, invadir a corrente sanguínea e gerar novos biofilmes em tecidos saudáveis, levando a quadros de sepse generalizada (MOTTA et al, 2021). Outro fator que preocupa é que essas estruturas conseguem se formar não apenas sobre as superfícies biológicas, mas também àquelas implantadas no organismo com o intuito de prolongar o tempo de vida do paciente, como cateteres, marca-passos e válvulas cardíacas, inviabilizando seu uso em até pouco tempo após sua implantação (KURMOO et al, 2020).

Cerca de 40-50% de válvulas cardíacas e até 70% de cateteres implantados em pacientes contaminados com *Enterococcus faecalis*, *Staphylococcus Aureus* e *pseudomonas aeruginosa* são trocados devido a deposição de biofilmes microbianos nesses dispositivos



(KHATOON et al, 2018). Muitas outras doenças são desencadeadas no organismo com a deposição de biofilmes, destacando-se endocardite, fibrose cística, periodontites, sinusites e infecções renais (POURNAJAF et al, 2018; XI et al, 2019; ALONSO et al, 2021; WU et al, 2018; LEE et al, 2019). Associada a facilidade de se aderirem às superfícies biológicas e dispositivos médicos, os biofilmes contam ainda com a resiliência frente às drogas antimicrobianas, dificultando seu tratamento e erradicação (VESTBY et al, 2020). Nesse sentido, a necessidade do desenvolvimento de drogas alternativas às quais os microrganismos não sejam capazes de tolerar e que possam auxiliar no tratamento e prevenção de doenças é urgente.

## **2.5 Peptídeos antimicrobianos (PAMs) naturais e suas características**

A prospecção de moléculas com alto potencial terapêutico e farmacológico tem se configurado como uma das áreas mais crescentes nas áreas de biologia, medicina e biotecnologia. Dentre as alternativas exploradas, os produtos naturais são fontes de novas moléculas biologicamente ativas como carboidratos, lipídios, proteínas e seus derivados. Entre estas, os peptídeos antimicrobianos naturais ganham um destaque especial pelo fato de serem encontrados em quase todos os organismos vivos, constituindo a primeira linha de defesa contra patógenos através da sua capacidade moduladora da resposta imunológica (LIMA et al, 2021).

O amplo espectro de atividade que essas moléculas possuem permite que sejam ativas contra uma gama de microrganismos incluindo bactérias, fungos, parasitas e vírus. Alguns trabalhos tem relatado também a atividade inseticida de peptídeos antimicrobianos, expandindo sua potencial aplicação também na agricultura (SOUZA et al, 2020). Tais atividades relatadas evidenciam uma forte relação com o principal mecanismo de ação desses peptídeos que envolve o ataque e desestabilização de membranas celulares, sendo capaz de atenuar ou impedir as probabilidades de desenvolvimento de mecanismos de resistência (LIMA et al, 2021).

Por serem moléculas globalmente difundidas, os peptídeos antimicrobianos possuem características em comum. Pode-se citar que estes peptídeos são formados por sequências que variam de 5 a 50 resíduos de aminoácidos e possuem carga peculiarmente positiva, a qual está relacionada com a presença de aminoácidos carregados positivamente como Lisina e Arginina, que garantem a interação com a membrana celular do microrganismo negativamente carregada do lado externo (OLIVEIRA et al, 2019). Associado a isso, o teor de aminoácidos hidrofóbicos varia de 40 a 50% entre as estruturas conhecidas e essa característica permite que os PAMs sejam capazes de interagir com as membranas biológicas, configurando-

lhes seu mecanismo de ação principal que consiste no ataque às membranas celulares. Porém, PAMs podem ser altamente tóxicos às células de mamíferos devido à presença em demasia de aminoácidos hidrofóbicos, o que causa lise celular inclusive nas células saudáveis do organismo hospedeiro (SOUZA et al, 2020).

Os resíduos de aminoácidos de caráter hidrofóbico e positivamente carregados permitem que os PAMs interajam especificamente com as membranas biológicas, desestabilizando-as. Essa atividade associa-se também à conformação adquirida pelos peptídeos em contato com o meio aquoso, sendo a estrutura em  $\alpha$ -hélice a mais estudada devido as características anfipáticas que essa organização confere. PAMs com estrutura em folha  $\beta$  apresentam resíduos de Cisteína bem conservados que se responsabilizam pela estabilização da estrutura através de pontes dissulfeto (LIMA et al, 2021). Algumas sequências ricas em conteúdo de Arginina, Triptofano e Prolina contribuem na determinação de uma estrutura estendida, sem formação de estrutura secundária aparente.

## **2.6 Mecanismos de ação dos PAMs**

Os componentes de estruturas celulares como membrana plasmática e parede celular devem ser as primeiras barreiras físicas superadas pelos PAMs para que se possa alcançar o interior da célula microbiana e desenvolver mecanismos alternativos de combate (LIMA et al, 2021). No entanto, essa superação deve levar em consideração inicialmente os componentes da parede celular como  $\beta$ -glucanos e polímeros de N-acetil-D-glicosamina que, em muitas vezes, são alvos de interação dos peptídeos, iniciando a desestabilização da estrutura celular ainda no primeiro contato (MAGANA et al, 2020). Alguns trabalhos, inclusive, relatam a existência de peptídeos com capacidade de interação com a quitina e outras estruturas da parede celular (AMARAL et al, 2021).

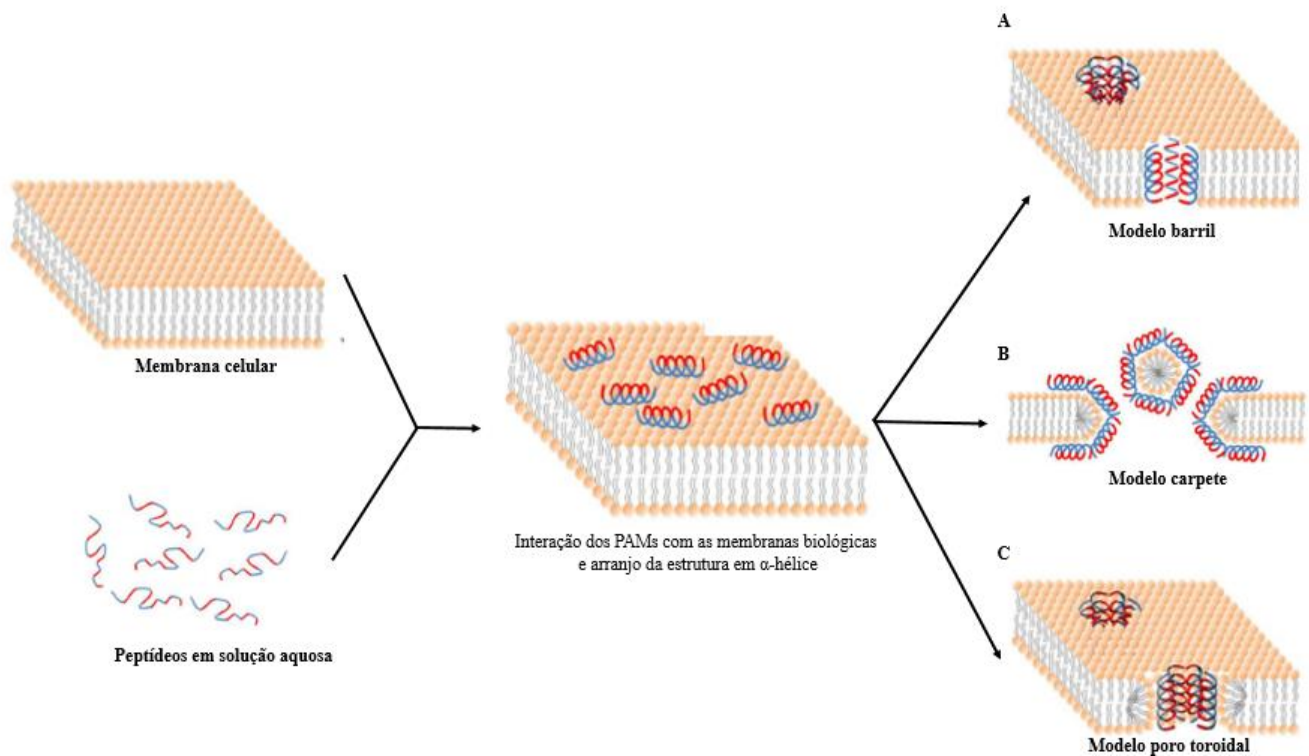
O rompimento da membrana e o acesso ao meio intracelular está intrinsecamente ligado à interação dos PAMs com a membrana celular que é garantida pelas características anteriormente descritas como carga líquida positiva (responsável por interagir com a carga negativa das porções polares dos lipídeos estruturais de membrana) e grau de hidrofobicidade (garantindo a interação com os fosfolipídios estruturais da bicamada lipídica) (AKBARI et al, 2018).

Estudos revelam os possíveis modos de interação com as membranas celulares dos microrganismos (Figura 3). Entre eles, o modelo de barril é responsável pela formação de um poro através da interação dos aminoácidos hidrofóbicos com os lipídeos de membrana. Em

determinada concentração, as unidades monoméricas peptídicas se organizam e interagem entre si de modo a atenuar a exibição dos resíduos hidrofóbicos formando poros inteiramente inseridos na porção lipídica da membrana celular (LIMA et al, 2021). Um outro mecanismo proposto e denominado modelo de poro toroidal explica que diferentemente do mecanismo anterior, os peptídeos não interagem entre si formando agregados peptídicos, mas permitem a interação dos seus grupos polares com as porções carregadas dos fosfolipídios de membrana (LIMA et al, 2021).

Adicionalmente, o modelo de tapete propõe que os peptídeos não promovem a formação de poros, mas agem de maneira aleatória sobre a membrana, desestabilizando-a com ação similar àquela apresentada pelas substâncias surfactantes. Esse mecanismo leva em consideração a interação entre as porções positivas e negativas dos peptídeos e dos fosfolipídios de membrana, respectivamente. Uma concentração elevada de PAMs depositados sobre a membrana leva a desestabilização da estrutura e, conseqüentemente, à formação de micelas (BOGDANOVA et al, 2020).

Figura 3: Exemplificação de alguns mecanismos de ação dos PAMs contra membranas



Fonte: LIMA et al, 2020 (com adaptações)

Modelo barril (A), Modelo tapete (B) e Modelo poro toroidal (C). Em azul, destacam-se as regiões hidrofílicas e em vermelho as regiões hidrofóbicas dos aminoácidos constituintes das PAMs

Apesar de ser o principal, a desestabilização e rompimento da membrana celular do patógeno não é o único mecanismo de ação desenvolvido pelos PAMs (CORRÊA et al, 2019). Muitos peptídeos conseguem atravessar as membranas biológicas sem causar dano algum, alcançam a matriz celular e interagem com alvos intracelulares específicos, impedindo o correto funcionamento de rotas metabólicas importantes ao desenvolvimento e manutenção das atividades biológicas dos microrganismos. Além disso, há estudos que evidenciam a participação dos PAMs em eventos de inibição da síntese de parede celular, replicação, transcrição, inibição de enzimas importantes e, inclusive, indução da morte celular programada (MORAVEJ et al, 2018). Alguns trabalhos relatam ainda a capacidade de PAMs desencadear uma superprodução de espécies reativas de oxigênio que leva a desestabilização de proteínas, carboidratos e ácidos nucleicos, gerando a desregulação de rotas metabólicas celulares, embora os fatores que iniciam esse processo ainda sejam desconhecidos (LIMA et al, 2020).

## **2.7 Peptídeos antimicrobianos sintéticos**

Embora os mecanismos de ação apresentados pelos PAMs naturais sejam promissores em atacar a membrana do microrganismo, desestabiliza-la e, assim, desenvolver seu potencial terapêutico, essas moléculas apresentam algumas características indesejáveis que acabam inviabilizando o seu uso (LIMA et al, 2021). Estudos mostram que os PAMs naturais são facilmente degradados por proteases do hospedeiro, apresentando ainda baixa seletividade e hidrossolubilidade. Além disso, estas moléculas podem ser altamente tóxicas para o organismo humano bem como causar hemólise em células sanguíneas saudáveis (CAPECCHI et al, 2021). Sua obtenção direta de produtos naturais também se configura como um problema pois os processos de purificação e obtenção dessas moléculas geralmente apresentam um baixo rendimento, inviabilizando sua produção de forma escalonada e acarretando em alto custo para sua obtenção (OLIVEIRA et al, 2019).

Com o intuito de superar tais adversidades, o desenho racional de peptídeos sintéticos tem se sobressaído como uma alternativa promissora na utilização de tais agentes como potentes mediadores farmacológicos (SOUZA et al, 2020). O desenho desses peptídeos consiste numa relação direta entre a estrutura dos peptídeos gerados com sua atividade, tendo em vista a possibilidade de manipulação dos aminoácidos constituintes da sequência peptídica afim de melhorar seu potencial terapêutico (TAN et al, 2021).

Dentre as ferramentas aplicadas para obtenção das sequências desejadas está a possibilidade de uso de uma proteína natural com atividade antimicrobiana conhecida para o desenho de peptídeos com características semelhantes. As ferramentas de bioinformática disponíveis também podem auxiliar na seleção das melhores sequências proteicas sugerindo quais fragmentos destas proteínas poderiam gerar peptídeos com atividade antimicrobiana (SOUZA et al, 2020). Softwares disponíveis gratuitamente garantem a realização de ensaios *in silico* para verificação do potencial antimicrobiano dos peptídeos gerados como também sugerem possíveis modificações afim de otimizar suas atividades (SOUZA et al, 2020). Características adicionais podem ser adotadas como aumento da concentração de resíduos de aminoácidos hidrofóbicos ou positivamente carregados, garantindo uma melhor interação com a membrana dos microrganismos (KUMAR et al, 2021; LIMA et al, 2021; SOUZA et al, 2020).

### **2.8 Peptídeos inspirados em *Mo*-CBP3 e uma quitinase de *A. thaliana*.**

Nosso grupo de pesquisa identificou, purificou e caracterizou uma proteína ligante à quitina de sementes de *Moringa oleífera*, a qual foi denominada *Mo*-CBP3. Tal proteína foi capaz de inibir a germinação e crescimento micelial dos fungos fitopatogênicos *Fusarium solani*, *Fusarium oxysporum*, *Colletotrichum musae* e *Colletotrichum gloeosporioides* mesmo em baixas concentrações (2,8 µM). Apesar dos bons resultados, a proteína não mostrou uma atividade eficiente contra patógenos humanos como fungos leveduriformes do gênero *Candida*, inclusive na sua concentração mais elevada de 299,30 µM. Ademais, o baixo rendimento durante o processo de purificação demonstrou ser um processo desfavorável (BATISTA et al, 2014; GIFONI et al, 2012; NETO et al, 2017).

Com isso, peptídeos sintéticos bioinspirados na sequência primária de *Mo*-CBP3 foram desenhados, com o objetivo de melhorar a atividade dessa proteína e os peptídeos gerados foram denominados *Mo*-CBP3-PepI, *Mo*-CBP3-PepII e *Mo*-CBP3-PepIII, de acordo com as metodologias descritas por OLIVEIRA et al, 2019 e DIAS et al, 2020. Além disso, um estudo inédito realizado também pelo nosso grupo de pesquisa visou o estabelecimento de um protocolo para determinação de sequências peptídicas com alto potencial antimicrobiano. Tal trabalho culminou no desenho de dois peptídeos baseados na sequência de uma quitinase de *Arabidopsis thaliana*, denominados PepGAT e PepKAA que mostraram ser eficientes contra células planctônicas de *Candida albicans*, *Bacillus subtilis*, *Staphylococcus aureus* e *Salmonella enterica*, bem como contra a germinação de esporos de fungos dermatófitos do gênero *Trichophyton* (SOUZA et al, 2020). A realização deste trabalho foi possível graças a

utilização de servidores disponíveis gratuitamente e de alta eficiência no campo da bioinformática.

A sequência de *Mo*-CBP3 de *M. oleifera* bem como a de uma quitinase de *A. thaliana* disponível no NCBI (número de acesso: NP\_181885.1) foram empregadas no desenho dos peptídeos através do servidor [http://bioserver-3.bioacademy.gr/Bioserver/CPAmP/Peptide\\_index.php](http://bioserver-3.bioacademy.gr/Bioserver/CPAmP/Peptide_index.php), disponível gratuitamente. Além disso, foram estabelecidos alguns parâmetros (Tabela 1) como carga líquida positiva, massa molecular variando de 600 a 1200 Da, índice de Bowman  $\leq 2,5$  e conteúdo de aminoácidos hidrofóbicos de, no mínimo, 40%. O Software Banco de Dados de Peptídeos (<http://aps.unmc.edu/AP/>) foi utilizado para avaliar os parâmetros estabelecidos e as pontuações  $T_m$  e  $sOPEP$  obtidas pelo servidor PEP-FOLD. (SOUZA et al, 2020)

Tabela 1 – Propriedades físico-química dos peptídeos sintéticos *Mo*-CBP3-PepI, *Mo*-CBP3-PepII, *Mo*-CBP3-PepIII, PepGAT e PepKAA

Propriedades físico-químicas	Peptídeos sintéticos				
	<i>Mo</i> -CBP3-PepI	<i>Mo</i> -CBP3-PepII	<i>Mo</i> -CBP3-PepIII	PepGAT	PepKAA
Sequência	CPAIQRCC	NIQPPCRCC	AIQRCC	GATIRAVNSR	KAANRIKYFQ
<sup>1</sup> Massa molecular calculada (Da)	893.12	1033.26	692.86	1044.18	1238.44
<sup>2</sup> Massa molecular experimental (Da)	893.10	1033.23	692.85	1044.90	1239.00
<sup>1</sup> Ponto Isoelétrico (pI)	7.97	7.97	8.11	12.00	10.29
<sup>3</sup> Índice de Bowman	1.23	2.03	1.86	2.19	2.28
<sup>3</sup> Razão Hidrofóbica Total (%)	62	44	66	40	40
<sup>3</sup> Carga líquida (+)	1	1	1	2	2
<sup>4</sup> Gráfico de Ramachandran (%)	100	67,7	83,3	98	75
<sup>5</sup> $T_m$	0,984	0,428	1,00	0,360	0,414
<sup>5</sup> $sOPEP$	-9.31	-8.16	-3.68	-7.39	-18.18

Fonte: OLIVEIRA et al, 2019; SOUZA et al, 2020.

<sup>1</sup>Obtido em ProtParam (<https://web.expasy.org/protparam/>)

<sup>2</sup>Resultados obtidos em função de espectrometria de massa conduzida.

<sup>3</sup>Obtido por APD3 ([http://aps.unmc.edu/AP/prediction/prediction\\_main.php](http://aps.unmc.edu/AP/prediction/prediction_main.php))

<sup>4</sup>Obtido por Rampage (<http://mordred.bioc.cam.ac.uk/~rapper/rampage.php>)

<sup>5</sup>Obtido por PepFOLD 3.0 (<http://mobylye.rpbs.univ-paris-diderot.fr/cgi-bin/portal.py#forms;PEP-FOLD>).

Para determinar as características antimicrobianas dos peptídeos gerados, as sequências peptídicas foram analisadas em alguns servidores disponíveis gratuitamente (Tabelas 2). A capacidade de cada peptídeo em interagir com membranas biológicas foi determinada através do servidor Cell Penetrating Peptides

([http://crdd.osdd.net/raghava/cellppd/multi\\_pep.php](http://crdd.osdd.net/raghava/cellppd/multi_pep.php)); O potencial antimicrobiano foi verificado utilizando o software iAMPpred (<http://cabgrid.res.in:8080/amppred/>); A previsão do potencial alergênico foi permitida com o auxílio da plataforma Predicting Antigenic Peptides (<http://imed.med.ucm.es/Tools/antigenic.pl>); A capacidade de resistência dos peptídeos gerados frente às enzimas proteolíticas foi determinada por Peptide Cutter (<http://imed.med.ucm.es/Tools/antigenic.pl>) e a meia-vida bem como a estabilidade de cada molécula em ambiente semelhante ao intestino foram determinadas usando o servidor HLP (<http://crdd.osdd.net/raghava/hlp/help.html>) (SOUZA et al, 2020).

Tabela 2 – Determinação do potencial antimicrobiano, resistência a proteólise e estabilidade de peptídeos sintéticos

Propriedades analisadas	Peptídeos sintéticos				
	<i>Mo</i> -CBP3-PepI	<i>Mo</i> -CBP3-PepII	<i>Mo</i> -CBP3-PepIII	PepGAT	PepKAA
<sup>1</sup> CPP	Sim	Sim	Sim	Sim	Sim
<sup>2</sup> Potencial alérgico	Não	Não	Não	Não	Não
<sup>3</sup> Potencial antimicrobiano (%)					
Antibacteriano	83	71	89	77	60
Antifúngico	87	80	92	60	89
<sup>4</sup> Sítios de clivagem					
Tripsina (pH)	1	1	1	Sim	Sim
Pepsina (pH 1.3)	0	0	0	Sim	Não
Pepsina (pH > 2)	0	0	0	Sim	Não
<sup>5</sup> Tempo de meia-vida	1.265	1.209	1.309	0,879	1.115
<sup>6</sup> Estabilidade	Alta	Alta	Alta	Normal	Alta

Fonte: OLIVEIRA et al, 2019; SOUZA et al, 2020.

<sup>1</sup>Obtido por Cell PPD ([http://crdd.osdd.net/raghava/cellppd/multi\\_pep.php](http://crdd.osdd.net/raghava/cellppd/multi_pep.php))

<sup>2</sup>Obtido por Antigenic Prediction tool (<http://imed.med.ucm.es/Tools/antigenic.pl>)

<sup>3</sup>Obtido por iAMPpred (<http://cabgrid.res.in:8080/amppred/>)

<sup>4</sup>Obtido por Peptide Cutter ([http://web.expasy.org/peptide\\_cutter/](http://web.expasy.org/peptide_cutter/))

<sup>5,6</sup>Obtido por Half Life Prediction (<http://crdd.osdd.net/raghava/hlp/help.html>)

Resultados preliminares mostraram a atividade de *Mo*-CBP3-PepI, *Mo*-CBP3-PepII e *Mo*-CBP3-PepIII contra as formas planctônicas das espécies *Staphylococcus aureus*, *Candida parapsilosis* e *Candida albicans*, bem como contra fungos dermatófitos do gênero *Trichophyton* (OLIVEIRA et al, 2019; LIMA et al, 2020). PepGAT e PepKAA apresentou atividade contra o fungo fitopatogênico *Penicillium digitatum* (LIMA et al, 2021) e contra as formas livres das bactérias patogênicas *S. aureus*, *B. subtilis*, *S. enterica* e *E. aerogenes*, bem como contra a levedura *C. albicans* (SOUZA et al, 2020). No entanto, mais estudos são necessários utilizando tais peptídeos contra as formação de biofilmes antimicrobianos, levando

em consideração que tais estruturas apresentam maiores chances de resistência às drogas atualmente disponíveis.

## 2.9 Sinergismo

O uso de fármacos antimicrobianos com mecanismos de ação iguais ou diferentes combinados entre si é conhecido por sinergismo. Essa atividade sinérgica ocorre quando o uso consoante de pelo menos dois fármacos diferentes resulta em uma maior atividade do que quando ambos atuam de maneira separada (PATRA et al, 2021). PAMs são capazes de interagir com drogas antifúngicas e antibióticos levando à formação de poros na membrana e promovendo a entrada desses agentes dentro da célula, facilitando a execução do seu potencial farmacológico que pode atuar sobre a replicação do DNA, inibição da síntese proteica e síntese os componentes da parede celular (GUCWA et al, 2018). Adicionalmente, essa combinação pode ser um indicativo de quebra da resistência desenvolvida pelos patógenos que conseguem impedir a entrada da droga no seu meio intracelular, resultando em baixa ou nenhuma atividade. Outro ponto importante é que o sinergismo é responsável por diminuir as concentrações de drogas específica que apresentam potencial tóxico para as células do hospedeiro, minimizando os efeitos deletérios ao organismo (LI et al, 2020). Dessa forma, além de haver uma redução no custo do tratamento, há a possibilidade de prevenir o desenvolvimento de mecanismos de resistência pelos microrganismos, permitindo que os PAMs atuem como moléculas adjuvantes às drogas já utilizadas para tratamento (LIMA et al, 2021).

Para determinar o potencial sinérgico de tais moléculas é usado o Índice de Concentração Inibitória Fracionada (ICIF), que é obtido com base na concentração inibitória média de cada composto em combinação dividido pela concentração inibitória média de cada composto atuando sozinho, conforme a formula:  $[ICIF = \frac{C_{IF}fármaco + C_{IF}peptídeos}{(C_{fármacocomb}/C_{fármacosozinho}) + (C_{peptídeoscomb}/C_{peptídeossozinho})}$ . Com isso, os resultado obtidos podem ser classificados em antagônico ( $ICIF \geq 4,0$ ), indiferente (cuja atividade não foi alterada por nenhuma combinação) ( $ICIF 0,5 - 4,0$ ) e efeito sinérgico ( $ICIF \leq 0,5$ ) (SOUZA et al, 2020).



### 3. HIPÓTESE

*Mo*-CBP3-PepI, *Mo*-CBP3-PepII, *Mo*-CBP3-PepIII, PepGAT e PepKAA são peptídeos antimicrobianos sintéticos que possuem atividade antibiofilme, atuando na inibição e na redução da biomassa de biofilmes de *Candida* spp. através da formação de poros na membrana celular e indução da superprodução de espécies reativas de oxigênio.

### 4. OBJETIVOS

#### 4.1 Objetivo geral

- Determinar o potencial antibiofilme dos peptídeos *Mo*-CBP3-PepI, *Mo*-CBP3-PepII, *Mo*-CBP3-PepIII, PepGAT e PepKAA *in vitro* e determinar os mecanismos de ação por trás de tal atividade.

#### 4.2 Objetivos específicos

- Avaliar as propriedades físico-químicas dos peptídeos sintéticos;
- Determinar a atividade antibiofilme de peptídeos contra biofilmes formados por espécies do gênero *Candida*;
- Elucidar os possíveis mecanismos de ação envolvidos em tal atividade através de técnicas de microscopia eletrônica e microscopia de fluorescência;
- Analisar o efeito de sinergismo estabelecido com antifúngicos comerciais como Nistatina e Itraconazol;
- Determinar os níveis de toxicidade dos peptídeos contra células humanas.

## **5. CAPÍTULO II – Artigo científico 1**

Para as sessões Metodologia, Resultados e Discussão foram utilizado artigos científicos submetidos em revistas científicas internacionais. O artigo Combined Antibiofilm Activity of Synthetic Peptides and antifungal drugs against *Candida spp*: Action mechanisms and clinical application to overcome the resistance towards antifungal drugs mostrou os índices de inibição bem como mecanismos de ação da atividade antifúngica de PepGAT e PepKAA contra biofilmes formados por leveduras das espécies *Candida albicans* e *C. krusei*.

### **5.1 Artigo científico 1**

Artigo científico submetido à revista *Frontiers in Microbiology* fator de impacto 5.76 (Qualis A1), status *under review*.

## Artigo científico 1

### **Combined Antibiofilm Activity of Synthetic Peptides and antifungal drugs against *Candida spp*: Action mechanisms and clinical application to overcome the resistance towards antifungal drugs**

Leandro P. Bezerra<sup>1,¥</sup>, Ayrles F.B. Silva<sup>2,¥</sup>, Ralph Santos-Oliveira<sup>3</sup>, Luciana M. Rebelo Alencar<sup>4</sup>, Jackson L. Amaral<sup>1,2</sup>, Nilton A.S. Neto<sup>1</sup>, Rafael G. G. Silva<sup>5</sup>, Mônica O. Belém<sup>6</sup>, Claudia R. de Andrade<sup>6</sup>, Jose T. A. Oliveira<sup>1</sup>, Cleverson D.T. Freitas<sup>1</sup>, Pedro F. N. Souza<sup>1,\*</sup>

<sup>1</sup>*Department of Biochemistry and Molecular Biology, Federal University of Ceará, Fortaleza, Ceará 60451, Brazil.*

<sup>2</sup>*Department of Physic, Federal University of Ceará, Fortaleza, Ceará 60451, Brazil.*

<sup>3</sup>*Nanoradiopharmaceuticals and Radiopharmacy, Zona Oeste State University, Rio de Janeiro, Rio de Janeiro 23070200, Brazil; Brazilian Nuclear Energy Commission, Nuclear*

<sup>4</sup>*Department of Physics, Laboratory of Biophysics and Nanosystems, Federal University of Maranhao, São Luís, Maranhão 65080-805, Brazil;*

<sup>5</sup>*Department of Biology, Federal University of Ceará, Fortaleza, Ceará 60451, Brazil*

<sup>6</sup>*Laboratory of Translational Research, Christus University Center, Fortaleza, Ceará 60192, Brazil*

¥ These authors contributed equally to this work.

#### **Corresponding Author**

\*Corresponding author: Biochemistry and Molecular Biology Department, Federal University of Ceará, CE, Brazil. Laboratory of Plant Defense Proteins, Av. Mister Hull, Caixa Postal 60451 Fortaleza, CE, Brazil. Tel: +55 85 33669823; Fax: +55 85 33669789.

E-mail: [pedrofilhobio@gmail.com](mailto:pedrofilhobio@gmail.com)

ORCID: **0000-0003-2524-4434** (P. F. N. Souza)

## 1 **Abstract**

2 Yeasts belonging to the *Candida* genus are important human pathogens. *Candida* biofilm  
3 is the most common resistance mechanism, increasing 1,000 times the resistance to  
4 antifungal drugs. This study aimed to evaluate the antibiofilm activity of synthetic  
5 peptides, as well as action mechanisms and synergistic effect with Nystatin (NYS) and  
6 Itraconazole (ITR) by Scanning Electron Microscopy (SEM) and Fluorescence  
7 Microscopy (FM). ITR (1000  $\mu\text{g. mL}^{-1}$ ) inhibited 10% biofilm formation of *C. krusei* and  
8 NYS (1000  $\mu\text{g. mL}^{-1}$ ) 40% of *C. albicans*. Regarding synergistic effect, peptides enhance  
9 7-fold the action of ITR to inhibit the biofilm formation of *C. krusei* and *C. albicans* and  
10 the degradation of formed biofilm of *C. krusei*. In combination with antifungal drugs,  
11 peptides' action mechanism involves cell wall damage, membrane pore formation, loss of  
12 cytoplasmic content, and overproduction of reactive oxygen species (ROS). Docking  
13 analysis revealed ionic and hydrophobic interactions between peptides and both drugs,  
14 which may explain the synergistic effect. Altogether, our results suggest the synthetic  
15 peptides enhance the antibiofilm activity of NYS and ITR have some potential to be  
16 employed as adjuvants and decrease the toxicity of drugs.

17 **Keywords:** Antibiofilm activity; Candidiasis; Synergism; *Candida*; Synthetic peptides;  
18 Antifungal drugs; Nystatin and Itraconazole; Action mechanisms; Clinical application.

## Introduction

The fast increase of antimicrobial resistance to drugs globally is driving humanity to a "post-antibiotic era" where the available drugs will no longer work (Lima et al., 2021). In this scenario, infections caused by fungi have gained attention. Estimates suggest 200 million new cases caused by resistant fungi every year of infections with approximately 1 million deaths (M et al., 2015). Among the fungi that affect humans, those belonging to *Candida* genus 6 have a higher prevalence, 7 cases per 100 patients (Morgan et al., 2005; GD et al., 2012; Sanguinetti et al., 2015).

*Candida* genera affect debilitated patients, as such transplanted, cancer patients, and immune-suppressed, leading to a bloodstream infection, prolonged hospital stays, and high mortality rates (Morgan et al., 2005; GD et al., 2012; Sanguinetti et al., 2015). Until 2010, *C. albicans* carrying resistance to multiple drugs was responsible for at least 60% of clinical infections (Sanguinetti et al., 2015). Nowadays, this scenario has changed. Today, infections caused by non-*C. albicans* reached 56.5% of *Candida* infections. The new cases are divided into *C. glabrata* (33.3%), *C. tropicalis* (20.3%), *C. krusei* (1.4%), and *C. kefyr* (1.4%) (Fu et al., 2017). Another important non-*albicans* pathogenic yeast is *C. auris*, first described in 2009 in Japan. Today, *C. auris* is considered a Pan-resistant yeast, presenting higher resistance rates to azoles, polyenes, and echinocandins (Ademe and Girma, 2020). Even though this change *C. albicans* still holds the higher number of cases, 43.5% (Fu et al., 2017).

Many pathogenic yeasts like *Candida* spp. have developed large drug spectra resistance mechanisms. Nevertheless, one of the most important is the ability to form biofilms. The production of biofilms could increase drug resistance up 1000-fold to conventional drugs compared to free cells (De La Fuente-Núñez et al., 2016). Besides protecting by altering the pH and

osmolarity, preventing the nutrients scarcity, and alleviating mechanical, and shear forces, the matrix of biofilms boosts the resistance by protecting yeasts cells from drugs and the host's immune response (De La Fuente-Núñez et al., 2016; Cavalheiro and Teixeira, 2018; Marak and Dhanashree, 2018; Costa-de-Oliveira and Rodrigues, 2020). It is not entirely clear the triggers to the *quorum sense* gene expression, but the composition of the matrix is known, which is rich in carbohydrates, proteins, lipids, nucleic acids, and water (Cavalheiro and Teixeira, 2018).

Biofilm development to a high level of fungal resistance with clinical implications worldwide given the small groups of antifungal agents bringing the concept of “post-antifungal” era (Chowdhary et al., 2017). In this context, the antimicrobial peptides active against biofilm could be an alternative to cope with this problem. Over the years, many researcher groups have sought antimicrobial peptides' active fungal biofilms alone or in combination with conventional drugs (Fjell et al., 2012). However, biofilm-active peptides have not yet achieved clinical trials and even commercial use. Therefore, such molecules' development, optimization, or design is needed to fight back fungal biofilms (Duncan and O'Neil, 2013).

To overcome the threat imposed by yeast's resistance to drugs, synthetic antimicrobial peptides (after that called synthetic AMPs) are an alternative either as a new drug to work alone or even as adjuvants enhancing the activity of commercial drugs (Mohamed et al., 2016; Lima et al., 2021). Synthetic AMPs were designed to have a positive charge (at least +1), amphipathic properties, acceptable hydrophobic rates (40 to 66%) (Oliveira et al., 2019; Dias et al., 2020; Souza et al., 2020b), and no-host toxicity. Breakthroughs in chemical synthesis technologies led to reduced costs for synthesis, high purity, and high amount of synthetic AMPs (Lima et al., 2021). The most advantageous technology developed allows the recovery and recycling of solvents used

during the synthesis leading to a reduced cost of synthesis, allowing the clinical application of synthetic peptides. For example, Fuzeon and Rybelsus are synthetic peptides already used to treat HIV and diabetes (Buckley et al., 2018; Pennington et al., 2021).

Recently, two synthetic peptides (PepGAT and PepKKA) were reported to strongly inhibit, at low concentrations, the growth of species of the *Candida* genus (Souza et al., 2020b). Thus, we reasoned that both peptides could be effective against biofilm from the *Candida* genus and develop synergistic effects with drugs that lost activity. The antibiofilm activity and action mechanisms PepGAT and PepKKA against *C. albicans* and *C. krusei* are described and characterized, employing advanced microscopy techniques. Furthermore, the results revealed that the synergistic effects of peptides enhanced the antibiofilm activity of commercial drugs, Nystatin (NYS) and Itraconazole (ITR), which were no longer active towards *Candida* biofilm.

## **Methods**

### **Ethical Statement**

Not applied for this study.

### **Biological materials**

The clinical isolates of *C. albicans*, *C. krusei*, and *C. parapsilosis* were from the laboratory of Plant Toxins at the Department of biochemistry and molecular biology of the Federal University of Ceará (UFC) Fortaleza, Brazil.

## Peptide synthesis

The synthetic peptides PepGAT and PepKAA (Souza et al., 2020b) were chemically synthesized by the company GenOne (São Paulo, Brazil), which analyzed their quality and purity ( $\geq 95\%$ ) by reverse-phase high-performance liquid chromatography (RP-HPLC) and mass spectrometry (Souza et al., 2020b).

## Biological activity

### *Antibiofilm and Combined effect between peptides and drugs assays*

The effect of PepGAT and PepKAA on the *Candida* spp. biofilm formation was evaluated in polystyrene flat-bottom 96-well microtiter plates (Dias et al., 2020) and as indicated by the Clinical and Laboratory Standards Institute (CLSI) M38-A2 method (M38-A2 Reference Method for Broth Dilution Antifungal Susceptibility Testing of Filamentous Fungi; Approved Standard-Second Edition, 2008). The cell suspensions were prepared from yeasts cultured for 18 h at 37 °C in the Sabouraud broth (Kasvi, Brazil). The cell concentration was diluted to  $10^6$  cells mL<sup>-1</sup> in the growth medium. One hundred microliters of the cell suspensions ( $10^6$  cells mL<sup>-1</sup>) were incubated at 37 °C for 48 h in the dark with 100  $\mu$ L of the synthetic peptides at concentration ( $50 \mu\text{g mL}^{-1}$ ) in a solution composed of 5% DMSO (Dimethyl sulfoxide) in 0.15 M NaCl (DMSO-NaCl). After that, the supernatant was discarded, and the wells were washed with sterile 0.15 M NaCl, air-dried for 30 min, and the biofilm formed was stained with an aqueous solution of 0.1% (m/v) crystal violet (Sigma Aldrich, São Paulo, Brazil), for 15 min at room temperature ( $24 \pm 2$  °C). The excess of crystal violet was removed by washing three times with sterile 0.15 M NaCl (Dias et al., 2020). Finally, 250  $\mu$ L of 95% (v/v) ethanol was added to solubilize the bound crystal violet, and absorbance was taken in a microplate reader (BioTek™ ELx800™, BioTek Instruments, Inc.,



USA) at a wavelength of 570 nm. The inhibition of biofilm formation was calculated by comparing the absorbance readings of cells treated with synthetic peptides and those obtained from cells treated with DMSO-NaCl solution (negative control), ITR (1000  $\mu\text{g mL}^{-1}$ ), and NYS (1000  $\mu\text{g mL}^{-1}$ ) both used as positive controls (Dias et al., 2020).

A second experiment was carried out to evaluate the effect of the peptides on the degradation of the preformed biofilms (Dias et al., 2020). Two hundred microliters of the cell suspensions ( $10^6$  cells  $\text{mL}^{-1}$ , prepared as described above) were incubated at 37 °C for 24 h in the dark to form the biofilm. Then, the supernatant was gently aspirated with a micropipette to remove the planktonic cells. In each well, 100  $\mu\text{L}$  of each synthetic peptide (50  $\mu\text{g mL}^{-1}$ ) or controls plus 100  $\mu\text{L}$  growth medium (Sabouraud broth, Kasvi, Brazil) were added. The plates were incubated for 24 h at 37 °C, in the dark. The culture medium was again discarded, and the same procedure described above was used to quantify the biofilm biomass remaining after incubation with the peptide (Dias et al., 2020). The controls use were the same from inhibition of biofilm formation.

The synergism assays were performed between peptides with either antifungals NYS or ITR: The combinations were constituted of each peptide (50  $\mu\text{g mL}^{-1}$ ) + NYS or ITR (1000  $\mu\text{g mL}^{-1}$ ) (Souza et al., 2020a). The control to evaluate the effectiveness of synergism was the activity presented by peptides or drugs alone. After the formulation of combinations, the antibiofilm assays for synergism analyses for *Candida* spp. were the same as described above.

## **Study of mechanisms of action of peptides against biofilms**

### ***Biofilm integrity by scanning electron microscopy (SEM)***

Morphological changes in the biofilm of *C. albicans* and *C. krusei* were evaluated by SEM, as previously described by Staniszewska et al. (2013) with modification. The assay was performed as described above (see the Antibiofilm section), but, this time, the biofilm was grown on the

coverslip (previously treated with 0.1% gelatin [Sigma Aldrich, São Paulo, Brazil]) inside a well of six-well plates. After, the biofilm was fixed with fixation buffer [in 1% (v/v) glutaraldehyde + 4% (v/v) formaldehyde in 0.15 M sodium phosphate buffer at pH 7.0]. Next, treated with 0.2% (m/v) osmium tetroxide (Sigma Aldrich, São Paulo, Brazil) for 30 min in the dark, and successively dehydrated with ethanol concentration (30, 70, 100, 100, and 100% [v/v]) for 10 min each, after each centrifugation wash the ethanol was aspirated with an automatic pipette. Finally, final dehydration was carried out with 50/50 ethanol/hexamethyldisilazane (HMDS) for 10 min and lastly with 100% HMDS (Sigma Aldrich, São Paulo, Brazil). Then, each coverslip was removed from each well and assembled on stubs and coated with a 20 nm gold layer using a positron-emission tomography (PET) coating machine (Emitech-Q150TES, Quorum Technologies, England). Images were made in an FEI Inspect<sup>TM</sup> 50 scanning electron microscope (Oregon, USA), equipped with a low energy detector (Everhart-Thornley) using acceleration beam voltage of 20,000 kV and 20,000x detector magnification (Souza et al., 2020a). The treatments for this assay were peptides alone, drugs alone, and solutions made by peptides and drugs.

#### ***Biofilm integrity determined by propidium iodide (PI) uptake***

The biofilms were produced as described in the biofilm assays and the SEM microscopy sections. After, peptide-, controls-, and drugs-peptides mixed solutions treated biofilm were incubated with  $10^{-3}$  M of propidium iodide (PI, Sigma Aldrich, São Paulo, Brazil), in the dark, at 37 °C for 30 min (Souza et al., 2020a). Then, the biofilm-containing coverslips were washed with 0.15 M of NaCl three times to remove the unbound PI and observed under a fluorescent microscope (Olympus System BX 60, Japan) with an excitation wavelength of 490 nm and an emission wavelength of 520 nm.

### ***Overproduction of reactive oxygen species (ROS) by biofilm***

The overproduction of ROS was evaluated as described by Dias et al. (2020) with modifications. The biofilms were produced as described in the biofilm assays and the SEM microscopy sections. After, peptide-, controls-, and drugs-peptides mixed solution treated biofilm were incubated with 10  $\mu\text{M}$  of 2',7' dichlorofluorescein diacetate (DCFH-DA, Sigma Aldrich, St., Louis, USA) at 37 °C in the dark for 30 min (Souza et al., 2020a). Then, the biofilm-containing coverslips were washed with 0.15 M of NaCl three times to remove the unbound PI and observed under a fluorescent microscope (Olympus System BX 60, Japan) with an excitation wavelength of 488 nm and an emission wavelength of 525 nm.

### **Hemolytic assay**

The hemolytic activity of synthetic peptides, NYS, ITR, and combination by then was tested in A, B, and O-types of human red blood cells (HRBC), according to Souza et al. (2020). The combined solutions of peptides and either NYS or ITR were the same as used in synergism assays. The HRBCs from A, B, and O were provided by the Ceará Hematology and Hemotherapy Center (Ceará, Brazil).

The blood was collected in the presence of heparin (5 IU mL<sup>-1</sup>, Sigma Aldrich, São Paulo, Brazil), centrifuged at 300 g for 5 min at 4 °C, and gently dissolved in sterile 0.15 M NaCl. The blood was washed three times with 0.15 M NaCl and diluted to a concentration of 2.5% in 0.15 M NaCl used in the assay. One hundred microliters of each blood type were incubated, individually, with solutions of synthetic peptides (50  $\mu\text{g mL}^{-1}$ ), NYS (1000  $\mu\text{g mL}^{-1}$ ), ITR (1000  $\mu\text{g mL}^{-1}$ ), the solution made by peptides and drugs, DMSO-NaCl, and 0.1% (v/v) Triton X-100 (the positive control for hemolysis) for 30 min at 37 °C, followed by centrifugation (300 g for 5 min at 4 °C, in centrifuge Eppendorf 5810, Germany). Then, the supernatants were collected and transferred to

96-well microtiter plates. Hemolysis (%) was calculated by measuring the supernatant absorbance at 414 nm using an automated absorbance microplate reader. Negative (0%) and positive (100%) hemolysis were determined by treating HRBCs with 5% DMSO in 0.15 M NaCl (vehicle for peptides) and 0.1% (v/v) Triton X-100, respectively. The equation calculated the hemolysis:  $[(\text{Abs}_{414\text{nm}}$  of HRBC treated with peptides -  $\text{Abs}_{414\text{nm}}$  HRBCs treated with 0.15 M NaCl) /  $[(\text{Abs}_{414\text{nm}}$  of HRBCs treated with 0.1% TritonX-100 -  $\text{Abs}_{414\text{nm}}$  of HRBCs treated with 0.15 M NaCl)] x 100.

### Statistical analysis

All the experiments were performed three times, and the statistics were expressed as the mean  $\pm$  standard error. The data were submitted to one-way analysis of variance (ANOVA) followed by the Tukey test, using GraphPad Prisma 5.01 (GraphPad Software company, California, USA), with the significance of  $p < 0.05$ .

## RESULTS

### Antibiofilm activity of peptides and synergistic effect with antifungal drugs

The peptides ( $50 \mu\text{g} \cdot \text{mL}^{-1}$ ) presented different behaviors toward the biofilm of *Candida* ssp (Fig. 1). Either the peptides, antifungal drugs, or combinations had any activity against the biofilm of *C. parapsilosis* or *C. tropicalis* (Supplementary Fig. 1C and D). The first assay was done to evaluate the ability of peptides to inhibit the biofilm formation of *C. krusei* and *C. albicans* (Fig. 1A and B). To *C. krusei*, both peptides barely reach 10% of inhibition. ITR and NYS reached 20 and 0% of inhibition of biofilm formation by *C. krusei* (Fig. 1A). In contrast, the combinations of both PepGAT ( $50 \mu\text{g} \cdot \text{mL}^{-1}$ ) + ITR ( $1000 \mu\text{g} \cdot \text{mL}^{-1}$ ) and PepKAA ( $50 \mu\text{g} \cdot \text{mL}^{-1}$ ) + ITR ( $1000 \mu\text{g} \cdot \text{mL}^{-1}$ ) led to an inhibition, respectively, of 80 and 76% of *C. krusei* biofilm (Fig. 1A). The combination of peptides with NYS was not effective. Regarding *C. albicans*, NYS, PepGAT, and PepKAA

inhibited biofilm formation, 40, 10, and 20%. An interesting result was the synergism found in the combinations made by PepGAT + ITR, PepGAT + NYS, and PepKAA + NYS that inhibited, respectively, 40%, 95%, and 98% the biofilm formation of *C. albicans* (Fig. 1B).

Regarding the degradation of formed biofilm, no results were found to *C. albicans*, *C. parapsilosis*, and *C. tropicalis* (Supplementary Fig. 1A and B), only toward *C. krusei* (Fig. 1C). ITR, PepGAT, and PepKAA alone did not reduce biomass of preformed biofilm of *C. krusei* (Fig. 1C). In contrast, NYS was able to reduce in 20% the biomass of *C. albicans* preformed biofilm (Fig. 1C). Except for the PepGAT + NYS combination that did not significantly decrease biomass reduction, PepGAT + ITR, PepKAA + ITR, and PepKAA + NYS reduced in, respectively, 50%, 30%, and 15% the preformed biofilm of *C. albicans* (Fig. 1C).

### **Biofilm integrity and ROS overproduction**

The evaluation of peptides alone and the combination with drugs affect the membrane of the biofilm cells. Fluorescence microscopy was employed (Figs. 2-5). Propidium iodide (PI) is a fluorophore that binds to DNA, releasing red fluorescence. However, PI only crosses the damaged cell membrane, and a healthy membrane blocks the movement of PI, leading to no fluorescence at all. As expected, all controls made by DMSO-NaCl solution (the vehicle of peptides) presented no fluorescence, suggesting the membranes in control cells have no type of pore formed (Figs. 2-5). An interesting result was the absence of fluorescence in biofilms treated with drugs (NYS and ITR) (Figs. 2-5).

Regarding the synthetic peptides, PepGAT did induce fluorescence in all treatments either in the inhibition of biofilm formation although at different intensities (Figs. 2-4) and degradation of preformed biofilm (Fig. 5). The PepKAA peptides presented a different behavior. In the case of the inhibition of biofilm formation by *C. krusei*, PepKAA alone could not induce damage in the

membrane to allow PI to pass by the membrane and emit fluorescence (Fig. 2). In contrast, PepKAA induced the fluorescence in inhibiting biofilm formation by *C. albicans* (Fig. 4). In the case of combinations made by peptides and antifungal drugs, all presented fluorescence (Figs. 2-5). This is an exciting result for three reasons: 1) drugs alone did not show any fluorescence (Figs. 2-5); 2) in the case of PepKAA, which did not show fluorescence, the combination with ITR led to a release of fluorescence (Figs. 2 and 3) in some cases, such as PepGAT+ITR (Figs. 3 and 5) fluorescence produced by the combination was higher than that produced by drugs alone, suggesting a bigger number of cell damage in the combination.

The experiments to evaluate the ROS overproduction in the biofilms revealed a different pattern than PI experiments. All positive or negative controls did not produce any fluorescence indicating no ROS production (Figs. 2-5). In inhibiting the biofilm formation of *C. krusei*, both peptides induced ROS production at different intensities, as revealed by fluorescence. In this case, the cells treated with PepGAT were brighter than those produced by PepKAA. Following this pattern, the combinations made to inhibit the biofilm formation by *C. krusei* produced only a slight fluorescence, indicating a low ROS level (Fig. 2). In the inhibition of biofilm formation by *C. albicans* to ROS production, only a slight production of ROS was indicated by a faint fluorescence in the treatment with PepKAA (Fig. 4). In contrast, brighter fluorescence indicates a higher production of ROS in both PepGAT alone and combined with ITR in the degradation of preformed biofilm of *C. krusei* (Fig. 5), suggesting that the ROS overproduction is, indeed, an important mechanism to degrade the biofilm.

### **Scanning electron microscopy (SEM) analyses of biofilm**

SEM images revealed severe that all control made with DMSO-NaCl solution the biofilm was in an excellent spherical shape, with no cracks or damage, and cells were seen with no visible

damage to membrane or cell wall (Figs. 6-8). The SEM analysis revealed that the cells involved in biofilm formation (Figs. 6 and 7) and preformed biofilm (Fig. 8) were not affected by the treatment with either ITR or NYS, both at  $1000 \mu\text{g mL}^{-1}$ .

SEM analysis strength the damages revealed by fluorescence microscopy in *Candida* cells (Figs. 2-5), which were confirmed by SEM analysis (Fig. 6-8). To inhibit the formation of *C. krusei*, PepGAT induced several damages to cells. It was possible to see a depression-like cavity on cells (Fig. 6, PepGAT and PepKAA Panels, white dashed circle), indicating damage to the cell wall. Also, tiny blebs, new buds, scars on new buds and cells, and rings of truncated bud scars were present in the treatment with both peptides (Fig. 6, white arrowheads). In both treatments with peptides, cells present wrinkles and scars all over the structure. Additionally, in both treatments with peptides alone is possible to see a lack of constriction in the solid point of the septum (Fig. 6, white open arrows).

In contrast to what was seen in the treatment with drugs alone, the combination of peptides and drugs lead to several damages to cells and thus inhibit biofilm formation. In both cases, many cells presented depression-like cavities (Fig. 6, PepGAT+ITR and PepKAA+ITR panels, white dashed circle), indicating damage to the cell wall. In addition, were noticed alterations in cell shape, wrinkles and scars all over the structure, small blebs, new buds, scars on new buds and cells, and rings of truncated bud scars in the treatment with both peptides (Fig. 6, white arrowheads), and no presence of a solid point in septum junction (Fig. 6, white open arrows).

SEM analysis revealed a different pattern in inhibiting biofilm formation of *C. albicans* (Fig. 7). The controls DMSO-NaCl solution, ITR, and NYS at  $1000 \mu\text{g mL}^{-1}$  showed no significant alteration on *C. albicans* cells (Fig. 7). Treatment with PepGAT induced small blebs, new buds,

scars on new buds and cells (Fig. 7, white arrowheads). In contrast, the treatment with PepKAA is possible to damage all cells. Cells stick together with all the present bad conformation and pieces of other cells on top of them (Fig. 7, panel PepKAA). SEM analysis revealed that the combination of PepGAT + ITR killed almost all cells (Fig. 7), and the leftovers are completely damaged unable to form biofilm. The combination of PepKAA + ITR is far less effective than PepGAT + ITR, causing scars and wrinkles on cells and abnormal shape. It is also possible to see the presence of small blebs, new buds, scars on new buds and cells, and rings of truncated bud scars in the treatment with both peptides (Fig. 7, white arrowheads). The combinations of both peptides + NYS were most efficient than with combination with ITR. In both cases, all cells were dead. It was only found isolated cell wholly damaged, with the signal of loss of internal content and with no ability to form biofilm at all (Fig. 7, PepGAT and PepKAA panels).

In the degradation of *C. krusei* preformed biofilm, the SEM analysis of ITR-treated biofilm revealed no damage on the biofilm (Fig. 8). In the treatment with peptides alone or combination with ITR, the biofilm constituting cells presented damage to the cell wall, loss of internal content, tiny blebs, new buds, many scars, and wrinkles on new buds and cells (Fig. 8 white arrowheads), and rings of truncated bud scars in the treatment with both peptides (Fig. 8, white open arrows).

### **Hemolytic Assay**

A previous study (Souza et al., 2020) showed that the synthetic peptides had no hemolytic activity against any human blood type tested (Table 1), even at 50  $\mu\text{g. mL}^{-1}$ . In contrast, NYS at 1000  $\mu\text{g. mL}^{-1}$  caused 100% hemolysis in all human blood types and ITR at 1000  $\mu\text{g. mL}^{-1}$  caused 80, 75, and 69% of hemolysis, respectively, to Type-A, B, and O of red blood cells (Table 1).



In general, synthetic peptides with antifungal drugs decreased their hemolytic effect (Table 1). PepGAT with NYS resulted in a reduced hemolytic effect of 54, 43, and 12%, respectively, to Type-A, B, and O of red blood cells. PepGAT with ITR caused 17, 45, and 43% of hemolysis, respectively, to Type-A, B, and O of red blood cells (Table 1). The combination of PepKAA with NYS hemolyzed 15, 10, and 21%, respectively, of Type-A, B, and O of red blood cells, whereas the combination of PepKAA with ITR 21, 34, 12%, respectively, of Type-A, B, and O of red blood cells (Table 1).

## Discussion

Fungal infection caused by yeasts from *Candida* species poses a critical problem in the healthcare field worldwide, leading to elevated mortality rates and high costs with medical care for hospitalized patients and governments (Pristov and Ghannoum, 2019; S et al., 2019). The drug-resistant *C. albicans* is the most severe threat to human health worldwide. It is responsible for infections caused in immunocompromised, HIV-positive, and intensive care unit patients (S et al., 2016; Costa-de-Oliveira and Rodrigues, 2020).

*C. albicans* and *C. krusei* have developed resistance to many antifungal drugs such as azoles (ITR), echinocandins, polyenes (NYS), among others (AT et al., 2021). Overall, the mechanisms of resistance developed by yeasts involve overexpression or alteration of the target, development of efflux pumps to remove the excess of drugs of cytoplasm, modification of the drug, and biofilm production (Orozco et al., 1998; Guinea et al., 2006; AT et al., 2021; Lima et al., 2021).

Biofilm is an excellent resistance structure and all yeasts on *Candida* genera could produce it (Cavalheiro and Teixeira, 2018). The biofilm production by *Candida* provides a different

behavior compared to planktonic life. For example, cells living in the biofilm community can attach irreversibly to any surface, inert material, living tissue, medical devices (e.i., prostheses and cardioverter defibrillators), in addition to increasing the expression of virulent factors and higher resistance to antifungal drugs (Cavalheiro and Teixeira, 2018; Lima et al., 2021). Based on that, biofilm formation is a serious threat to overcome.

The effect of synthetic peptides has already been tested toward *Candida* biofilms. For instance, the synthetic peptides KU4 ( $96 \mu\text{g mL}^{-1}$ ), uperin 3.6 ( $96 \mu\text{g mL}^{-1}$ ), upn-lys4 ( $96 \mu\text{g mL}^{-1}$ ), upn-lys5 ( $192 \mu\text{g mL}^{-1}$ ), and upn-lys6 ( $96 \mu\text{g mL}^{-1}$ ) reduced the viability of the biofilm of *C. albicans* only in 20, 35, 15, 40, and 30%, respectively (KY et al., 2015). In the case of *C. krusei*, the synthetic peptide VLL-28 at  $72 \mu\text{g mL}^{-1}$  reduced the viability of *C. krusei* biofilms by 35% (Roschetto et al., 2018). Paulone et al. (2017) reported a peptide that presented an  $\text{IC}_{50}$  value against *C. albicans* biofilm of  $126 \mu\text{g mL}^{-1}$  (Paulone et al., 2017).

Despite those activities of synthetic peptides against *Candida* biofilms, there also some studies reporting the synergism of synthetic peptides with antifungal drugs such as fluconazole and Amphotericin B but only against candida planktonic cells of (MacCallum et al., 2013; Park et al., 2017; do Nascimento Dias et al., 2020; Czechowicz et al., 2021; Maione et al., 2022). For example, the combination of synthetic peptide WMR ( $110 \mu\text{g mL}^{-1}$ ) + fluconazole ( $10 \mu\text{g mL}^{-1}$ ) inhibit in 50% the growth of *C. albicans* (Maione et al., 2022). Regarding the synergistic effect of peptides and antifungal drugs toward candida biofilm the studies are a little scarce and this number is even lower with synthetic peptides. The combination of peptide HsLin06\_18 ( $100 \mu\text{g mL}^{-1}$ ) with caspofungin ( $10 \mu\text{g mL}^{-1}$ ) inhibit in 50% the biofilm formation of *C. albicans* (Cools et al., 2017). The analysis of mechanism of action revealed that only the combination lead to membrane permeabilization of *C. albicans* cells on biofilm (Cools et al., 2017).

In another study, the synergistic action of the lipopeptide AC7BS (1000  $\mu\text{g mL}^{-1}$ ) + flucanazole (1000  $\mu\text{g mL}^{-1}$ ) reduced in 60% the preformed biofilm of *C. albicans* (Ceresa et al., 2017). Mora-Navarro et al. (2015) showed that a  $\beta$ -synthetic peptide (200  $\mu\text{g mL}^{-1}$ ) + ketoconazole (200  $\mu\text{g mL}^{-1}$ ) inhibit in 60% the biofilm formation. In this study, the authors did not report any mechanism of action of the combination. Compared to those above-mentioned results, here was found exciting results about synergic effect of peptides + antifungal drugs to inhibit the biofilm formation and reduced the mass of preformed biofilm (Fig. 1) toward *Candida* biofilms. PepKAA + NYS inhibited in 98% the biofilm formation of *C. albicans* and PepGAT + ITR reduced in 55% the biomass of preformed biofilm of *C. krusei* (Fig. 1). It is important to notice that none of those above-mentioned work showed any result about the reduction of biomass of preformed biofilms. This is the great novelty of this work.

Regarding the mechanism of action only Cools et al. (2017) and Maione et al. (2022) provided a clue about how the combination between peptides and drugs act on *C. albicans* biofilm. In both studie the authors just the membrane permeabilization. Here, fluorescence (Figs. 2-5) and SEM (Figs. 5-9) analysis revealed the mechanisms behind revealed lethal damage of those combinations to *Candida* biofilms. Here, additionally, fluorescence analyses revealed an exciting result. In some cases, the combinations of peptides with antifungal drugs lead to ROS overproduction (Fig. 2 panels PepGAT + ITR and PepKAA + ITR and Fig. 3 PepGAT + ITR). Interestingly, ROS overproduction was all in the combinations of either PepGAT or PepKAA with ITR and presented the best results even to inhibit the formation of biofilm (Fig. 1A) or degrade preformed biofilm (Fig. 1C). ROS is essential to biofilm biogenesis, development, formation, the genetic variability of cells (Čáp et al., 2012). However, the line of benefits and lethal effects are tiny and easy to cross. A slight unbalance in ROS levels could lead to ROS accumulation, which

is lethal because they inactivate vital molecules such as carbohydrates, nucleic acids, proteins, and lipids, triggering programmed cell death (PCD) (Maurya et al., 2011).

Our results clearly suggest peptides enhance the antibiofilm activity of NYS and ITR. There are two hypotheses to explain the improvement of antifungal drugs by peptides. The first one is directly related to the mechanism of action ITR and NYS. Although being of different classes, ITR and NYS have the same target. ITR interacts with the enzyme lanosterol 14 $\alpha$ -demethylase to inhibit the ergosterol biosynthesis, and NYS interacts with the ergosterol in the membrane, causing an unbalance in the membrane (Borgers and Ven, 1989; AG et al., 2017). By interacting with chitin in the cell wall, both PepGAT and PepKAA cause a rupture in the cell wall (Figs. 6-8), facilitating the access of lanosterol 14 $\alpha$ -demethylase and ergosterol, respectively, by ITR and NYS and thus enhancing their activity. The second explanation is based on the peptides attacking the membrane directly, as revealed by fluorescence microscopy (Figs. 2-5). During the treatment of yeasts with combinations made by peptides and antifungal drugs, membranes are double attacked. Peptides attack the membrane to form pores, and drugs attack their target in the membranes.

Both ITR and NYS have many collateral effects. ITR may cause vomiting, diarrhea, headache, and dizziness. Besides these collateral effects, cardiotoxicity and hypertension were attributed to ITR use (F et al., 2001). Regarding NYS, the collateral effects are poor taste (the incidence was 61.5% in one study) and gastrointestinal adverse reactions, including vomiting, nausea, diarrhea, anorexia, and abdominal pain (Macesic and Wingard, 2020). The interesting result was that the association of peptides with antifungal drugs reduced their toxicity in human erythrocytes (Table 1). In all treatments made with combinations, were found a reduction in toxicity of antifungal drugs, at least 2-fold reaching up to 8.3-fold (Table 1).

## **Conclusion**

Here is a pioneer study showing the activity, action mechanism, and synergistic effects of two synthetic peptides (PepGAT and PepKAA) with NYS and ITR against biofilms of *C. albicans* and *C. krusei*. In the best combinations, peptides enhanced the antibiofilm activity of both drugs at least five-fold and reduced up to ten-fold their toxic effect against red blood cells. Therefore, the ability to improve the antibiofilm activity of NYS and ITR suggests that synthetic peptides can be employed as adjuvants and decrease the toxicity of these drugs.

## **Funding and Acknowledgments**

This work was supported by grants from the following Brazilian agencies: Conselho Nacional de Desenvolvimento Científico e Tecnológico; Coordenação de Aperfeiçoamento de Pessoal de Nível Superior (CAPES); Fundação Cearense de Apoio ao Desenvolvimento Científico e Tecnológico (FUNCAP). A special thanks to CAPES for providing the grant (grant number 88887.318820/2019-00) for postdoctoral position for Pedro F. N. Souza. We are also grateful to the central analytical facilities of UFC, Brazil.

### **Credit Author Statement:**

**Conceptualization:** L.P.B., and P.F.N.S.

**Data curation:** L.P.B., A.F.B.S., J.L.A., N.A.S.N., C.R.A., R.G.G.S., R.S.O., and L.M.R.A., and P.F.N.S.

**Formal analysis:** C.D.T.F., J.T.A.O., and P.F.N.S.

**Funding acquisition:** C.D.T.F., R.S.O., L.M.R.A., and J.T.A.O.

**Methodology:** L.P.B., A.F.B.S., J.L.A., N.A.S.N., M.O.B., R.G.G.S., and P.F.N.S.

**Resources:** C.D.T.F., R.S.O., L.M.R.A., and J.T.A.O.

**Supervision:** P.F.N.S.

**Writing original draft:** M.O.B., C.R.A., R.S.O, L.M.R.A., and P.F.N.S.

**Writing, review, and editing:** R.S.O, L.M.R.A., and P.F.N.S.

**Conflict of interest**

All authors declare no conflict of interest.

## References

Ademe, M., and Girma, F. (2020). Candida auris: From Multidrug Resistance to Pan-Resistant Strains. *Infect. Drug Resist.* 13, 1287. doi:10.2147/IDR.S249864.

AG, D. S., JT, M., AC, C., IR, C., AS, V., MP, M.-L., et al. (2017). The molecular mechanism of Nystatin action is dependent on the membrane biophysical properties and lipid composition. *Phys. Chem. Chem. Phys.* 19, 30078–30088. doi:10.1039/C7CP05353C.

AT, J., J, A., OM, S., and CH, P. (2021). Update on Candida krusei, a potential multidrug-resistant pathogen. *Med. Mycol.* 59, 14–30. doi:10.1093/MMY/MYAA031.

Biggest Threats and Data | Antibiotic/Antimicrobial Resistance | CDC Available at:

<https://www.cdc.gov/drugresistance/biggest-threats.html> [Accessed September 15, 2021].

Borgers, M., and Ven, M.-A. Van de (1989). Mode of Action of Itraconazole: Morphological Aspects. *Mycoses* 32, 53–59. doi:10.1111/J.1439-0507.1989.TB02294.X.

Buckley, S. T., Bækdal, T. A., Vegge, A., Maarbjerg, S. J., Pyke, C., Ahnfelt-Rønne, J., et al. (2018). Transcellular stomach absorption of a derivatized glucagon-like peptide-1 receptor

- agonist. *Sci. Transl. Med.* 10, 7047. doi:10.1126/scitranslmed.aar7047.
- Čáp, M., Váchová, L., and Palková, Z. (2012). Reactive Oxygen Species in the Signaling and Adaptation of Multicellular Microbial Communities. *Oxid. Med. Cell. Longev.* 2012, 13. doi:10.1155/2012/976753.
- Cavalheiro, M., and Teixeira, M. C. (2018). Candida Biofilms: Threats, Challenges, and Promising Strategies. *Front. Med.* 5, 28. doi:10.3389/FMED.2018.00028.
- Ceresa, C., Rinaldi, M., and Fracchia, L. (2017). Synergistic activity of antifungal drugs and lipopeptide AC7 against *Candida albicans* biofilm on silicone. *AIMS Bioeng.* 4, 318–334. doi:10.3934/bioeng.2017.2.318.
- Chowdhary, A., Sharma, C., and Meis, J. F. (2017). Azole-resistant aspergillosis: epidemiology, molecular mechanisms, and treatment. *J. Infect. Dis.* 216, S436–S444.
- Cools, T. L., Struyfs, C., Drijfhout, J. W., Kucharíková, S., Romero, C. L., Dijck, P. Van, et al. (2017). A linear 19-mer plant defensin-derived peptide acts synergistically with caspofungin against *Candida albicans* biofilms. *Front. Microbiol.* 8, 1–14. doi:10.3389/fmicb.2017.02051.
- Costa-de-Oliveira, S., and Rodrigues, A. G. (2020). *Candida albicans* Antifungal Resistance and Tolerance in Bloodstream Infections: The Triad Yeast-Host-Antifungal. *Microorganisms* 8. doi:10.3390/MICROORGANISMS8020154.
- Czechowicz, P., Neubauer, D., Nowicka, J., Kamysz, W., and Gościński, G. (2021). Antifungal activity of linear and disulfide-cyclized ultrashort cationic lipopeptides alone and in combination with fluconazole against vulvovaginal *Candida* spp. *Pharmaceutics* 13.

doi:10.3390/pharmaceutics13101589.

De La Fuente-Núñez, C., Cardoso, M. H., De Souza Cândido, E., Franco, O. L., and Hancock, R. E. W. (2016). Synthetic antibiofilm peptides. *Biochim. Biophys. Acta - Biomembr.* 1858, 1061–1069. doi:10.1016/j.bbamem.2015.12.015.

Dias, L. P., Souza, P. F. N., Oliveira, J. T. A., Vasconcelos, I. M., Araújo, N. M. S., Tilburg, M. F. V., et al. (2020). RcAlb-PepII, a synthetic small peptide bioinspired in the 2S albumin from the seed cake of *Ricinus communis*, is a potent antimicrobial agent against *Klebsiella pneumoniae* and *Candida parapsilosis*. *Biochim. Biophys. Acta - Biomembr.* 1862, 183092. doi:10.1016/j.bbamem.2019.183092.

do Nascimento Dias, J., de Souza Silva, C., de Araújo, A. R., Souza, J. M. T., de Holanda Veloso Júnior, P. H., Cabral, W. F., et al. (2020). Mechanisms of action of antimicrobial peptides ToAP2 and NDBP-5.7 against *Candida albicans* planktonic and biofilm cells. *Sci. Rep.* 10, 1–14. doi:10.1038/s41598-020-67041-2.

Duncan, V. M. S., and O’Neil, D. A. (2013). Commercialization of antifungal peptides. *Fungal Biol. Rev.* 26, 156–165.

F, C., M, M., C, G., R, M., S, C., AI, R., et al. (2021). Mechanism of Antifungal Activity by 5-Aminoimidazole-4-Carbohydrazonamide Derivatives against *Candida albicans* and *Candida krusei*. *Antibiot. (Basel, Switzerland)* 10, 1–13. doi:10.3390/ANTIBIOTICS10020183.

F, Q.-T., N, S., MM, C., AP, A., D, da M., MG, B., et al. (2001). Evaluation of efficacy and safety of itraconazole oral solution for the treatment of oropharyngeal candidiasis in aids patients. *Braz. J. Infect. Dis.* 5, 60–66. doi:10.1590/S1413-86702001000200003.



- Fjell, C. D., Hiss, J. A., Hancock, R. E. W., and Schneider, G. (2012). Designing antimicrobial peptides: form follows function. *Nat. Rev. Drug Discov.* 11, 37–51.
- Fu, J., Ding, Y., Wei, B., Wang, L., Xu, S., Qin, P., et al. (2017). Epidemiology of *Candida albicans* and non-*C. albicans* of neonatal candidemia at a tertiary care hospital in western China. *BMC Infect. Dis.* 17, 329. doi:10.1186/s12879-017-2423-8.
- GD, B., DW, D., NA, G., SM, L., MG, N., and TC, W. (2012). Hidden killers: human fungal infections. *Sci. Transl. Med.* 4. doi:10.1126/SCITRANSLMED.3004404.
- Guinea, J., Sánchez-Somolinos, M., Cuevas, O., Peláez, T., and Bouza, E. (2006). Fluconazole resistance mechanisms in *Candida krusei*: The contribution of efflux-pumps. *Med. Mycol.* 44, 575–578. doi:10.1080/13693780600561544.
- KY, L., ST, T., CF, L., VS, L., NH, S., RD, V., et al. (2015). Activity of Novel Synthetic Peptides against *Candida albicans*. *Sci. Rep.* 5. doi:10.1038/SREP09657.
- Lima, P. G., Oliveira, J. T. A., Amaral, J. L., Freitas, C. D. T., and Souza, P. F. N. (2021). Synthetic antimicrobial peptides: Characteristics, design, and potential as alternative molecules to overcome microbial resistance. *Life Sci.* 278, 119647. doi:10.1016/J.LFS.2021.119647.
- M, S., B, P., and C, L.-F. (2015). Antifungal drug resistance among *Candida* species: mechanisms and clinical impact. *Mycoses* 58 Suppl 2, 2–13. doi:10.1111/MYC.12330.
- M38-A2 Reference Method for Broth Dilution Antifungal Susceptibility Testing of Filamentous Fungi; Approved Standard-Second Edition (2008). Available at: [www.clsi.org](http://www.clsi.org).
- MacCallum, D. M., Desbois, A. P., and Coote, P. J. (2013). Enhanced efficacy of synergistic

combinations of antimicrobial peptides with caspofungin versus *Candida albicans* in insect and murine models of systemic infection. *Eur. J. Clin. Microbiol. Infect. Dis.* 32, 1055–1062. doi:10.1007/s10096-013-1850-8.

Macesic, N., and Wingard, J. R. (2020). Nystatin. *Kucers Use Antibiot. A Clin. Rev. Antibacterial, Antifung. Antiparasit. Antivir. Drugs, Seventh Ed.*, 2646–2652. Available at: <https://www.ncbi.nlm.nih.gov/books/NBK548581/> [Accessed September 15, 2021].

Maione, A., Bellavita, R., Alteriis, E. De, Galdiero, S., Albarano, L., Pietra, A. La, et al. (2022). WMR Peptide as Antifungal and Antibiofilm against *Albicans* and Non-*Albicans* *Candida* Species : Shreds of Evidence on the Mechanism of Action. 1–20.

Marak, M. B., and Dhanashree, B. (2018). Antifungal susceptibility and biofilm production of *candida* spp. Isolated from clinical samples. *Int. J. Microbiol.* 2018. doi:10.1155/2018/7495218.

Maurya, I. K., Pathak, S., Sharma, M., Sanwal, H., Chaudhary, P., Tupe, S., et al. (2011). Antifungal activity of novel synthetic peptides by accumulation of reactive oxygen species (ROS) and disruption of cell wall against *Candida albicans*. *Peptides* 32, 1732–1740. doi:10.1016/J.PEPTIDES.2011.06.003.

Mohamed, M. F., Abdelkhalek, A., and Seleem, M. N. (2016). Evaluation of short synthetic antimicrobial peptides for treatment of drug-resistant and intracellular *Staphylococcus aureus*. *Sci. Reports* 2016 61 6, 1–14. doi:10.1038/srep29707.

Mora-Navarro, C., Caraballo-León, J., Torres-Lugo, M., and Ortiz-Bermúdez, P. (2015). Synthetic antimicrobial  $\beta$ -peptide in dual-treatment with fluconazole or ketoconazole enhances the in vitro inhibition of planktonic and biofilm *Candida albicans*. *J. Pept. Sci.* 21,

853–861. doi:10.1002/psc.2827.

Morgan, J., Meltzer, M. I., Plikaytis, B. D., Sofair, A. N., Huie-White, S., Wilcox, S., et al. (2005). Excess Mortality, Hospital Stay, and Cost Due to Candidemia: A Case-Control Study Using Data From Population-Based Candidemia Surveillance. *Infect. Control Hosp. Epidemiol.* 26, 540–547. doi:10.1086/502581.

Nystatin Side Effects: Common, Severe, Long Term - Drugs.com Available at:

<https://www.drugs.com/sfx/nystatin-side-effects.html> [Accessed September 15, 2021].

Oliveira, J. T. A., Souza, P. F. N., Vasconcelos, I. M., Dias, L. P., Martins, T. F., Van Tilburg, M. F., et al. (2019). Mo-CBP3-PepI, Mo-CBP3-PepII, and Mo-CBP3-PepIII are synthetic antimicrobial peptides active against human pathogens by stimulating ROS generation and increasing plasma membrane permeability. *Biochimie* 157, 10–21. doi:10.1016/j.biochi.2018.10.016.

Orozco, A. S., Higginbotham, L. M., Hitchcock, C. A., Parkinson, T., Falconer, D., Ibrahim, A. S., et al. (1998). Mechanism of Fluconazole Resistance in *Candida krusei*. *Antimicrob. Agents Chemother.* 42, 2645. Available at: </pmc/articles/PMC105912/> [Accessed September 11, 2021].

Park, S. C., Kim, Y. M., Lee, J. K., Kim, N. H., Kim, E. J., Heo, H., et al. (2017). Targeting and synergistic action of an antifungal peptide in an antibiotic drug-delivery system. *J. Control. Release* 256, 46–55. doi:10.1016/j.jconrel.2017.04.023.

Paulone, S., Ardizzoni, A., Tavanti, A., Piccinelli, S., Rizzato, C., Lupetti, A., et al. (2017). The synthetic killer peptide KP impairs *Candida albicans* biofilm in vitro. *PLoS One* 12, e0181278. doi:10.1371/JOURNAL.PONE.0181278.

- Pennington, M. W., Zell, B., and Bai, C. J. (2021). Commercial manufacturing of current good manufacturing practice peptides spanning the gamut from neoantigen to commercial large-scale products. *Med. Drug Discov.* 9, 100071. doi:10.1016/j.medidd.2020.100071.
- Pristov, K. E., and Ghannoum, M. A. (2019). Resistance of *Candida* to azoles and echinocandins worldwide. *Clin. Microbiol. Infect.* 25, 792–798. doi:10.1016/J.CMI.2019.03.028.
- Roschetto, E., Contursi, P., Vollaro, A., Fusco, S., Notomista, E., and Catania, M. R. (2018). Antifungal and anti-biofilm activity of the first cryptic antimicrobial peptide from an archaeal protein against *Candida* spp. clinical isolates. *Sci. Reports* 2018 81 8, 1–11. doi:10.1038/s41598-018-35530-0.
- S, A., L, M., S, S., M, G., and M, C. (2016). Candidemia and invasive candidiasis in adults: A narrative review. *Eur. J. Intern. Med.* 34, 21–28. doi:10.1016/J.EJIM.2016.06.029.
- S, N., R, M., M, V., K, K., H, M., and H, M. (2019). Fungal vaccines, mechanism of actions and immunology: A comprehensive review. *Biomed. Pharmacother.* 109, 333–344. doi:10.1016/J.BIOPHA.2018.10.075.
- Souza, P. F. N., Lima, P. G., Freitas, C. D. T., Sousa, D. O. B., Neto, N. A. S., Dias, L. P., et al. (2020a). Antidermatophytic activity of synthetic peptides: Action mechanisms and clinical application as adjuvants to enhance the activity and decrease the toxicity of Griseofulvin. *Mycoses* 63, 979–992. doi:10.1111/myc.13138.
- Souza, P. F. N., Marques, L. S. M., Oliveira, J. T. A., Lima, P. G., Dias, L. P., Neto, N. A. S., et al. (2020b). Synthetic antimicrobial peptides: From choice of the best sequences to action mechanisms. *Biochimie* 175, 132–145. doi:10.1016/j.biochi.2020.05.016.

Staniszewska, M., Bondaryk, M., Swoboda-Kopec, E., Siennicka, K., Sygitowicz, G., and

Kurzatkowski, W. (2013). *Candida albicans* morphologies revealed by scanning electron microscopy analysis. *Brazilian J. Microbiol.* 44, 813–821. doi:10.1590/S1517-83822013005000056.

T, S., T, K., K, Y., E, Y., N, F., M, K., et al. (2019). Antifungal susceptibility trend and analysis of resistance mechanism for *Candida* species isolated from bloodstream at a Japanese university hospital. *J. Infect. Chemother.* 25, 34–40. doi:10.1016/J.JIAC.2018.10.007.

TTH, D., P, T., P, P., P, P., L, B., W, S., et al. (2021). Interaction Between Dendritic Cells and *Candida krusei*  $\beta$ -Glucan Partially Depends on Dectin-1 and It Promotes High IL-10 Production by T Cells. *Front. Cell. Infect. Microbiol.* 10. doi:10.3389/FCIMB.2020.566661.

## Figure Legends

**Figure 1. Antibiofilm activity and synergistic effect with Nystatin and Itraconazole of synthetic peptides PepGAT and PepKAA.** (A and B) Inhibition of biofilm formation, respectively, of *C. krusei* and *C. albicans*. (B) Biofilm degradation of *C. krusei*. All peptides were used at 50  $\mu\text{g mL}^{-1}$ . Nystatin and Itraconazole at 1000  $\mu\text{g mL}^{-1}$ . DMSO-NaCl as a negative control. The letters represent the mean  $\pm$  standard deviation of three replicates. \*Different lowercase letters indicate statically significant differences compared to DMSO by analysis of variance ( $p < 0.05$ ).

**Figure 2. Fluorescence images showing membrane pore formation and ROS overproduction as a mechanism of action to inhibit biofilm formation of *C. krusei*.** Control solution of DMSO-NaCl, treated with ITR alone at 1000  $\mu\text{g mL}^{-1}$ , PepGAT and PepKAA both alone at 50  $\mu\text{g mL}^{-1}$ , and synergistic activity of PepGAT and PepKAA with Itraconazole. The propidium iodide uptake assay measured the membrane pore formation and ROS overproduction using 2', 7' dichlorofluorescein diacetate (DCFH-DA). Bars: 100  $\mu\text{m}$ .

**Figure 3. Fluorescence images showing membrane pore formation and ROS overproduction as mechanisms of action to inhibit biofilm formation of *C. albicans*.** Control solution of DMSO-NaCl, treated with ITR alone at 1000  $\mu\text{g mL}^{-1}$ , PepGAT and PepKAA both alone at 50  $\mu\text{g mL}^{-1}$ , and synergistic activity of PepGAT and PepKAA with ITR. The propidium iodide uptake assay

measured the membrane pore formation and ROS overproduction using 2', 7' dichlorofluorescein diacetate (DCFH-DA). Bars: 100  $\mu\text{m}$ .

**Figure 4. Fluorescence images showing membrane pore formation and ROS overproduction as mechanisms of action to inhibit biofilm formation of *C. albicans*.** Control solution of DMSO-NaCl, treated with NYS alone at 1000  $\mu\text{g mL}^{-1}$ , PepGAT and PepKAA both alone at 50  $\mu\text{g mL}^{-1}$ , and synergistic activity of PepGAT and PepKAA with NYS. The propidium iodide uptake assay measured the membrane pore formation and ROS overproduction using 2', 7' dichlorofluorescein diacetate (DCFH-DA). Bars: 100  $\mu\text{m}$ .

**Figure 5. Fluorescence images showing membrane pore formation and ROS overproduction as mechanisms of action to degrade biofilm formation of *C. krusei*.** Control solution of DMSO-NaCl, treated with ITR alone at 1000  $\mu\text{g mL}^{-1}$ , PepGAT and PepKAA both alone at 50  $\mu\text{g mL}^{-1}$ , and synergistic activity of PepGAT and PepKAA with ITR. The propidium iodide uptake assay measured the membrane pore formation and ROS overproduction using 2', 7' dichlorofluorescein diacetate (DCFH-DA). Bars: 100  $\mu\text{m}$ .

**Figure 6. SEM images showing alterations in the biofilm of *C. krusei* cells after incubation with synthetic peptides, antifungal drugs, and combination by them.** The surface of biofilm control (DMSO-NaCl panel) cells is covered by well-defined and organized structures. Biofilm cells exposed to ITR show few alterations in the cell surface. PepGAT and PepKAA-treated cells, showing some alterations in cell structure, such as scars, buds scars, and distortion in the shape of the cells. Biofilm cells were incubated with PepGAT and PepKAA in contact with Itraconazole, resulting in strong alterations in the cell membrane, scars, bud scars, and deformation of the cells.

**Figure 7. SEM images showing alterations in the biofilm of *C. albicans* cells after incubation with synthetic peptides, antifungal drugs, and combination by them.** The surface of biofilm control (DMSO-NaCl panel) cells is covered by well-defined structures. No relevant changes were seen in the biofilm exposed to ITR and NYS. PepGAT and PepKAA-treated biofilm, showing alterations in the cell membrane, scars, bud scars, and distortion in the biofilm structure. Biofilm exposed to combinations made by PepGAT and PepKAA in a synergistic action with ITR, showing strong alterations in the shape of cells and buds scars. Biofilm incubated with PepGAT and PepKAA in contact with NYS, what is seen is no biofilm anymore, are only the remaining dead cells.

**Figure 8. SEM images show alterations in the preformed biofilm of *C. krusei* cells after incubation with synthetic peptides, antifungal drugs, and combination.** The surface of biofilm

control (DMSO-NaCl solution) is well-defined and organized. Biofilm exposed to ITR, showing few alterations in the cell surface. PepGAT and PepKAA-treated biofilm, showing alterations in cell structure, such as scars, bud scars, and distortion in the shape of the cells. Biofilm incubated with a combination of PepGAT or PepKAA and ITR, resulting in strong alterations in the cell membrane, scars, bud scars, deformation of the cells structures, and leakage of internal content.

**Supplementary Figure 1. Antibiofilm activity and synergistic effect with Nystatin and Itraconazole of synthetic peptides PepGAT and PepKAA. (A and B)** Inhibition of biofilm formation, respectively, of *C. parapsilosis* and *C. tropicalis*. **(C and D)** Biofilm degradation of *C. parapsilosis* and *C. tropicalis*. All peptides were used at 50  $\mu\text{g mL}^{-1}$ . Nystatin and Itraconazole at 1000  $\mu\text{g mL}^{-1}$ . DMSO-NaCl as a negative control. The letters represent the mean  $\pm$  standard deviation of three replicates. \*Different lowercase letters indicate statically significant differences compared to DMSO by analysis of variance ( $p < 0.05$ ).

## Figures

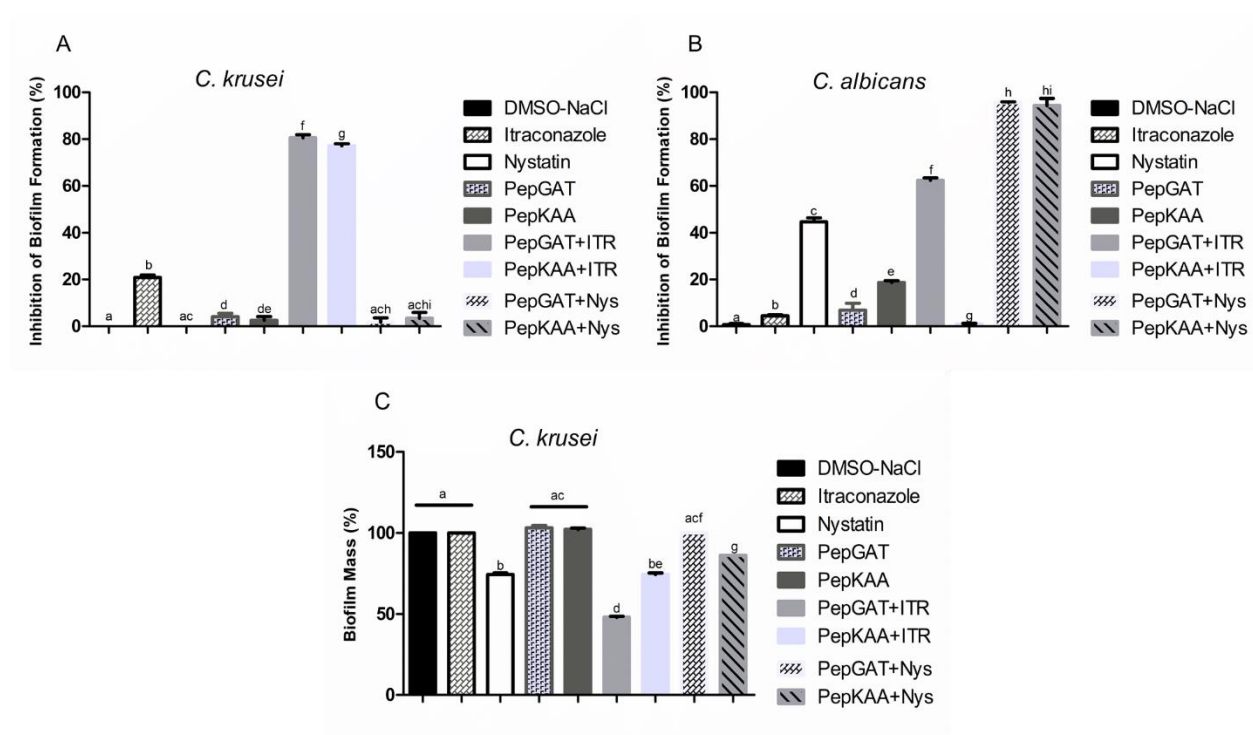


Fig. 1



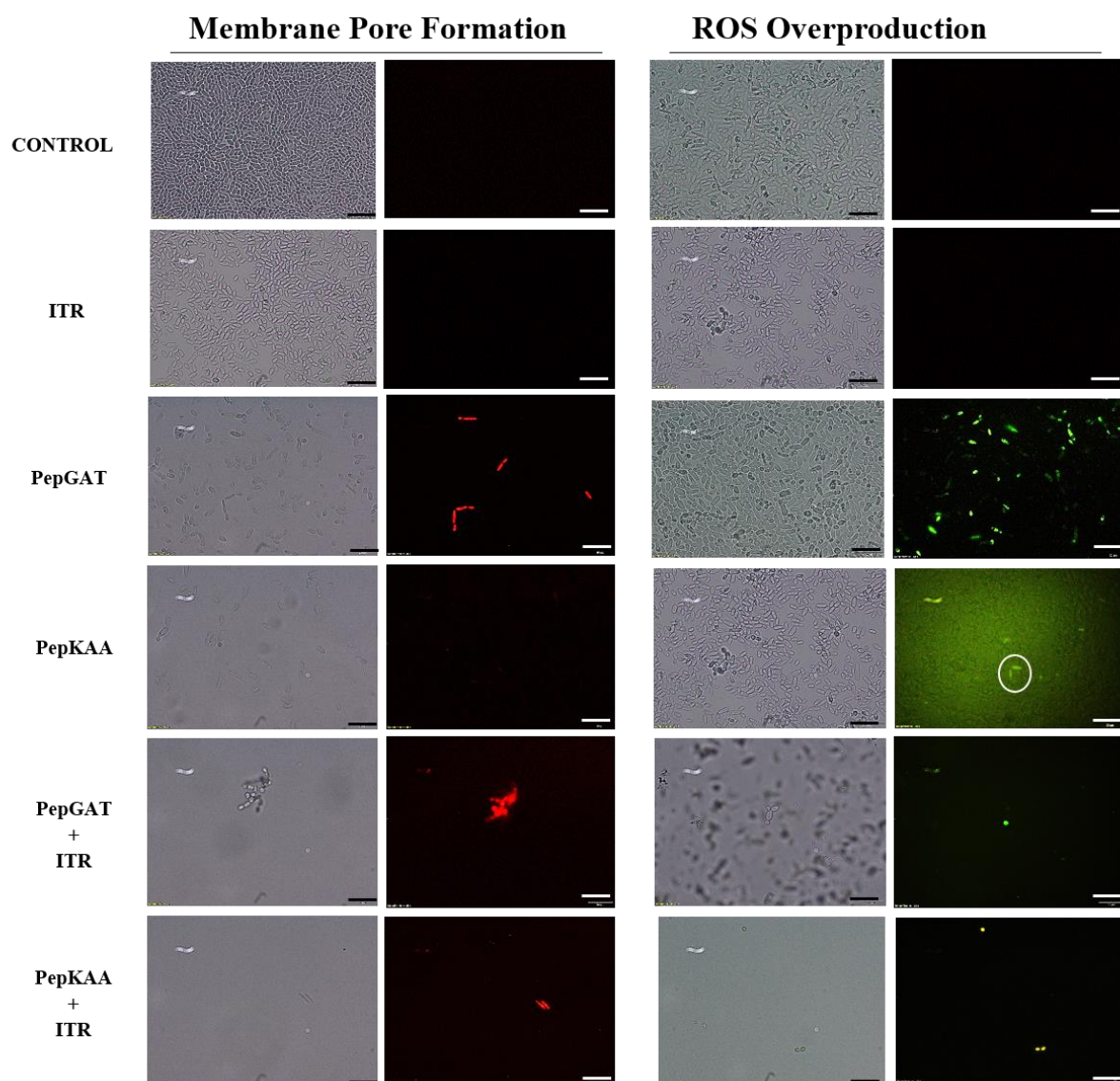


Fig. 2

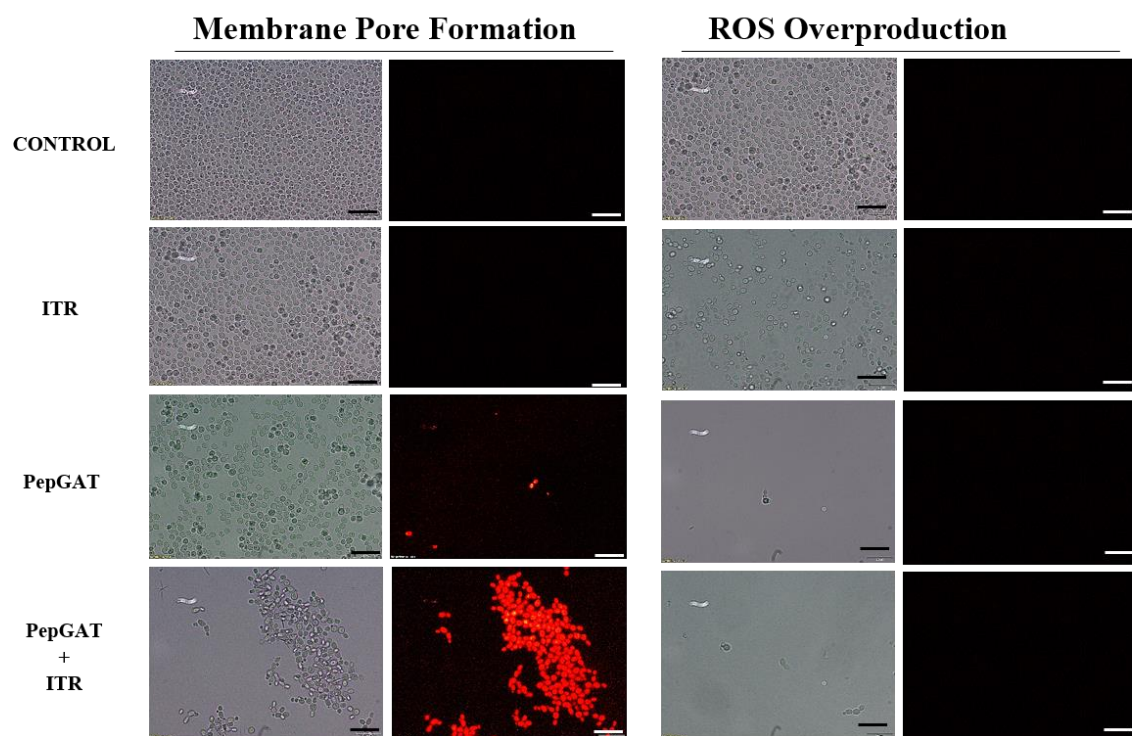


Fig. 3

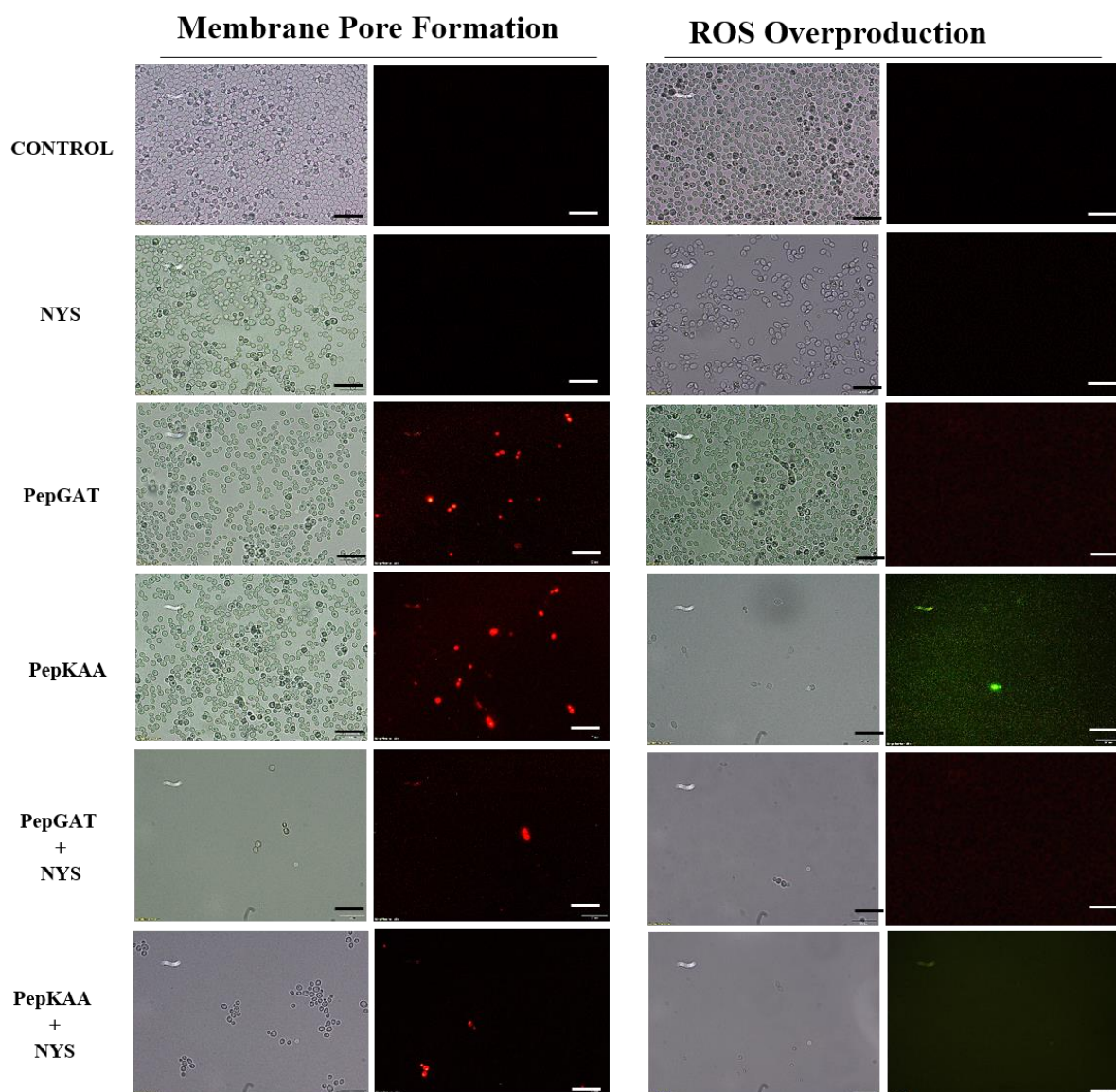


Fig. 4



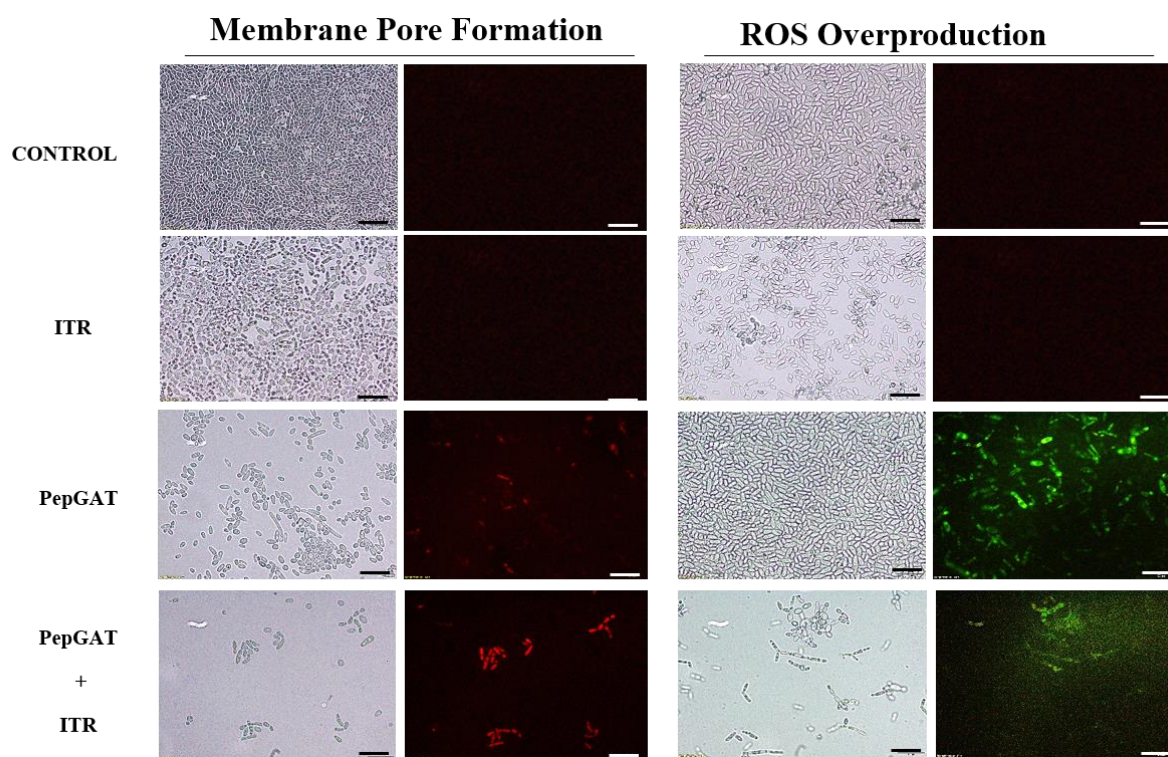


Fig. 5



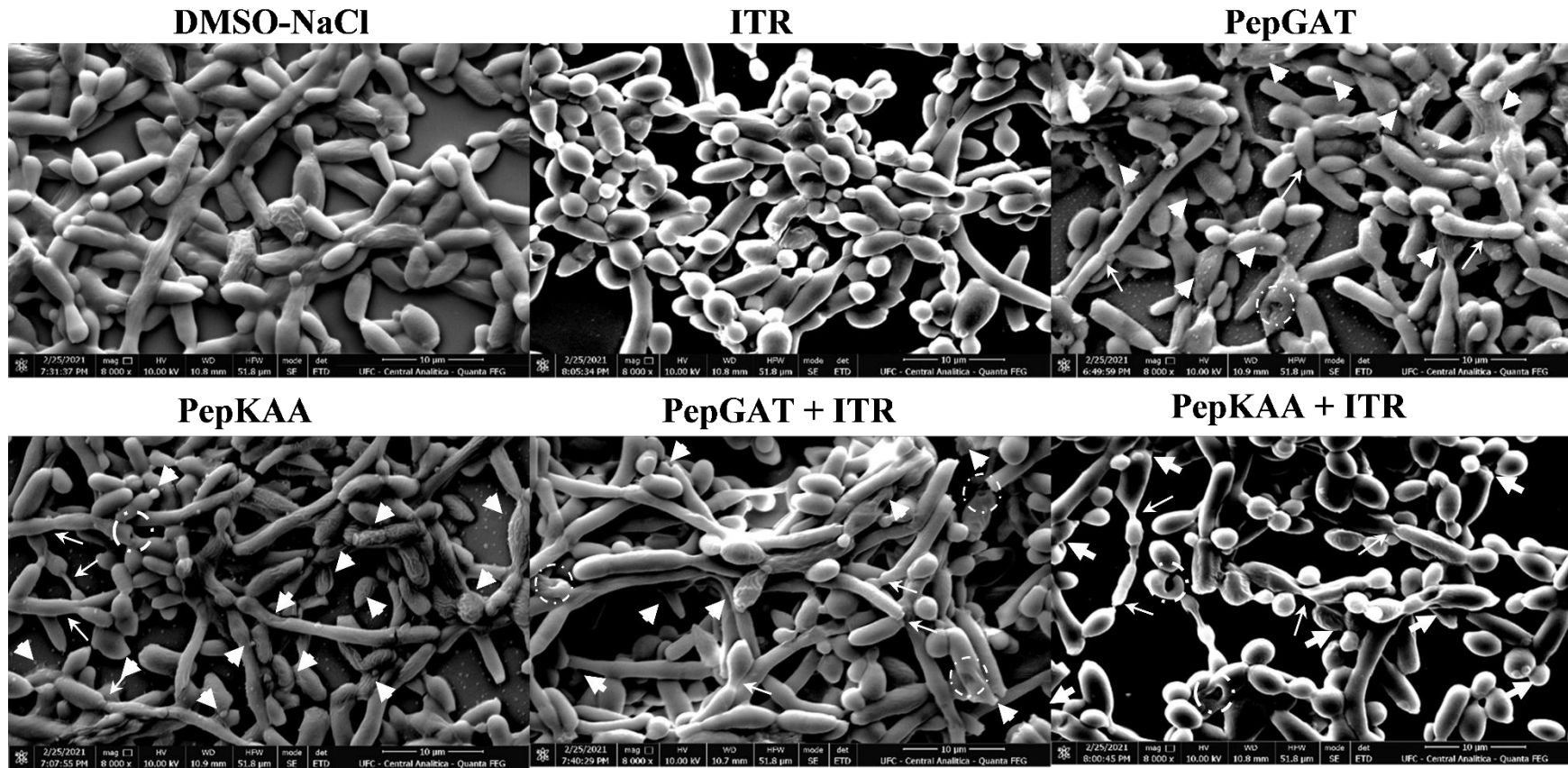


Fig. 6

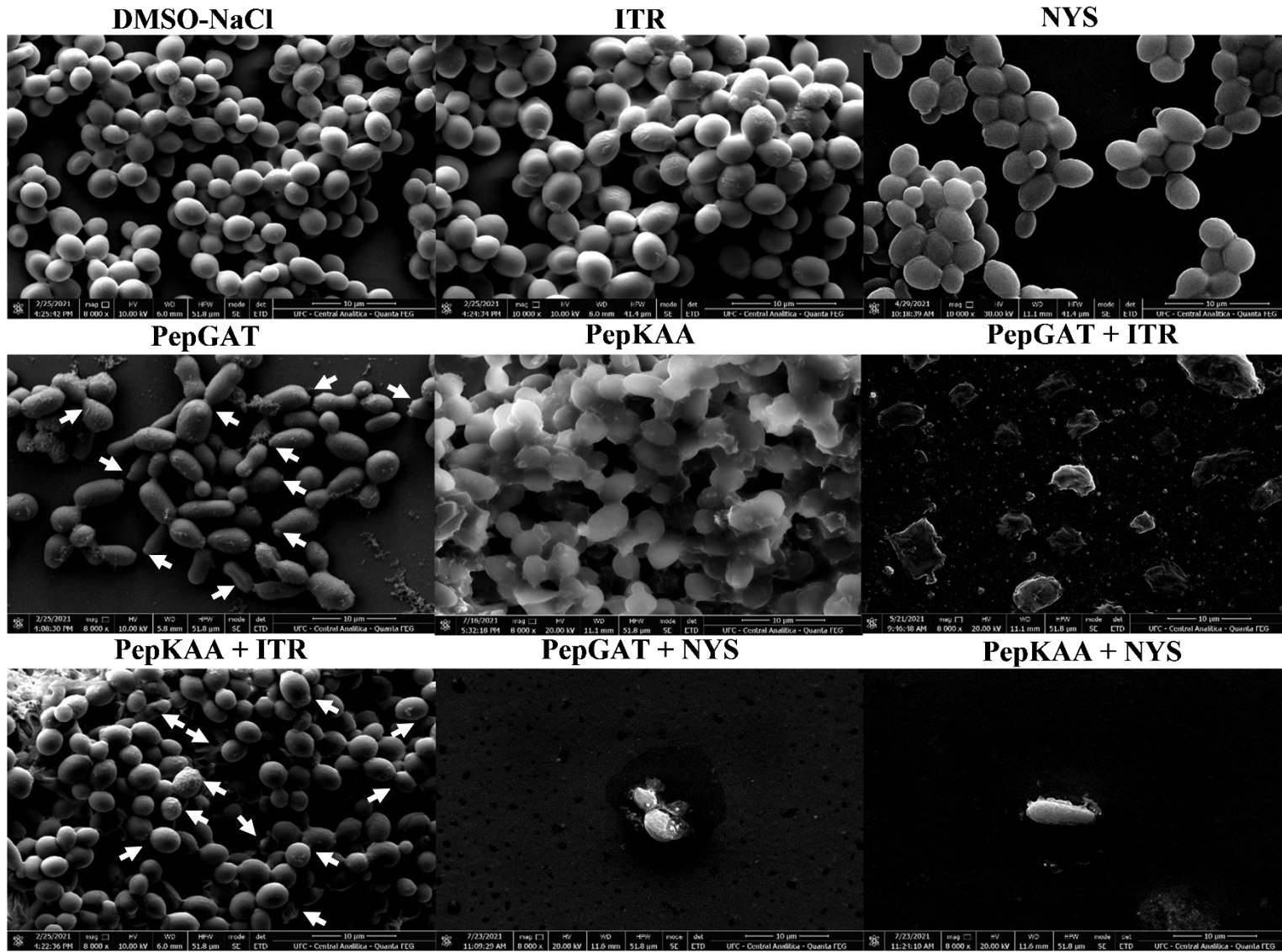


Fig. 7

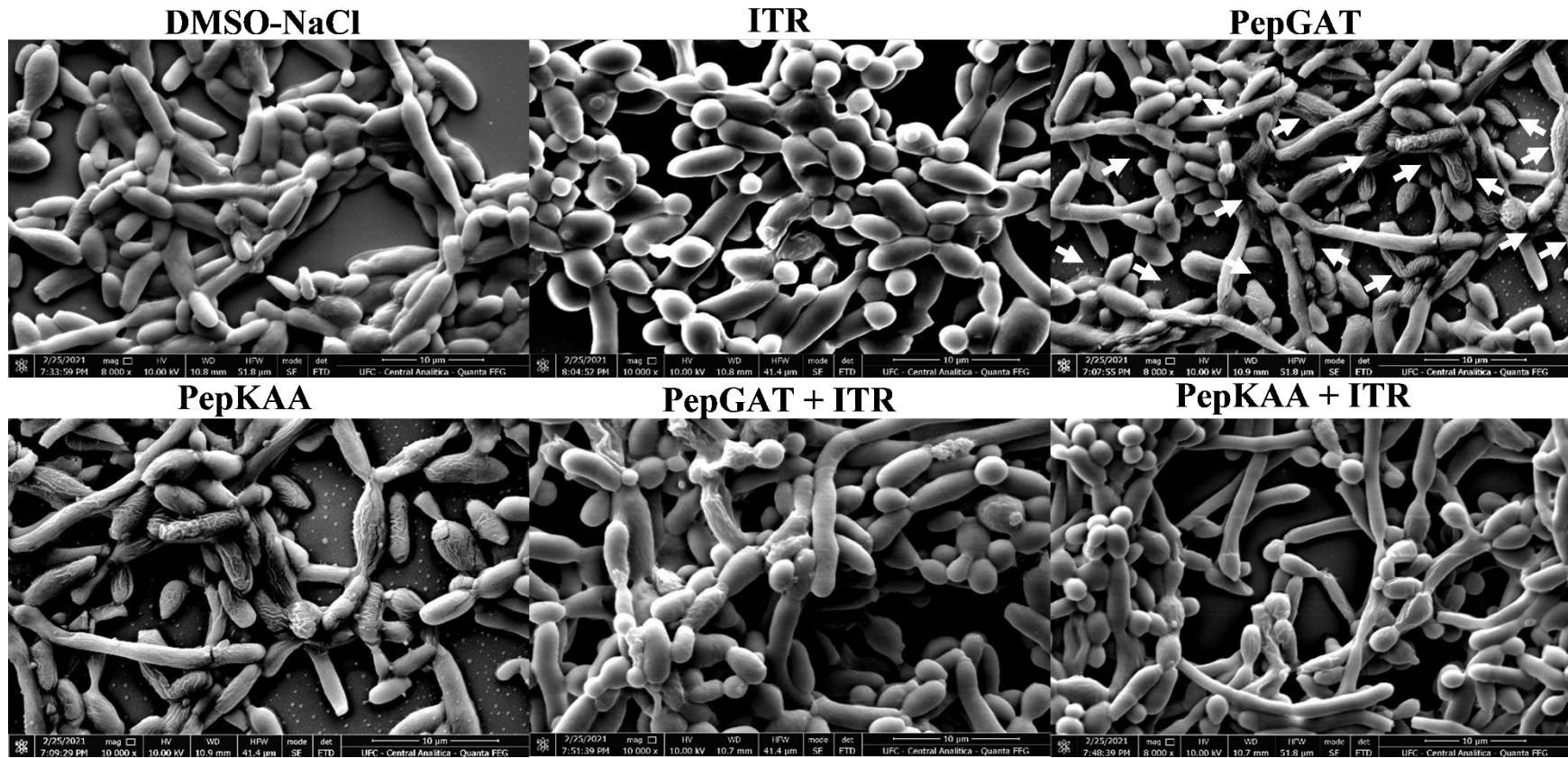
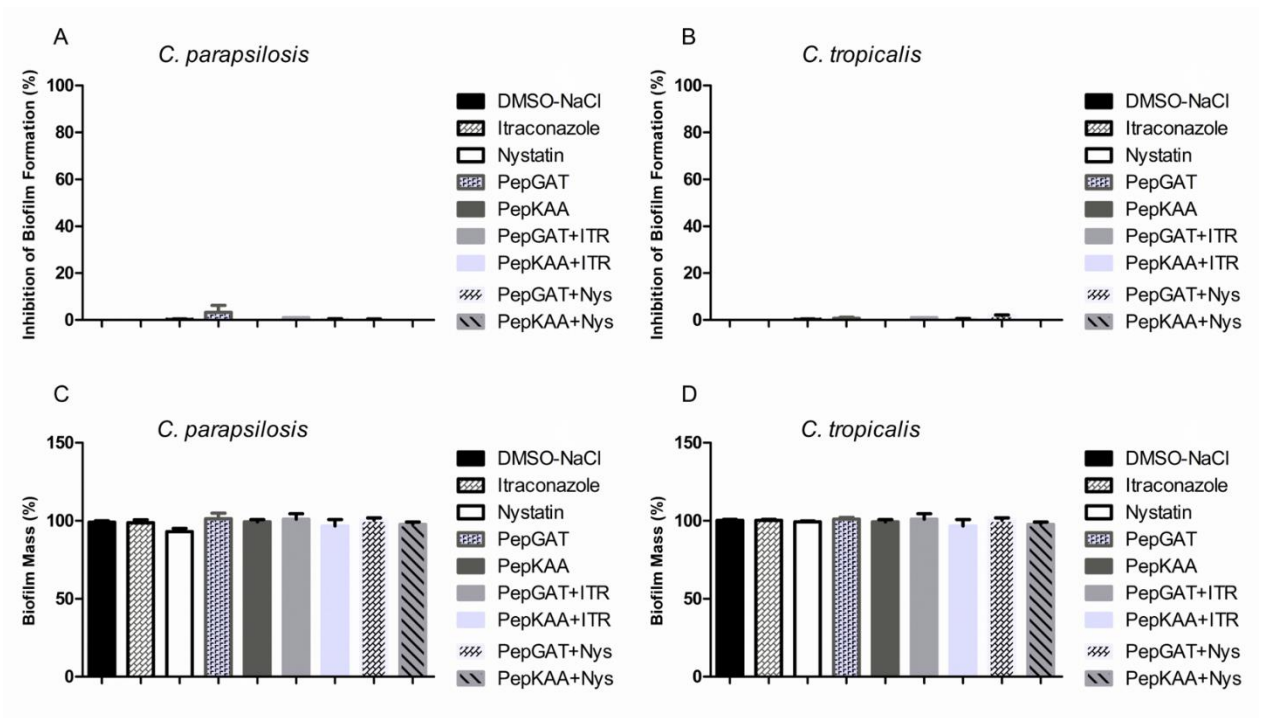


Fig. 8



**Table 1.** Hemolytic activity of synthetic peptides, antifungal drugs, and their combination toward human red blood cells

Peptides/Combinations	% Hemolysis		
	Type-A Blood	Type-B Blood	Type-O Blood
0.1% Triton X-100	100	100	100
DMSO-NaCl Solution	0	0	0
NYS (1000 $\mu\text{g mL}^{-1}$ )	100	100	100
ITR (1000 $\mu\text{g mL}^{-1}$ )	80	75	69
PepGAT (50 $\mu\text{g mL}^{-1}$ )	0	0	0
PepKAA (50 $\mu\text{g mL}^{-1}$ )	0	0	0
PepGAT (50 $\mu\text{g mL}^{-1}$ ) + NYS (1000 $\mu\text{g mL}^{-1}$ )	54	43	12
PepGAT (50 $\mu\text{g mL}^{-1}$ ) + ITR (1000 $\mu\text{g mL}^{-1}$ )	17	45	43
PepKAA (50 $\mu\text{g mL}^{-1}$ ) + NYS (1000 $\mu\text{g mL}^{-1}$ )	15	10	21
PepKAA (50 $\mu\text{g mL}^{-1}$ ) + ITR (1000 $\mu\text{g mL}^{-1}$ )	21	34	12



Supl. Fig. 1

### **CAPÍTULO III – Artigo científico 2**

As sessões Metodologia, Resultados e Discussão serão apresentadas na forma de um artigo científico submetido em uma revista científica internacional. Sucintamente, os resultados mostram que os peptídeos sintéticos Mo-CBP3-PepI e Mo-CBP3-PepIII apresentaram atividade contra biofilmes formados por espécies de *C. albicans* e *C. parapsilosis*, levando à formação de poros na membrana e superprodução de espécies reativas de oxigênio, inibindo a formação de novos biofilmes e inviabilizando as estruturas pré-formadas.

#### **Artigo científico 2**

Artigo científico submetido à revista *Biofouling* fator de impacto 3.2 (Qualis A1) status *under review*.

## Artigo científico 2

### **Synergistic antifungal activity of synthetic peptides and antifungal drugs against *Candida ssp* biofilms**

Leandro P. Bezerra<sup>1</sup>, Cleverson D.T. Freitas<sup>1</sup>, \*, Ayrles F.B. Silva<sup>2</sup>, Jackson L. Amaral<sup>1</sup>,  
Nilton A.S. Neto<sup>1</sup>, Rafael G. G. Silva<sup>3</sup>, Aura L.C. Parra<sup>1</sup>, Gustavo H. Goldman<sup>4</sup>, Jose T.  
A. Oliveira<sup>1</sup>, Pedro F. N. Souza<sup>1,\*</sup>

<sup>1</sup>*Department of Biochemistry and Molecular Biology, Federal University of Ceará, Fortaleza, Ceará 60451, Brazil.*

<sup>2</sup>*Department of Physics, Federal University of Ceará, Fortaleza, Ceará 60451, Brazil.*

<sup>3</sup>*Department of Biology, Federal University of Ceará, Fortaleza, Ceará 60451, Brazil*

<sup>4</sup>*Faculty of Pharmaceutical Sciences of Ribeirão Preto, University of São Paulo, Brazil*

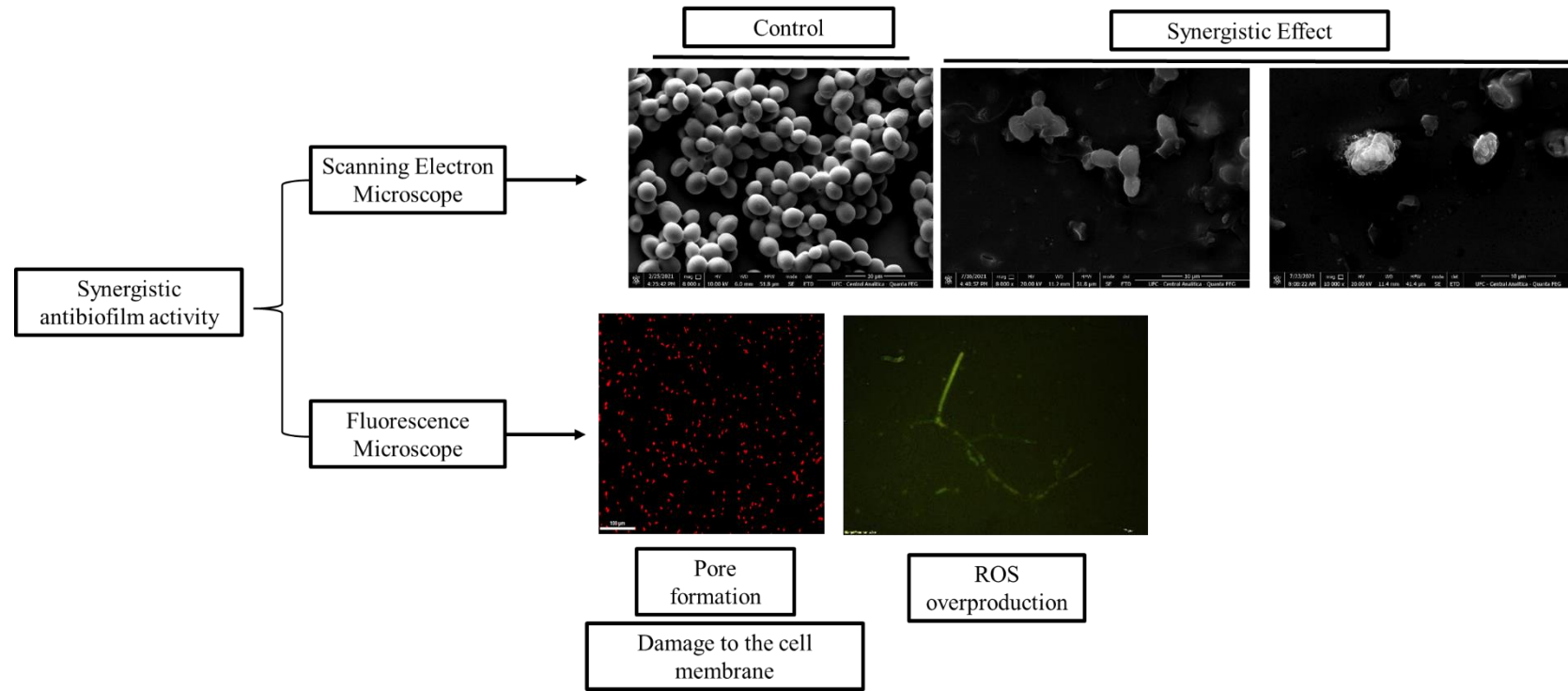
#### **Corresponding Author**

\*Corresponding authors: Biochemistry and Molecular Biology Department, Federal University of Ceará, CE, Brazil. Laboratory of Plant Defense Proteins, Av. Mister Hull, Caixa Postal 60451 Fortaleza, CE, Brazil. Tel: +55 85 33669823; Fax: +55 85 33669789.

E-mail: [cleversondiniz@hotmail.com](mailto:cleversondiniz@hotmail.com) and [pedrofilhobio@gmail.com](mailto:pedrofilhobio@gmail.com)

ORCID: **0000-0002-2203-1575** (C. D. T. Freitas) and **0000-0003-2524-4434** (P. F. N. Souza)

Graphical Abstract



## 1 **Abstract**

2 Biofilm-forming *Candida albicans* and *C. parapsilosis* are responsible for bloodstream  
3 infections leading individuals to death. Synthetic antimicrobial peptides (SAMPs) are  
4 considered new weapons to combat infections alone or conjugated with drugs. Here, two  
5 SAMPs named *Mo*-CBP<sub>3</sub>-PepI and *Mo*-CBP<sub>3</sub>-PepIII were tested alone or combined with  
6 Nystatin (NYS) and Itraconazole (ITR) against *C. albicans* and *C. parapsilosis* biofilms.  
7 Furthermore, the mechanism of antibiofilm activity was evaluated by fluorescence and  
8 scanning electron microscopies. When combined with peptides, the results revealed an  
9 improvement of 2 up to 4-fold in NYS and ITR antibiofilm activity. Microscopic analyses  
10 showed cell wall degradation, ROS overproduction, and membrane pore formation  
11 causing leakage of internal content and leading biofilm cells to death. Taken together,  
12 these results suggest the potential of *Mo*-CBP<sub>3</sub>-PepI and *Mo*-CBP<sub>3</sub>-PepIII as new drugs  
13 and adjuvants to increase the activity of conventional drugs for the treatment of clinical  
14 infections caused by *C. albicans* and *C. parapsilosis*.

15 **Keywords:** Antibiofilm activity; Candidiasis; Synergism; Synthetic peptides; Antifungal  
16 drugs;

## 17 **Introduction**

18           Candida species are the primary fungus responsible for up to 15% of hospital-  
19 acquired cases of sepsis. Biofilms are established by microbial cells on an inert or living  
20 surface, promoting the development of microcolonies with polymeric matrices,  
21 enhancing the resistance to various antimicrobial agents (Kumar et al. 2017; Lima et al.  
22 2021). A mature biofilm formed by *Candida spp.* is coated by an extracellular matrix  
23 composed of glycoproteins (55%), carbohydrates (25%), lipids (15%), and nucleic acids  
24 (5%) that protect the microbial cells (Zarnowski et al. 2014). The National Institutes of  
25 Health (NIH) in the USA considered biofilms a public health problem and estimates  
26 biofilms are responsible for 80% of the difficulties to cure human infections (Fox &  
27 Nobile 2012; Zarnowski et al. 2014; Kumar et al. 2017; Lima et al. 2021). The most  
28 susceptible are immunocompromised patients, AIDS<sup>+</sup> patients, patients under  
29 chemotherapy treatment or immunosuppressive therapies, and patients carrying medical  
30 devices (catheters, pacemakers, and heart valves) (Weig 1998; Kullberg & Oude Lashof  
31 2002).

32           *C. albicans* and *C. parapsilosis* are common opportunistic fungal pathogens  
33 asymptotically colonizing mucosal surfaces and skin of healthy individuals leading to  
34 an infection called candidiasis (Baillie 2000). In addition, *C. albicans* and *C. parapsilosis*  
35 are responsible for bloodstream infections called candidemia in immunocompromised  
36 patients, including those in intensive care units (Sasso et al. 2017). Currently, the  
37 treatment of *C. albicans* and *C. parapsilosis* infections involves applying antifungals  
38 agents that can interrupt different metabolic pathways of the cell. However, many studies  
39 have reported *Candida* resistance to these antifungal molecules (Ramage 2002; LaFleur  
40 et al. 2006; Arendrup & Patterson 2017). A study developed by Katiyar and collaborators  
41 (Katiyar et al. 2006) reported clinical isolates of *Candida sp* to carry genes conferring

42 resistance to all antifungal agents making those drugs useless (Katiyar et al. 2006). To  
43 overcome this situation, synthetic antimicrobial peptides (SAMPs) could be an alternative  
44 either alone or combined with antifungal drugs to control *Candida* infection and fight  
45 these pathogens' resistance (Lima et al. 2021). SAMPs have some important antimicrobial  
46 characteristics found in natural antimicrobial peptides, such as positive net charge,  $\alpha$ -helix  
47 structure, low molecular weight (600-1200 Da), high hydrophobic ratio (40 – 60%), and  
48 amphipathicity (Pedro F.N. Souza et al. 2020; Lima et al. 2021).

49         Recently, our research group designed, characterized, and evaluated the  
50 antimicrobial activity of three synthetic peptides *Mo*-CBP3-PepI (CPIAQRCC, positive  
51 charge of +1 and hydrophobic ratio of 66%), *Mo*-CBP3-PepII (NIQPPCRCC, positive  
52 charge of +1, and hydrophobic ratio of 44%), and *Mo*-CBP3-PepIII (AIQRCC, positive  
53 charge of +1, and hydrophobic ratio of 44%). These peptides were designed based on the  
54 structure of *Mo*-CBP<sub>3</sub>, a chitin-binding protein purified from *Moringa oleifera* seeds  
55 (Oliveira et al. 2019; Lima et al. 2020). The anticandidal activity and mechanism of action  
56 of these peptides were evaluated by Oliveira et al. (2019) and Lima et al. (2020).

57         Here, we advanced these studies by investigating the antifungal effects of *Mo*-  
58 CBP<sub>3</sub>-PepI, and *Mo*-CBP<sub>3</sub>-PepIII tested alone or combined with Nystatin (NYS) and  
59 Itraconazole (ITR) against *C. albicans* and *C. parapsilosis* biofilms. We demonstrated the  
60 potential of *Mo*-CBP<sub>3</sub>-PepI and *Mo*-CBP<sub>3</sub>-PepIII as new drugs and adjuvants to increase  
61 the activity of conventional drugs for the treatment of *C. albicans* and *C. parapsilosis*  
62 biofilm formation. At the same time, it reduces drugs' toxicity to human erythrocytes.



## 63 **Materials and methods**

### 64 **Ethics Statement**

65 Not applied for this study.

### 66 **Biological materials**

67 *C. albicans* (ATCC 10231) and *C. parapsilosis* (ATCC 22019) were obtained from the  
68 Laboratory of Plant Toxins at the Department of Biochemistry and Molecular Biology at  
69 the Federal University of Ceará. All other chemicals were purchased from Sigma-Aldrich  
70 Co. (St. Louis, USA).

### 71 **Peptide synthesis**

72 The Synthetic peptides *Mo*-CBP3-PepI, *Mo*-CBP3-PepII, and *Mo*-CBP3-PepIII  
73 (Oliveira et al. 2019; Lima et al. 2020) were chemically synthesized by GenOne, which  
74 had their quality and purity ( $\geq 95\%$ ) analyzed by Reverse-Phase High-Performance Liquid  
75 Chromatography (RP-HPLC) and mass spectrometry.

### 76 **Biological activity**

#### 77 *Antibiofilm assay*

78 The antibiofilm assays against *C. albicans* and *C. parapsilosis* were performed  
79 following the methodology described by Dias et al. (Dias et al. 2020), with some  
80 modifications. To evaluate the inhibition of the biofilm formation, 100  $\mu\text{L}$  of *C. albicans*  
81 and *C. parapsilosis* suspension ( $2.5 \times 10^3$  CFU/mL) in Sabouraud broth were incubated  
82 in a flat bottom of 96-well plate with 100  $\mu\text{L}$  of *Mo*-CBP3-PepI, *Mo*-CBP3-PepII, *Mo*-  
83 CBP3-PepIII ( $50 \mu\text{g. mL}^{-1}$ ), at 37 °C for 48 hours. The supernatant was removed to  
84 quantify the biofilm formed, and wells were washed three times with sterile 0.15 M NaCl  
85 solution. Next, the cells were fixed with 100  $\mu\text{L}$  of methanol for 15 min at 37 °C and  
86 plates were air-dried under the same conditions. Then, 200  $\mu\text{L}$  of an aqueous solution of

87 0.1% of crystal violet was added and incubated for 30 min at room temperature ( $\pm 22$  °C).  
88 To remove the excess stain, the plates were washed three times with distilled water and  
89 finally added 100  $\mu$ L of 33% of acetic acid to solubilize the dye bound in the biofilm.  
90 After 15 min, the absorbance was measured at 600 nm using an automated microplate  
91 reader (Epoch, Biotek).

92 To perform the degradation of preformed biofilm assay, in a flat-bottom 96-well  
93 plate, 100  $\mu$ L of the cell suspensions of both yeasts were incubated at 37 °C for 24 hours.  
94 Then, the supernatant was removed, and 100  $\mu$ L of the Sabouraud broth media and 100  
95  $\mu$ L of each peptide were added and incubated again for 24 hours. The culture medium  
96 was again discarded, and the same procedure described above was used to quantify the  
97 biofilm mass after incubation with each peptide. In both experiments, DMSO-NaCl was  
98 used as a negative control. NYS (1000  $\mu$ g mL<sup>-1</sup>) and ITR (1000  $\mu$ g mL<sup>-1</sup>) as a positive  
99 control.

100 The synergism assays were carried out by combining peptides with either  
101 antifungals NYS or ITR: The combinations were constituted of each peptide (50  $\mu$ g mL<sup>-1</sup>)  
102 + NYS or ITR (1000  $\mu$ g mL<sup>-1</sup>). The control to evaluate the effectiveness of synergism  
103 was the activity presented by peptides or drugs alone. After the formulation of  
104 combinations, the antibiofilm assays for synergism analyses for *Candida* ssp. were the  
105 same as described above.

106

### 107 ***Overproduction of reactive oxygen species (ROS)***

108 To evaluate ROS overproduction, it followed the methodology described by Dias et  
109 al.(Dias et al. 2020) with some modifications. *C. albicans* and *C. parapsilosis* were  
110 incubated with peptides for 24 hours under the same conditions as described above  
111 (Inhibition of the biofilm formation and degradation of preformed biofilm assays). Then,  
112 50  $\mu$ L of cell suspension ( $2.5 \times 10^3$  CFU/mL in contact with 50  $\mu$ L of each peptide placed

113 in a coverslip with its respective positive and negative controls. Next, the formed biofilm  
114 in the coverslip was washed with 0.15 M NaCl three times to remove the Sabouraud  
115 media. Thus, 20  $\mu$ L of 2',7' dichlorofluorescein diacetate (DCFH-DA) were added and  
116 incubated in the dark for 30 min at room temperature ( $\pm 22$  °C). The coverslips were  
117 rewashed with 0.15 M NaCl to remove the excess stain and observed under a fluorescence  
118 microscope (Olympus System BX 41, at Plant Cell Biology Lab) with an excitation  
119 wavelength of 488 nm and emission wavelength of 525 nm.

### 120 *Cell membrane integrity assay*

121 *C. albicans* and *C. parapsilosis*, the experiment to evaluate pore formation, were  
122 done as described by Dias et al.(Dias et al. 2020) with modifications. The biofilms were  
123 treated as the same described for ROS overproduction analysis. Thus, 20  $\mu$ L of Propidium  
124 Iodide (PI) was added to the coverslip and incubated in a dark place for 30 min at room  
125 temperature ( $\pm 22$  °C). Then, the samples were washed three times with 0.15 M of NaCl  
126 to remove the excess of PI and observed in a fluorescence microscope (Olympus System  
127 BX 41, at Plant Cell Biology Lab) with an excitation wavelength of 548 nm and emission  
128 wavelength of 650 nm.

129

### 130 *Scanning electron microscopy (SEM) analysis*

131 The morphological changes in the cells of *C. albicans* and *C. parapsilosis* were  
132 evaluated by SEM, using the method described by Staniszewska et al.(Staniszewska et al.  
133 2013). Biofilms were fixed with 1% (v/v) glutaraldehyde in 0.15 M of sodium phosphate  
134 buffer at pH 7.0 for 16 hours. Then, the coverslips were washed with 0.15 M sodium  
135 phosphate buffer pH 7.0 three times. Next, 0.2% (v/v) osmium tetroxide was added to the  
136 samples and incubated for 30 min at 37 °C and washed again under the same conditions  
137 described above. Samples were successively dehydrated with increased ethanol

138 concentration (30%, 50%, 70% 100% and 100% [v/v]) for 10 minutes each at room  
139 temperature. At last, the final dehydration was realized with 50% hexamethyldisilane  
140 (HMDS) diluted in ethanol for 10 min and then 100% HDMS. The coverslips were placed  
141 on stubs and coated with a 20 nm gold layer using positron-emission tomography (PET)  
142 coating machine (Emitech-Q150TES, Quorum Technologies, England). The images were  
143 obtained with an FEI inspect<sup>TM</sup>50 scanning electron microscopy, equipped with a low  
144 energy detector (Everhart-Thornley), and the acceleration used was 20.000 kV and  
145 20.000x detector magnification.

146

### 147 **Obtaining, files preparation, and Molecular Docking**

148 The *Mo*-CBP<sub>3</sub>-PepI and *Mo*-CBP<sub>3</sub>-PepIII three-dimensional (3D) structures were  
149 predicted using the PepFold server 3 (Lamiabile et al. 2016). The amino acid protonation  
150 of the peptides was adjusted to pH 7.4 in ProteinPrepare (Martínez-Rosell et al. 2017).  
151 NYS (accession number CID 16219709) and ITR (accession number CID 55283) 3D  
152 structures were obtained from the database PubChem (Kim et al. 2019). The protonation  
153 of the ligands was adjusted using the software Marvin Sketch version 15.6.15. The energy  
154 minimization of the peptide hydrogens and the ligand was conducted in Discovery Studio  
155 v. 20.1 and Open Babel version 2.4.0.

156 Molecular docking assays were carried out in Autodock Vina, version 1.1.2 (Trott  
157 & Olson 2009). Additionally, the Autodock graphical interface version 1.5.6 was used to  
158 maintain polar hydrogens and provide charges to peptides and drugs using the Kollman  
159 united charges (Morris et al. 2009). The *Mo*-CBP<sub>3</sub>-PepI and *Mo*-CBP<sub>3</sub>-PepIII were  
160 considered rigid molecules, and NYS and ITR were docked as flexible molecules. The  
161 grid box was defined as a 24 Å x 24 Å x 24 Å cube with the peptides in the center. The  
162 exhaustiveness was set up to 16, and all other parameters were used as default. The

163 software Discovery Studio v. 20.1 and the 3D interaction representations were realized in  
164 Pymol v. 1.3

## 165 **Hemolytic assay**

166 The hemolytic activity of *Mo*-CBP<sub>3</sub>-PepI, *Mo*-CBP<sub>3</sub>-PepIII, NYS, ITR, and  
167 combination by then was assessed in A, B, and O-types of erythrocytes as described by  
168 Souza et al.(Pedro F.N. Souza et al. 2020). The concentrations of all solutions were the  
169 same as used in synergism assays. The HRBCs from A, B, and O were provided by the  
170 Cear Hematology and Hemotherapy Center (Brazil).

171 The blood was collected in a tube with heparin (5 IU mL<sup>-1</sup>), centrifuged at 300 g  
172 for 5 min at 4 °C, dissolved, washed, and diluted to a concentration of 2.5% in sterile 0.15  
173 M NaCl. Each blood type was incubated (100 µL), with solutions of *Mo*-CBP<sub>3</sub>-PepI, *Mo*-  
174 CBP<sub>3</sub>-PepIII (50 µg mL<sup>-1</sup>), NYS (1000 µg mL<sup>-1</sup>), ITR (1000 µg mL<sup>-1</sup>), the solution made  
175 by peptides and drugs, DMSO-NaCl, and 0.1% (v/v) Triton X-100 (the positive control  
176 for hemolysis) for 30 min at 37 °C, followed by centrifugation (300 g for 5 min at 4 °C),  
177 supernatants were collected and transferred to 96-well microtiter plates. Hemolysis (%)  
178 was calculated by taking absorbance at 414 nm using an automated absorbance microplate  
179 reader. Negative (0%) and positive (100%) hemolysis were determined by treating  
180 HRBCs with 5% DMSO in 0.15 M NaCl (vehicle for peptides) and 0.1% (v/v) Triton X-  
181 100, respectively. The hemolysis was calculated by the equation: [(Abs<sub>414nm</sub> of HRBC  
182 treated with Solution-Abs<sub>414nm</sub> HRBCs treated with 0.15 M NaCl) / [(Abs<sub>414nm</sub> of HRBCs  
183 treated with 0.1% TritonX-100-Abs<sub>414nm</sub> of HRBCs treated with 0.15 M NaCl)] x 100.

184

## 185 **Statistical analysis**

186

187 All the assays were performed individually three times with the statistics  
188 expressed as the mean ± standard error. The data were submitted to ANOVA software  
189 followed by the Tukey test. GraphPad Prism 5.01. was used to perform all graphics, with  
190 a significance of P<0.05.

## 191 **Results**

### 192 **Antibiofilm activity of synthetic peptides and two commercial drugs**

193 The antibiofilm activity of *Mo*-CBP<sub>3</sub>-PepI and *Mo*-CBP<sub>3</sub>-PepIII, both at 50 µg  
194 mL<sup>-1</sup> against *C. albicans* and *C. parapsilosis*, are shown in Figure 1. ITR and NYS alone  
195 inhibited *C. albicans* 7% and 40% biofilm formation, respectively (Fig. 1A). *Mo*-CBP<sub>3</sub>-  
196 PepI alone inhibited 10% of the biofilm formation of *C. albicans*. Regarding the  
197 synergistic effect, *Mo*-CBP<sub>3</sub>-PepI and *Mo*-CBP<sub>3</sub>-PepIII enhanced the ITR biofilm  
198 inhibition formation in *C. albicans* about 3.5- and 4.0-fold, respectively (Fig. 1A).  
199 Combining both peptides with NYS increased the inhibition of *C. albicans* biofilm  
200 formation from 40% (NYS alone) to 90% (Fig. 1).

201 ITR or NYS alone inhibited, respectively, 45 and 43% of *C. parapsilosis* biofilm  
202 formation of (Fig. 1B) while combinations of *Mo*-CBP<sub>3</sub>-PepI + ITR, *Mo*-CBP<sub>3</sub>-PepIII +  
203 ITR, *Mo*-CBP<sub>3</sub>-PepI + NYS, and *Mo*-CBP<sub>3</sub>-PepIII + NYS inhibited 98%, 96%, 79%, and  
204 82%, respectively, *C. parapsilosis* biofilm formation (Fig. 1B). In contrast, *Mo*-CBP<sub>3</sub>-  
205 PepI and *Mo*-CBP<sub>3</sub>-PepIII inhibited 15% and 25%, respectively, *C. parapsilosis* biofilm  
206 formation (Fig. 1B). The combinations of peptides and antifungal drugs showed higher  
207 biofilm inhibition than conventional drugs. This combination was more efficient in  
208 inhibiting biofilm formation in *C. parapsilosis* than in *C. albicans*.

209 Regarding the degradation of preformed *C. albicans* biofilm, ITR and NYS  
210 degraded the biofilm by about 50% and 30%, respectively (Fig. 1C). *Mo*-CBP<sub>3</sub>-PepI and  
211 *Mo*-CBP<sub>3</sub>-PepIII showed a stronger action by degrading 60% and 30% of preformed *C.*  
212 *albicans* biofilm. The combinations *Mo*-CBP<sub>3</sub>-PepI + ITR and *Mo*-CBP<sub>3</sub>-PepIII + ITR  
213 did not present any effect (Fig. 1C). However, the combinations *Mo*-CBP<sub>3</sub>-PepI + NYS  
214 showed 85% degradation of *C. albicans* preformed biofilm while *Mo*-CBP<sub>3</sub>-PepIII + NYS  
215 degraded 50% of *C. albicans* preformed biofilm (Fig. 1C). Regarding the degradation of

216 *C. parapsilosis* preformed biofilm, only the combination *Mo*-CBP<sub>3</sub>-PepI + NYS reduced  
217 50% of the biofilm biomass (Fig. 1D). Any other treatments were effective against the *C.*  
218 *parapsilosis* preformed biofilm (Fig. 1D).

### 219 ***Analysis of Candida biofilm morphology***

220 Scanning Electron Microscopy (SEM) is a powerful tool to assess the damage of  
221 antifungal treatment on *C. albicans* and *C. parapsilosis* biofilm formation (Figs. 2 and 3).  
222 Regarding inhibition of *C. albicans* and *C. parapsilosis* biofilm formation, control cells  
223 did not show any damage or alterations on the cell surface since spherical cellular shape  
224 can be observed without cracks or scars (Figs. 2A and 3A). The treatment with peptides  
225 and drugs alone presented only mild damage such as wrinkles and slight changes on  
226 morphology of cells but nonlethal effects showing a very similar appearance to the control  
227 in the number of cells (Fig. 2B-E).

228 The combination *Mo*-CBP<sub>3</sub>-PepI + ITR and *Mo*-CBP<sub>3</sub>-PepIII + ITR showed a  
229 significant reduction in the biofilm formed compared to control (Fig. 2F and G). In these  
230 treatments, it was possible to see damage such as small blebs, new buds, scars on new  
231 buds and cells, and rings of truncated bud scars (Fig. 2F and G). The *Mo*-CBP<sub>3</sub>-PepI +  
232 NYS and *Mo*-CBP<sub>3</sub>-PepIII + NYS are by far the most lethal to *C. albicans* (Fig. 2F and  
233 G). In those treatments, the cells are entirely damaged with high roughness levels, severe  
234 alterations in morphology, and a clear indication of cellular lysis leading to loss of  
235 cytoplasm.

236 In the inhibition of *C. parapsilosis* biofilm formation, SEM analysis revealed the  
237 treatment with drugs alone (Fig. 3B and C) did not prevent the biofilm formation of *C.*  
238 *parapsilosis*. Although the treatment with peptides alone caused severe damage to cells,  
239 such as cell morphology and lysis alteration, this was not sufficient to inhibit the *C.*  
240 *parapsilosis* biofilm formation (Fig. 3D and E). SEM images revealed that all peptides



241 and drug combinations were lethal to *C. parapsilosis* (Fig. 3F-I). The synergistic effect  
242 led to severe injuries such as distortions and alterations on the cell surface and shape, cell  
243 wall damage, distortion of the cell membrane, and internal content loss, without any  
244 possibility for *C. parapsilosis* to form a biofilm (Fig. 3F-I).

245 SEM analysis revealed *Mo*-CBP<sub>3</sub>-PepI + NYS was the most efficient treatment in  
246 degrading the *C. albicans* and *C. parapsilosis* preformed biofilms (Figs. 4 and 5). The  
247 control biofilm (treated with DMSO) did not present any damage (Figs. 4A and 5A). The  
248 biofilms treated alone with NYS (Figs. 4B and 5B) and *Mo*-CBP<sub>3</sub>-PepI (Figs. 4C and 5C)  
249 presented mild damage such as altered morphology and wrinkles, distortion and apparent  
250 reduction in biomass compared to controls. The *Mo*-CBP<sub>3</sub>-PepI + NYS presented higher  
251 lethality to *C. albicans*, and *C. parapsilosis* preformed biofilms (Figs. 4D and 5D). After  
252 the treatment, biofilms presented a high reduction in the biomass of both biofilms in  
253 addition to severe damage such as cell depression-like cavities and damage to the cell  
254 wall, in addition to alterations in cell shape, wrinkles and scars all over the structure, and  
255 loss of internal content (Figs. 4D and 5D).

### 256 ***Membrane pore formation***

257 PI incorporation was used to evaluate the pore formation on the yeast membrane.  
258 PI interacts with DNA releasing red fluorescence, but this is only possible in membranes  
259 that are damaged. Healthy membranes block the PI from moving into the cell. The  
260 negative control DMSO did not damage the membranes, and thus no fluorescence was  
261 detected (Figs. 6-10). NYS and ITR tested alone did not show fluorescence in any  
262 treatment (Figs. 6-10). However, *Mo*-CBP<sub>3</sub>-PepI and *Mo*-CBP<sub>3</sub>-PepIII alone and in  
263 combination with NYS induced red fluorescence in *C. albicans* cells, indicating these  
264 cells are damaged and could present challenges to form a biofilm (Fig. 6). Similar results  
265 were found with *C. parapsilosis* cells (Figs. 7 and 8). Both peptides, either alone or

266 combined with ITR or NYS, induced pore formation in the *C. parapsilosis* cell  
267 membrane, thus inhibiting biofilm formation (Figs. 7 and 8). In preformed biofilms, *Mo*-  
268 CBP<sub>3</sub>-PepI alone or combined with NYS induced pore formation in the *C. albicans* and  
269 *C. parapsilosis* cell membranes, as revealed by red fluorescence (Figs. 9 and 10).

### 270 ***ROS production***

271 The analysis of ROS production revealed this is a mechanism employed by  
272 peptides alone and in synergism with drugs to damage the biofilms of *Candida* species  
273 (Figs. 6-10). The results showed that in *C. albicans* cells NYS did not induce ROS  
274 overproduction. Nevertheless, *Mo*-CBP<sub>3</sub>-PepIII, *Mo*-CBP<sub>3</sub>-PepI + NYS, and *Mo*-CBP<sub>3</sub>-  
275 PepIII + NYS induced a slight production of ROS (Fig. 6). None of the treatments induced  
276 ROS production during the inhibition of biofilm formation of *C. parapsilosis* (Figs. 7 and  
277 8).

278 Regarding degradation of preformed biofilm, no ROS overproduction was  
279 detected with any treatment towards *C. albicans* biofilm (Fig. 9). The fluorescence  
280 images obtained from the degradation of *C. parapsilosis* preformed biofilm indicated that  
281 NYS alone is ineffective in promoting ROS generation. However, *Mo*-CBP<sub>3</sub>-PepI alone  
282 or combined with NYS induced a strong ROS production (Fig. 10).

### 283 **Molecular docking**

284 We performed molecular docking to evaluate and understand the possible  
285 interactions of the peptides with the antifungal drugs. *Mo*-CBP<sub>3</sub>-PepI interacts with ITR  
286 and NYS with the lowest binding interaction energy (LBIE) of -4.5 and -4.2 kcal.mol<sup>-1</sup>,  
287 respectively (Fig. S1A and B). The amino acid residues Pro<sup>2</sup> and Ile<sup>4</sup> of the *Mo*-CBP<sub>3</sub>-  
288 PepI peptide show Pi-Alkyl interactions with the phenyl (4.5 Å), piperazine (4.2 Å), and  
289 dichlorophenyl (4.5 Å) groups, respectively, with ITR. Cys<sup>8</sup> has a Pi-Anion (3.4 Å,

290 triazole group) and a Pi-Sulfur (5.1 Å, dichlorophenyl group) interaction from ITR, and  
291 Arg<sup>6</sup> presents only van der Waals interaction (Fig. S1A and C). The *Mo*-CBP<sub>3</sub>-PepI  
292 interacts with NYS by van der Waals interactions of Cys<sup>8</sup>, Gln<sup>5</sup>, Cys<sup>1</sup>. An Alkyl (5.0 Å)  
293 interaction with Pro<sup>2</sup> and an unfavorable donor-donor (1.3 Å) with Arg<sup>6</sup> are also  
294 established (Fig. S1B and D).

295 *Mo*-CBP<sub>3</sub>-PepIII presents a docking score of -4.0 and -4.1 kcal.mol<sup>-1</sup> with ITR  
296 and NYS, respectively (Fig. S1E and F). *Mo*-CBP<sub>3</sub>-PepIII interacts through van der Waals  
297 interactions by residues Ala<sup>1</sup>, Gln<sup>3</sup>, and Cys<sup>6</sup> with ITR. Cys<sup>5</sup> interacts through an Amide-  
298 Pi stacked (3.8 Å) with the phenyl group of ITR. The Arg<sup>4</sup> of the *Mo*-CBP<sub>3</sub>-PepIII  
299 establishes a Pi-Cation interaction with the dichlorophenyl group (3.8 Å) and a Pi-Alkyl  
300 interaction (4.7 Å) with the methoxyphenyl group of itraconazole (Fig. S1E and G). The  
301 interaction between *Mo*-CBP<sub>3</sub>-PepIII and NYS is supported by hydrogen bonds between  
302 residues Arg<sup>4</sup> (2.0 Å) and Cys<sup>6</sup> (1.9 Å), as well as through van der Waals interactions  
303 through residues Gln<sup>3</sup> and Cys<sup>5</sup> (Fig. S1F and H). Taken together, these results suggest  
304 possible direct interactions between the peptides and NYS and ITR.

### 305 **Hemolytic Assay**

306 As shown in a previous study (Oliveira et al. 2019), the *Mo*-CBP<sub>3</sub>-PepI and *Mo*-  
307 CBP<sub>3</sub>-PepIII had no hemolytic activity against any human blood type tested (Table S1),  
308 even at 50 µg. mL<sup>-1</sup>. In contrast, NYS at 1000 µg. mL<sup>-1</sup> caused 100% hemolysis in all  
309 human blood types and ITR at 1000 µg. mL<sup>-1</sup> caused 75, 68, and 58% of hemolysis,  
310 respectively, to Type-A, B, and O of red blood cells (Table S1).

311 In general, the combination of synthetic peptides with antifungal drugs decreased  
312 their hemolytic effect (Table S1). The combination of *Mo*-CBP<sub>3</sub>-PepI with NYS resulted  
313 in a hemolytic effect of 14, 23, and 2%, respectively, to Type-A, B, and O of red blood

314 cells, and combination of *Mo*-CBP<sub>3</sub>-PepI with ITR caused in 0, 4, and 8% of hemolysis,  
315 respectively, to Type-A, B, and O of red blood cells (Table S1). The combination of *Mo*-  
316 CBP<sub>3</sub>-PepIII with NYS hemolyzed 45, 30, and 18%, respectively, of Type-A, B, and O  
317 of red blood cells, whereas the combination of *Mo*-CBP<sub>3</sub>-PepIII with ITR 50, 15, 2%,  
318 respectively, of Type-A, B, and O of red blood cells (Table S1).

## 319 **Discussion**

320 *Candida spp* yeasts represent a serious threat to human health worldwide. The  
321 infections by these fungi include bloodstream and systemic infections leading patients to  
322 death. Some immunocompromised patients (e.g., HIV+ and diabetics) develop an  
323 untreatable infection by *Candida spp* (Weig 1998; Kullberg & Oude Lashof 2002). These  
324 opportunistic pathogens have also established resistance to several antifungal agents  
325 (Baillie 2000; Ramage 2002; Arendrup & Patterson 2017; Sasso et al. 2017).  
326 Nevertheless, these microorganisms can organize themselves into compact microcolonies  
327 called biofilms enhancing their drug resistance and complicating the treatment.  
328 Additionally, higher concentrations of drugs employed in treatments could lead to  
329 collateral effects on patients (Baillie 2000; LaFleur et al. 2006; Kumar et al. 2017).  
330 Therefore, it is urgent to seek new alternative drugs to face this scenario and help patients  
331 to recover and survive.

332 Natural Antimicrobial Peptides (AMPs) are promising molecules to act as  
333 substitutes or adjuvants to treat infections. However, they present some disadvantages,  
334 such as high toxicity, low resistance to proteolysis, and high cost of isolation and  
335 purification processes. The development of SAMPs is an alternative solution to bypass  
336 this problem (Pedro F.N. Souza et al. 2020; Lima et al. 2021). SAMPs are potentially  
337 promising molecules to be used as novel therapeutic drugs against pathogens, in addition  
338 to other characteristics such as low or absence of toxicity to mammalian cells, low chance

339 to develop antimicrobial resistance based on their mechanism of action (Pedro F.N. Souza  
340 et al. 2020; Lima et al. 2021).

341 Bioinspired SAMPs based on natural AMPs can offer attributes that are not  
342 present in the natural molecule (Mason et al. 2006; Mason et al. 2009). A good example  
343 is the synthetic peptide LAH4 designed based on Magainin 2 sequence that presented a  
344 potent activity against *Escherichia coli* and *Staphylococcus aureus* compared with the  
345 natural peptide Magainin 2 (Mason et al. 2006; Mason et al. 2009). Recently, our research  
346 group designed three peptides derived from *Mo*-CBP<sub>3</sub> and antifungal Chitin-binding  
347 protein from *M. oleifera* seeds. *Mo*-CBP<sub>3</sub>-PepI, *Mo*-CBP<sub>3</sub>-pepII, and *Mo*-CBP<sub>3</sub>-pepIII  
348 inhibited the growth of *C. albicans* and *C. parapsilosis* planktonic cells by the stimulation  
349 of ROS production, cell wall damage, and membrane pore formation, leading to death  
350 (Oliveira et al. 2019; Lima et al. 2020). It is essential to notice that *Mo*-CBP<sub>3</sub> does not  
351 present anticandidal activity. Those cited are two examples of gain of function presented  
352 by SAMPs related to NAMPs. Based on that, we decided to evaluate the potential of *Mo*-  
353 CBP<sub>3</sub>-PepI, *Mo*-CBP<sub>3</sub>-pepII, and *Mo*-CBP<sub>3</sub>-pepIII to inhibit biofilm formation and its  
354 capacity to promote degradation of preformed biofilm in *C. albicans* and *C. parapsilosis*  
355 cells. This study evaluated the mechanisms of action to understand how these molecules  
356 work and their possible applications.

357 Regarding degradation of preformed biofilm of *C. albicans* cells, *Mo*-CBP<sub>3</sub>-PepI  
358 and *Mo*-CBP<sub>3</sub>-PepIII were active by 40% and 70%, respectively (Fig. 1). These results  
359 corroborate with Galdiero et al. (Galdiero et al. 2020) for gH625, analog from gH625-M,  
360 which reduced by 61% the biomass of preformed biofilm of *C. albicans*. SEM analysis  
361 of *C. albicans* and *C. parapsilosis* treated with *Mo*-CBP<sub>3</sub>-PepI and *Mo*-CBP<sub>3</sub>-PepIII  
362 showed that biofilm suffered severe damage leading biofilm structure to disorder.  
363 Furthermore, SEM analysis suggests all peptides induce rupture of the cell wall and

364 membrane-pore formation, leading the cell to internal content loss and death (Figs. 2-5).  
365 The images also showed the presence of scars, buds scars, and cracks in biofilm-treated  
366 cells. These results corroborate the work developed by Belmadani et al. (Belmadani et al.  
367 2018) observed that Dermaseptin-S1, an antimicrobial peptide from *Phyllomedusa*  
368 *sauvagii*, decreased *C. albicans* biofilm formation by alterations on the cell wall structure,  
369 membrane pore formation, and leakage of internal content (Belmadani et al. 2018).

370 The effects of *Mo*-CBP<sub>3</sub>-PepI and *Mo*-CBP<sub>3</sub>-PepIII on *C. albicans* and *C.*  
371 *parapsilosis* biofilm growth were either cytolysis or cell membrane disruption, leading to  
372 cell death. A previous study of our research group demonstrated that *Mo*-CBP<sub>3</sub>-PepIII  
373 presented a potent activity against *C. parapsilosis* planktonic cells, causing severe  
374 damage to the cell wall and membrane and leading to death through leakage of internal  
375 content (Oliveira et al. 2019). Similar behavior was observed by Sierra et al., where *C.*  
376 *albicans* biofilm suffered severe damage by the antimicrobial peptide Histatin-5 (Sierra  
377 et al. 2017).

378 These severe damages observed in the cell wall of both cells via SEM analysis can  
379 be explained considering that *Mo*-CBP<sub>3</sub>-PepI and *Mo*-CBP<sub>3</sub>-PepIII are designed based  
380 on the sequence of *Mo*-CBP<sub>3</sub>, a chitin-binding protein from *M. oleifera* seeds (Oliveira  
381 et al. 2019). Both peptides can interact with chitin present in the fungal cell wall and cause  
382 destabilization of the cell, leading to rupture, electrolyte imbalance, and thus cell death.

383 Unlike many commercial drugs with specific targets in enzymes from the  
384 metabolism or inactivation of protein synthesis, SAMPs target the cell membrane leading  
385 to pore formation and damage of the cell wall (Pedro F.N. Souza et al. 2020). The ability  
386 of SAMPs to alter the microbial membrane permeabilization is considered the most  
387 common mechanism of action of these molecules, making the development of resistance  
388 mechanisms by microorganisms (Pedro F.N. Souza et al. 2020; Lima et al. 2021).

389 Fluorescence microscopy analyses were performed to evaluate if our peptides could  
390 induce membrane-pore formation (Figs. 6-10). *Mo*-CBP<sub>3</sub>-PepI and *Mo*-CBP<sub>3</sub>-PepIII  
391 induced PI uptake in *C. albicans* and *C. parapsilosis* biofilm, suggesting pore formation  
392 and cell membrane damage (Figs. 6-10). The fluorescence microscopy corroborates the  
393 data observed by SEM analysis, strongly indicating damage in the cell membrane.  
394 Peptides enhanced the activity of NYS and ITR towards *C. albicans* and *C. parapsilosis*  
395 biofilms. In some cases, alone, neither peptides nor drugs had any action against biofilms;  
396 however, the combinations between them were much more efficient. It is known that *Mo*-  
397 CBP<sub>3</sub>-PepI and *Mo*-CBP<sub>3</sub>-PepIII form pores, respectively, of 6 and 20 kDa on *C. albicans*  
398 and *C. parapsilosis* membrane (Oliveira et al. 2019; Lima et al. 2020). NYS and ITR have  
399 molecular weights, respectively, of 926.1 and 705 Da. So, it is feasible to suggest that  
400 both NYS and ITR are passing through the pores formed by peptides on the membrane  
401 and somehow displaying damage in components of the cytoplasm.

402         Although the major mechanisms of action of synthetic peptides are to attack the  
403 cell membrane and the cell wall, these molecules can also be internalized by the cell and  
404 induce different responses, such as inhibition of cell wall synthesis or its maintenance,  
405 protein synthesis, and folding (Huang et al. 2010). Similar behavior was described by  
406 Maurya et al. [29], which showed that the peptides VS2 and VS3 can induce pore  
407 formation in *C. albicans* cells and develop distinct inhibitory activities in different targets  
408 inside the cell (Maurya et al. 2011).

409         Furthermore, *Mo*-CBP<sub>3</sub>-PepI induced ROS overproduction in *C. parapsilosis*  
410 biofilm in both degradation and inhibition of biofilm. *Mo*-CBP<sub>3</sub>-PepIII induced slight  
411 ROS generation in the inhibition of *C. albicans* biofilm formation (Fig. 6). A similar  
412 profile was observed using the killer peptides KP and MCh-AMP1, which are synthetic  
413 peptides able to induce ROS overproduction in *C. albicans* biofilm, leading to cell death

414 (Seyedjavadi et al. 2020). ROS are involved in the damage of essential molecules such as  
415 proteins, lipids, and DNA.

416 Additionally, we performed a pioneer molecular docking study to evaluate if our  
417 peptides could interact with NYS and ITR predominantly used to treat infections caused  
418 by *Candida spp* (Fig. S1). Similar behavior was detected by Souza et al. (Pedro F N Souza  
419 et al. 2020) where *Mo*-CBP<sub>3</sub>-PepI and *Mo*-CBP<sub>3</sub>-PepIII interacted with griseofulvin by  
420 weak interactions, such as hydrogen bonds and hydrophobic interactions. The interaction  
421 of peptides with griseofulvin enhanced its activity against dermatophytes and reduced the  
422 toxicity of the drug. The interactions between both peptides and each drug can explain  
423 the great synergistic activity obtained in our results, where both peptides enhanced the  
424 activity of both drugs.

425 A possible clinical application of synthetic peptides is that these molecules could  
426 act as adjuvants to drugs becoming less active due to the development of antifungal  
427 clinical resistance. *Mo*-CBP<sub>3</sub>-PepI and *Mo*-CBP<sub>3</sub>-PepIII improved the activity of NYS  
428 and ITR by up to 50% on inhibition of biofilm formation of *C. albicans* and *C.*  
429 *parapsilosis*. Moreover, the results showed that *Mo*-CBP<sub>3</sub>-PepI enhanced NYS activity  
430 up to 60% to degrade the preformed biofilm of both yeasts. NYS (polyene) very likely  
431 promotes an antibiofilm activity by interacting with ergosterol in the fungal cell  
432 membrane, making it an efficient drug to treat skin infections caused by *Candida* species.  
433 Nevertheless, NYS presents a high hemolytic activity to human blood cells, limiting its  
434 application.

435 Besides improve the antibiofilm activity of NYS and ITR, peptides also reduced  
436 the hemolytic effect (Table S1). However, ITR and NYS presented undesired effects,  
437 such as vomiting, nausea, diarrhea, anorexia, abdominal pain, and dizziness. Besides  
438 these collateral effects, cardiotoxicity and hypertension were attributed to ITR usage. An



439 unexpected and interesting result was that the association of peptides with antifungal  
440 drugs reduced their toxicity in human erythrocytes (Table S1). For example, NYS alone  
441 caused hemolysis of 100% on type-A erythrocytes. The *Mo*-CBP<sub>3</sub>-PepI + NYS and *Mo*-  
442 CBP<sub>3</sub>-PepIII + NYS induced hemolysis of 0 and 45%, respectively, of type-A blood. This  
443 is a reduction of 100 and 55% in the toxicity of NYS to type-A blood cells. All treatments  
444 combining peptides with antifungal drugs were able to reduce the hemolytic effect of  
445 drugs. These results make peptides potential molecules to be applied as adjuvants of these  
446 drugs because they enhance their activity toward biofilm and, at the same, reduce their  
447 toxicity.

448         Molecular docking analysis between peptides and drugs revealed a clue about how  
449 peptides reduced the hemolytic effect of drugs. It seems that all rely on hydrophobicity.  
450 The membrane of erythrocytes has neutral phospholipids, which means that any  
451 interaction with those membranes must be driven by hydrophobic interactions (Huang et  
452 al. 2010). It is known that NYS and ITR are hydrophobic drugs (B et al. 2016; C et al.  
453 2019). Hydrophobic interactions with membranes of erythrocytes may drive the  
454 hemolytic activity of NYS and ITR. The molecular docking experiments revealed that  
455 peptides performed hydrophobic interactions with NYS and ITR. Our results suggest that  
456 the hydrophobic interactions between peptides and both drugs prevent the interaction with  
457 the erythrocyte membranes reducing their hemolytic effect.

## 458 **Conclusion**

459         Antibiofilm activity, no toxicity, and synergistic effect enhancing the activity of  
460 NYS and ITR, strongly indicate that *Mo*-CBP<sub>3</sub>-PepI and *Mo*-CBP<sub>3</sub>-PepIII are promising  
461 antibiofilm peptides to act as new antimicrobial agents. We also highlight their use for  
462 clinical application or adjuvants to conventional drugs to overcome resistance developed  
463 by *Candida species*.

**464 Acknowledgments**

465 This work was supported by grants from the following Brazilian agencies: Conselho  
466 Nacional de Desenvolvimento Científico e Tecnológico (CNPq) (process numbers  
467 308107/2013-6 and 306202/2017-4); Coordenação de Aperfeiçoamento de Pessoal de  
468 Nível Superior (CAPES); Instituto Nacional de Ciências e Tecnologia de Bioinspiração  
469 (Process Number: 465507/2014-0) and Fundação Cearense de Apoio ao  
470 Desenvolvimento Científico e Tecnológico (FUNCAP). A special thanks to CAPES for  
471 providing the grant for postdoctoral position for Pedro F. N. Souza. We are also grateful  
472 to the central analytical facilities of UFC, Brazil.

473

**474 Credit Author Statement:**

475 All authors made substantial contributions. The conception and design of the study and  
476 acquisition of data, analysis, docking analysis, and interpretation were performed by LPB,  
477 CDTF, AFBS, NASN, ALCP, JTAO and PFNS. Microscopic analyses were carried out  
478 by RGGs and AFBS. Writing or revising this article was done by LPB, ALCP, GHG, and  
479 PFNS. PFNS did final approval of the version to be submitted.

480

**481 Declaration of interest**

482 The authors report no conflicts of interest. The authors alone are responsible for the  
483 content and the writing of the paper.

484

**485 Data Availability**

486 The data that support the findings of this study are available on request from the  
487 corresponding author.

488

**489 References**

490 Arendrup MC, Patterson TF. 2017. Multidrug-Resistant Candida: Epidemiology,  
491 Molecular Mechanisms, and Treatment. J Infect Dis [Internet]. 216(suppl\_3):S445--

- 492 S451.  
493 [http://academic.oup.com/jid/article/216/suppl\\_3/S445/4107052/MultidrugResistant-](http://academic.oup.com/jid/article/216/suppl_3/S445/4107052/MultidrugResistant-Candida-Epidemiology-Molecular)  
494 [Candida-Epidemiology-Molecular](http://academic.oup.com/jid/article/216/suppl_3/S445/4107052/MultidrugResistant-Candida-Epidemiology-Molecular)
- 495 B L, S L, JW M, RO W. 2016. Effect of hydrophilic additives on the dissolution and  
496 pharmacokinetic properties of itraconazole-enteric polymer hot-melt extruded  
497 amorphous solid dispersions. *Drug Dev Ind Pharm* [Internet]. [accessed 2021 Oct 17]  
498 42(3):429–445. <https://pubmed.ncbi.nlm.nih.gov/26355819/>
- 499 Baillie GS. 2000. Matrix polymers of *Candida* biofilms and their possible role in  
500 biofilm resistance to antifungal agents. *J Antimicrob Chemother* [Internet]. 46(3):397–  
501 403. <https://academic.oup.com/jac/article-lookup/doi/10.1093/jac/46.3.397>
- 502 Belmadani A, Semlali A, Rouabhia M. 2018. Dermaseptin-S1 decreases *Candida*  
503 *albicans* growth, biofilm formation and the expression of hyphal wall protein 1 and  
504 aspartic protease genes. *J Appl Microbiol* [Internet]. 125(1):72–83.  
505 <https://onlinelibrary.wiley.com/doi/10.1111/jam.13745>
- 506 C B, V G-H, C T, S T-S. 2019. Nystatin antifungal micellar systems on endotracheal  
507 tubes: development, characterization and in vitro evaluation. *Pharmazie* [Internet].  
508 [accessed 2021 Oct 17] 74(1):34–38. <https://pubmed.ncbi.nlm.nih.gov/30782248/>
- 509 Dias LP, Souza PFN, Oliveira JTA, Vasconcelos IM, Araújo NMS, Tilburg MF V,  
510 Guedes MIF, Carneiro RF, Lopes JLS, Sousa DOB. 2020. RcAlb-PepII, a synthetic  
511 small peptide bioinspired in the 2S albumin from the seed cake of *Ricinus communis*, is  
512 a potent antimicrobial agent against *Klebsiella pneumoniae* and *Candida parapsilosis*.  
513 *Biochim Biophys Acta - Biomembr* [Internet]. 1862(2):183092.  
514 <https://doi.org/10.1016/j.bbmem.2019.183092>
- 515 Fox EP, Nobile CJ. 2012. A sticky situation. *Transcription* [Internet]. 3(6):315–322.  
516 <http://www.tandfonline.com/doi/abs/10.4161/trns.22281>
- 517 Galdiero E, de Alteriis E, De Natale A, D'Alterio A, Siciliano A, Guida M, Lombardi  
518 L, Falanga A, Galdiero S. 2020. Eradication of *Candida albicans* persister cell biofilm  
519 by the membranotropic peptide gH625. *Sci Rep* [Internet]. 10(1):5780.  
520 <http://www.nature.com/articles/s41598-020-62746-w>
- 521 Huang Y, Huang J, Chen Y. 2010. Alpha-helical cationic antimicrobial peptides:  
522 Relationships of structure and function. *Protein Cell*. 1(2):143–152.
- 523 Katiyar S, Pfaller M, Edlind T. 2006. *Candida albicans* and *Candida glabrata* Clinical  
524 Isolates Exhibiting Reduced Echinocandin Susceptibility. *Antimicrob Agents*  
525 *Chemother* [Internet]. 50(8):2892–2894.  
526 <https://journals.asm.org/doi/10.1128/AAC.00349-06>
- 527 Kim S, Chen J, Cheng T, Gindulyte A, He J, He S, Li Q, Shoemaker BA, Thiessen PA,  
528 Yu B, et al. 2019. PubChem 2019 update: improved access to chemical data. *Nucleic*  
529 *Acids Res* [Internet]. 47(D1):D1102–D1109.  
530 <https://academic.oup.com/nar/article/47/D1/D1102/5146201>
- 531 Kullberg BJ, Oude Lashof AML. 2002. Epidemiology of opportunistic invasive  
532 mycoses. *Eur J Med Res* [Internet]. 7(5):183–191.  
533 <http://www.ncbi.nlm.nih.gov/pubmed/12069910>
- 534 Kumar A, Alam A, Rani M, Ehtesham NZ, Hasnain SE. 2017. Biofilms: Survival and

- 535 defense strategy for pathogens. *Int J Med Microbiol* [Internet]. 307(8):481–489.  
536 <https://linkinghub.elsevier.com/retrieve/pii/S1438422117300280>
- 537 LaFleur MD, Kumamoto CA, Lewis K. 2006. *Candida albicans* Biofilms Produce  
538 Antifungal-Tolerant Persister Cells. *Antimicrob Agents Chemother* [Internet].  
539 50(11):3839–3846. <https://journals.asm.org/doi/10.1128/AAC.00684-06>
- 540 Lamiable A, Thévenet P, Rey J, Vavrusa M, Derreumaux P, Tufféry P. 2016. PEP-  
541 FOLD3: faster de novo structure prediction for linear peptides in solution and in  
542 complex. *Nucleic Acids Res* [Internet]. 44(W1):W449--W454.  
543 <https://academic.oup.com/nar/article-lookup/doi/10.1093/nar/gkw329>
- 544 Lima PG, Oliveira JTA, Amaral JL, Freitas CDT, Souza PFN. 2021. Synthetic  
545 antimicrobial peptides: Characteristics, design, and potential as alternative molecules to  
546 overcome microbial resistance. *Life Sci*. 278:119647.
- 547 Lima PG, Souza PFN, Freitas CDT, Oliveira JTA, Dias LP, Neto JXS, Vasconcelos IM,  
548 Lopes JLS, Sousa DOB. 2020. Anticandidal activity of synthetic peptides: Mechanism  
549 of action revealed by scanning electron and fluorescence microscopies and synergism  
550 effect with nystatin. *J Pept Sci.(January)*:1–13.
- 551 Martínez-Rosell G, Giorgino T, Fabritiis G De. 2017. PlayMolecule ProteinPrepare: A  
552 Web Application for Protein Preparation for Molecular Dynamics Simulations. *J Chem*  
553 *Inf Model* [Internet]. [accessed 2021 Sep 15] 57(7):1511–1516.  
554 <https://pubs.acs.org/doi/abs/10.1021/acs.jcim.7b00190>
- 555 Mason AJ, Gasnier C, Kichler A, Prévost G, Aunis D, Metz-Boutigue MH, Bechinger  
556 B. 2006. Enhanced membrane disruption and antibiotic action against pathogenic  
557 bacteria by designed histidine-rich peptides at acidic pH. *Antimicrob Agents*  
558 *Chemother*. 50(10):3305–3311.
- 559 Mason AJ, Moussaoui W, Abdelrahman T, Boukhari A, Bertani P, Marquette A,  
560 Shooshtarizaheh P, Moulay G, Boehm N, Guerold B, et al. 2009. Structural  
561 Determinants of Antimicrobial and Antiplasmodial Activity and Selectivity in  
562 Histidine-rich Amphipathic Cationic Peptides. *J Biol Chem* [Internet]. 284(1):119–133.  
563 <https://linkinghub.elsevier.com/retrieve/pii/S0021925820682989>
- 564 Maurya IK, Pathak S, Sharma M, Sanwal H, Chaudhary P, Tupe S, Deshpande M,  
565 Chauhan VS, Prasad R. 2011. Antifungal activity of novel synthetic peptides by  
566 accumulation of reactive oxygen species (ROS) and disruption of cell wall against  
567 *Candida albicans*. *Peptides* [Internet]. [accessed 2019 Apr 23] 32(8):1732–1740.  
568 <https://www.sciencedirect.com/science/article/pii/S0196978111002270>
- 569 Morris GM, Huey R, Lindstrom W, Sanner MF, Belew RK, Goodsell DS, Olson AJ.  
570 2009. AutoDock4 and AutoDockTools4: Automated docking with selective receptor  
571 flexibility. *J Comput Chem* [Internet]. 30(16):2785–2791.  
572 <https://onlinelibrary.wiley.com/doi/10.1002/jcc.21256>
- 573 Oliveira JTA, Souza PFN, Vasconcelos IM, Dias LP, Martins TF, Van Tilburg MF,  
574 Guedes MIF, Sousa DOB. 2019. Mo-CBP3-PepI, Mo-CBP3-PepII, and Mo-CBP3-  
575 PepIII are synthetic antimicrobial peptides active against human pathogens by  
576 stimulating ROS generation and increasing plasma membrane permeability. *Biochimie*  
577 [Internet]. [accessed 2019 Apr 8] 157:10–21.  
578 <http://www.ncbi.nlm.nih.gov/pubmed/30389515>

- 579 Ramage G. 2002. Investigation of multidrug efflux pumps in relation to fluconazole  
580 resistance in *Candida albicans* biofilms. *J Antimicrob Chemother* [Internet]. 49(6):973–  
581 980. <https://academic.oup.com/jac/article-lookup/doi/10.1093/jac/dkf049>
- 582 Sasso Milène, Roger C, Sasso Magali, Poujol H, Barbar S, Lefrant J-Y, Lachaud L.  
583 2017. Changes in the distribution of colonising and infecting *Candida* spp. isolates,  
584 antifungal drug consumption and susceptibility in a French intensive care unit: A 10-  
585 year study. *Mycoses* [Internet]. 60(12):770–780.  
586 <https://onlinelibrary.wiley.com/doi/10.1111/myc.12661>
- 587 Seyedjavadi SS, Khani S, Eslamifar A, Ajdary S, Goudarzi M, Halabian R, Akbari R,  
588 Zare-Zardini H, Imani Fooladi AA, Amani J, Razzaghi-Abyaneh M. 2020. The  
589 Antifungal Peptide MCh-AMP1 Derived From *Matricaria chamomilla* Inhibits *Candida*  
590 *albicans* Growth via Inducing ROS Generation and Altering Fungal Cell Membrane  
591 Permeability. *Front Microbiol* [Internet]. 10.  
592 <https://www.frontiersin.org/article/10.3389/fmicb.2019.03150/full>
- 593 Sierra JM, Fusté E, Rabanal F, Vinuesa T, Viñas M. 2017. An overview of  
594 antimicrobial peptides and the latest advances in their development. *Expert Opin Biol*  
595 *Ther.* 17(6):663–676.
- 596 Souza Pedro F N, Lima PG, Freitas CDT, Sousa DOB, Neto NAS, Dias LP,  
597 Vasconcelos IM, Freitas LBN, Silva RGG, Sousa JS, et al. 2020. Antidermatophytic  
598 activity of synthetic peptides: Action mechanisms and clinical application as adjuvants  
599 to enhance the activity and decrease the toxicity of Griseofulvin. *Mycoses* [Internet].  
600 63(9):979–992. <https://onlinelibrary.wiley.com/doi/10.1111/myc.13138>
- 601 Souza Pedro F.N., Marques LSM, Oliveira JTA, Lima PG, Dias LP, Neto NAS, Lopes  
602 FES, Sousa JS, Silva AFB, Caneiro RF, et al. 2020. Synthetic antimicrobial peptides:  
603 From choice of the best sequences to action mechanisms. *Biochimie.* 175:132–145.
- 604 Staniszewska M, Bondaryk M, Swoboda-Kopec E, Siennicka K, Sygitowicz G,  
605 Kurzatkowski W. 2013. *Candida albicans* morphologies revealed by scanning electron  
606 microscopy analysis. *Brazilian J Microbiol.* 44(3):813–821.
- 607 Trott O, Olson AJ. 2009. AutoDock Vina: Improving the speed and accuracy of docking  
608 with a new scoring function, efficient optimization, and multithreading. *J Comput Chem*  
609 [Internet]. [accessed 2020 Jul 3] 31(2):NA-NA.  
610 [/pmc/articles/PMC3041641/?report=abstract](https://pubs.rsc.org/doi/10.1039/B8PY00034G)
- 611 Weig M. 1998. Clinical aspects and pathogenesis of *Candida* infection. *Trends*  
612 *Microbiol* [Internet]. 6(12):468–470.  
613 <https://linkinghub.elsevier.com/retrieve/pii/S0966842X98014073>
- 614 Zarnowski R, Westler WM, Lacmbouh GA, Marita JM, Bothe JR, Bernhardt J, Lounes-  
615 Hadj Sahraoui A, Fontaine J, Sanchez H, Hatfield RD, et al. 2014. Novel Entries in a  
616 Fungal Biofilm Matrix Encyclopedia. Lopez-Ribot J, Berman J, editors. *MBio* [Internet].  
617 5(4). <https://journals.asm.org/doi/10.1128/mBio.01333-14>
- 618

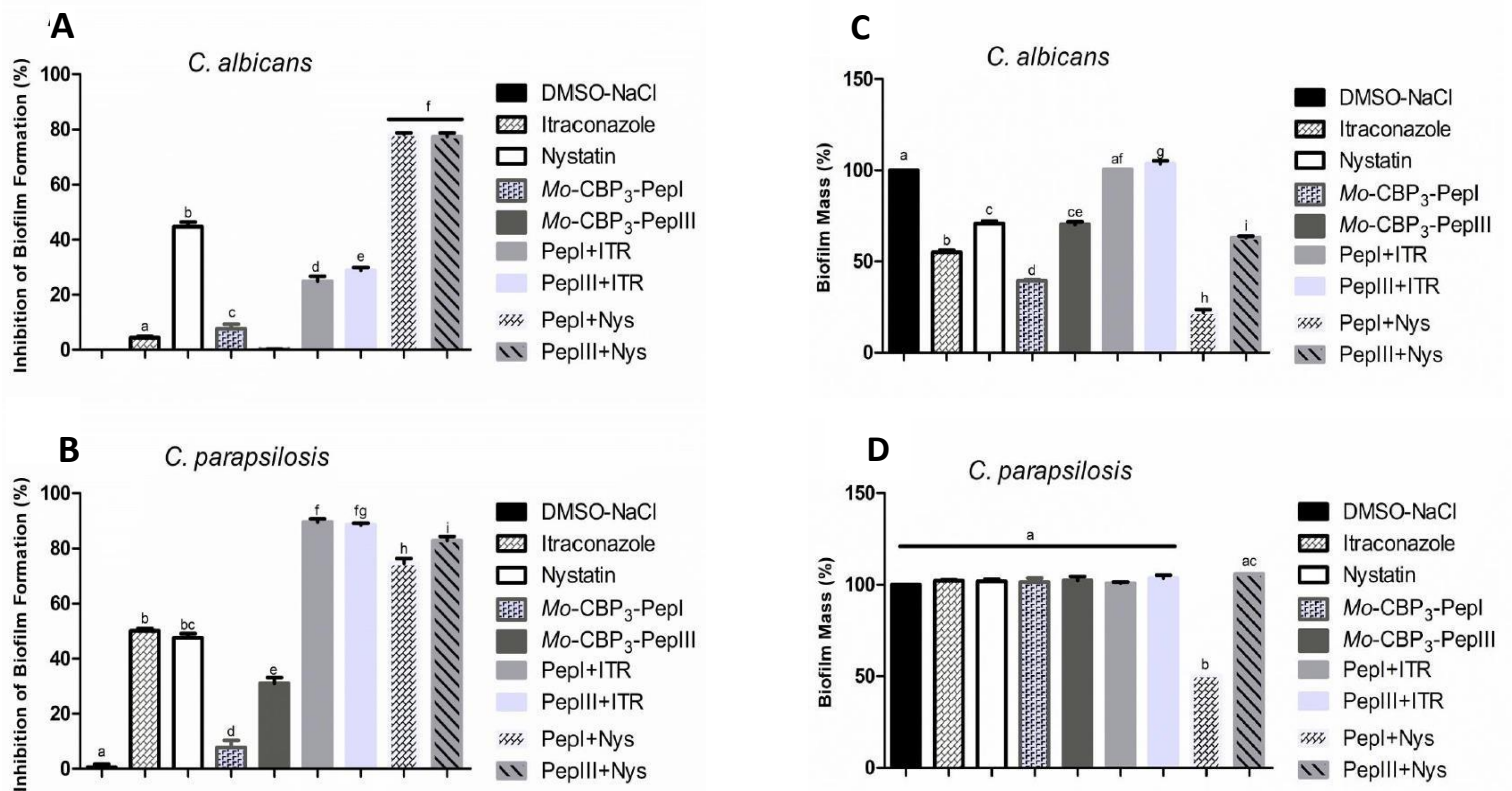


**Figure 1.** (A and B) Inhibitory activity of biofilm formation exhibited by Mo-CBP3-PepI and Mo-CBP3-PepIII against *C. albicans* and *C. parapsilosis*. (C and D) Degradation of preformed biofilm of *C. albicans* and *C. parapsilosis* exerted by Mo-CBP3-PepI and Mo-CBP3-PepIII. DMSO-NaCl was used as a negative control and ITR and NYS as a positive control. The letters represent the mean  $\pm$  standard deviation of three replicates. \*Different lowercase letters indicate statically significant difference compared to DMSO by analysis of variance ( $p < 0.05$ ).

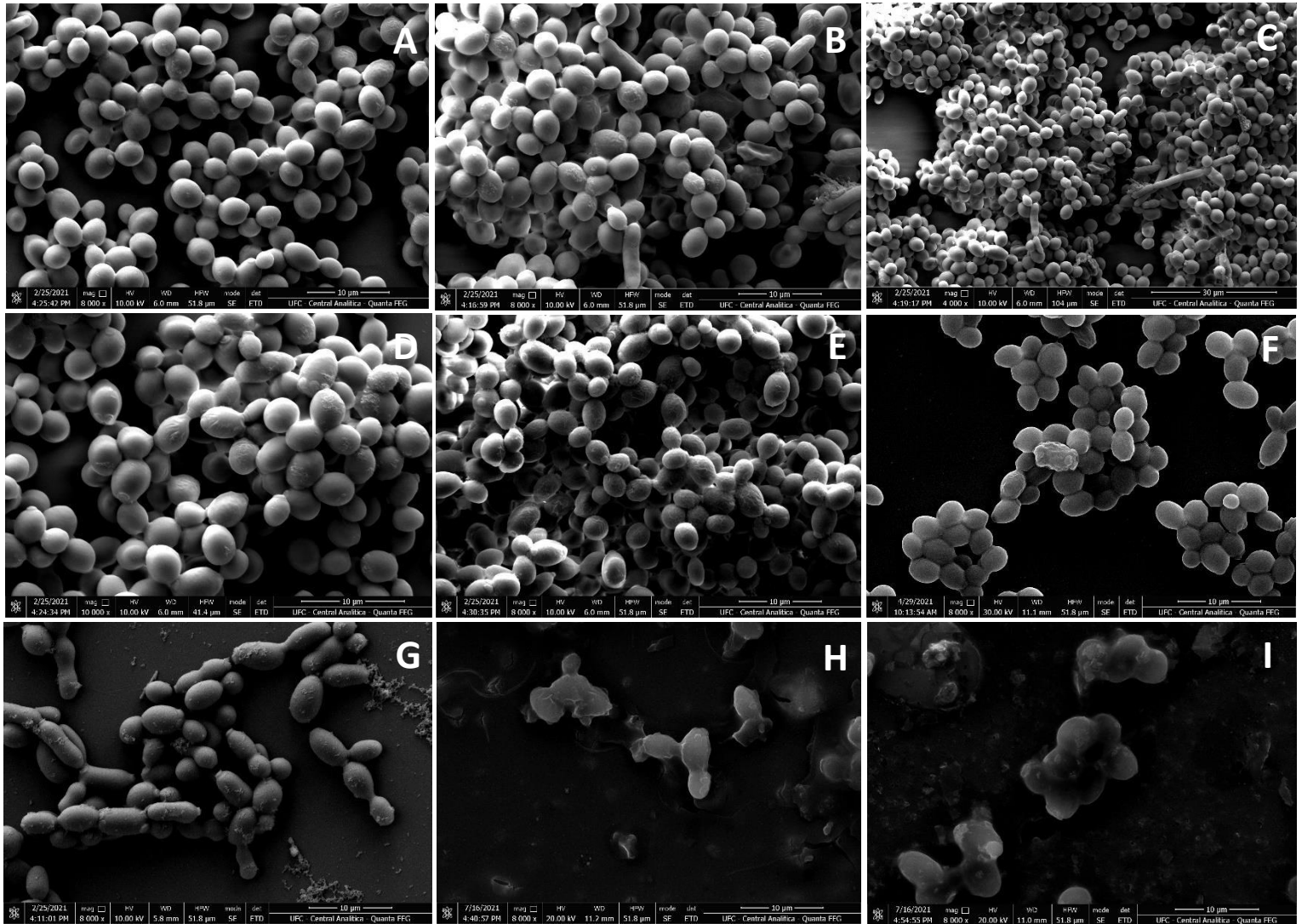


**Figure 2.** Scanning Electron Microscopy (SEM) images showing alterations on biofilm of *C. albicans* cells after incubation with *Mo-CBP<sub>3</sub>-PepI* and *Mo-CBP<sub>3</sub>-PepIII*. **(A)** The surface of biofilm control cells is covered by well-defined and organized structures. **(B- C)** Biofilm cells exposed to ITR and NYS, without major changes in the cell surface. **(D-E)** *Mo-CBP<sub>3</sub>-PepI* and *Mo-CBP<sub>3</sub>-PepIII*-treated cells, showing alterations in cell membrane, scars, and buds scars. **(F-G)** Biofilm cells in contact with *Mo-CBP<sub>3</sub>-PepI* and *Mo-CBP<sub>3</sub>-PepIII* in a synergistic action with ITR, showing considerable changes in the shape of cells and buds scars. **(H-I)** Biofilm cells incubated with *Mo-CBP<sub>3</sub>-PepI* and *Mo-CBP<sub>3</sub>-PepIII* in contact with NYS, resulting into strong alterations in the shape of the cells, cell wall damage and leakage of internal content.

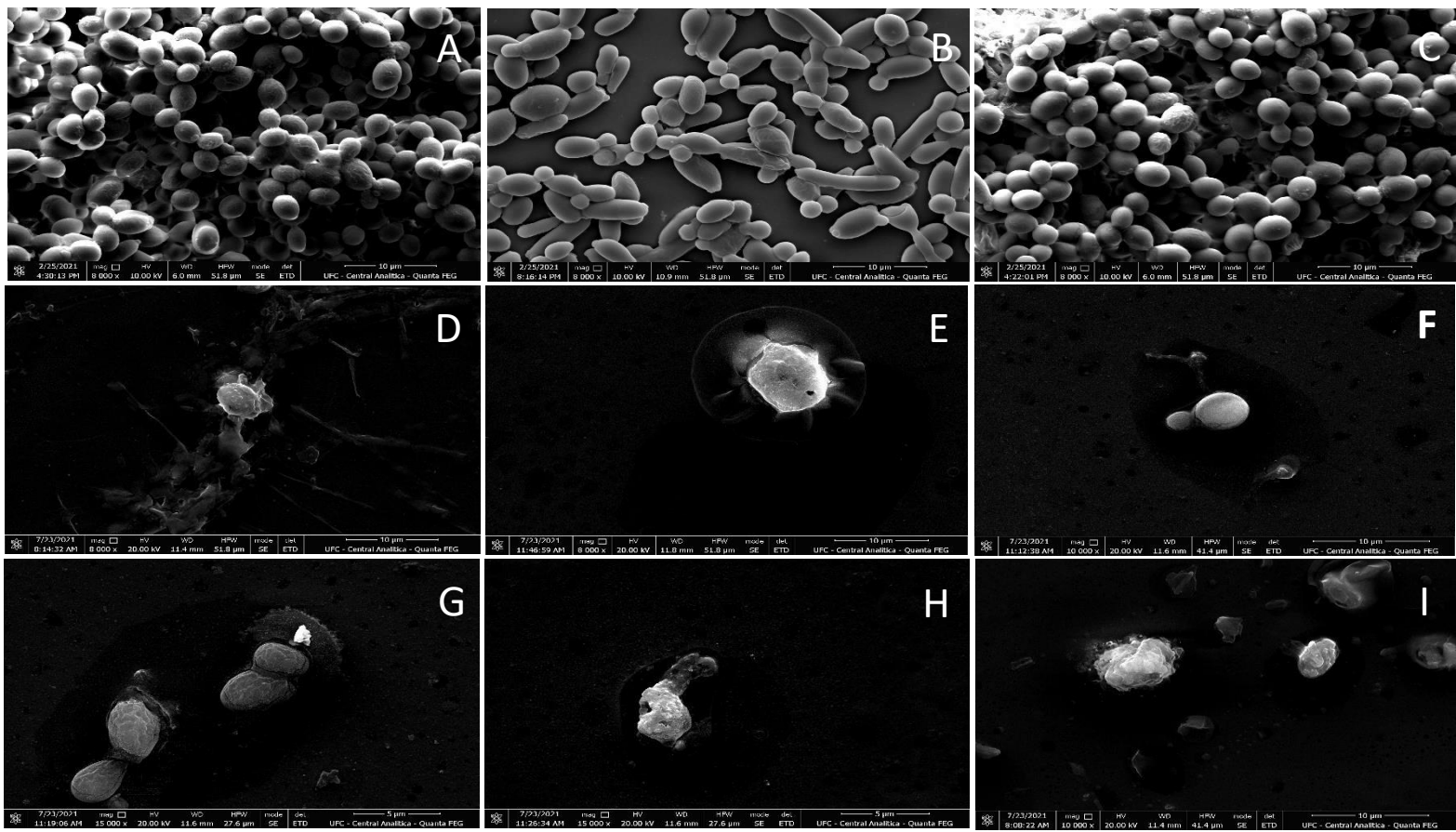


**Figure 3.** Scanning Electron Microscopy (SEM) images showing alterations on biofilm of *C. parapsilosis* cells after incubation with *Mo-CBP<sub>3</sub>-PepI* and *Mo-CBP<sub>3</sub>-PepIII*. (A) The surface of biofilm control cells is covered by well-defined and organized structures. (B-C) Biofilm cells exposed to ITR and NYS, without major changes in the cell surface. (D-E) *Mo-CBP<sub>3</sub>-PepI* and *Mo-CBP<sub>3</sub>-PepIII*-treated cells, showing major alterations in cell membrane, such as deformation, cell wall damage and internal content loss. (F-G) Biofilm cells in contact with *Mo-CBP<sub>3</sub>-PepI* and *Mo-CBP<sub>3</sub>-PepIII* in a synergistic action with ITR, showing considerable changes in the shape of cells and internal content loss. (H-I) Biofilm cells incubated with *Mo-CBP<sub>3</sub>-PepI* and *Mo-CBP<sub>3</sub>-PepIII* in contact with NYS, resulting into strong alterations in the membrane cell surface, cell wall damage and internal content loss.



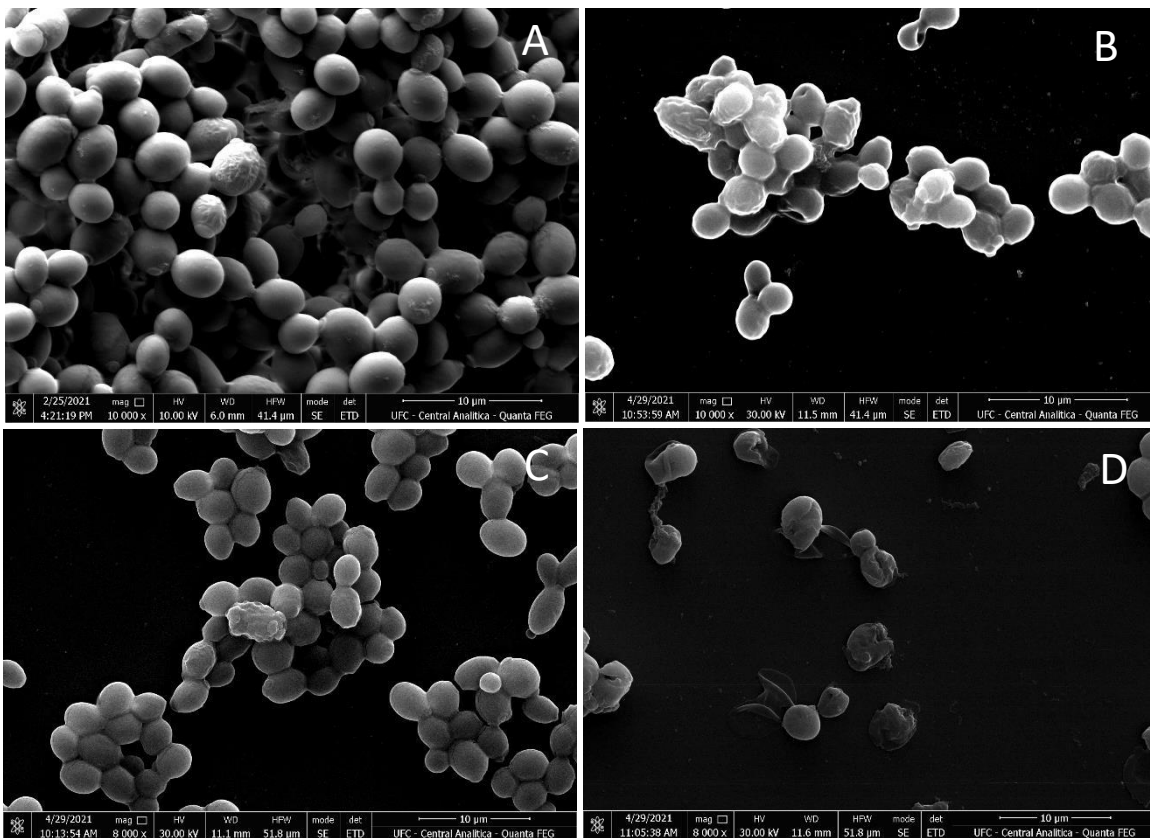


**Figure 4.** Scanning Electron Microscopy (SEM) images showing alterations on preformed biofilm of *C. albicans* cells after incubation with *Mo-CBP<sub>3</sub>-Pepl*. **(A)** The surface of biofilm control cells is covered by well-defined and organized structures. **(B)** Biofilm cells exposed to NYS, showing few alterations in the cell surface. **(C)** *Mo-CBP<sub>3</sub>-Pepl*-treated cells, showing some alterations in cell membrane, such as scars and cell wall damage. **(D)** Biofilm cells incubated with *Mo-CBP<sub>3</sub>-Pepl* in contact with NYS, resulting into strong alterations in the shape of the cells, cell wall damage and leakage of internal content.

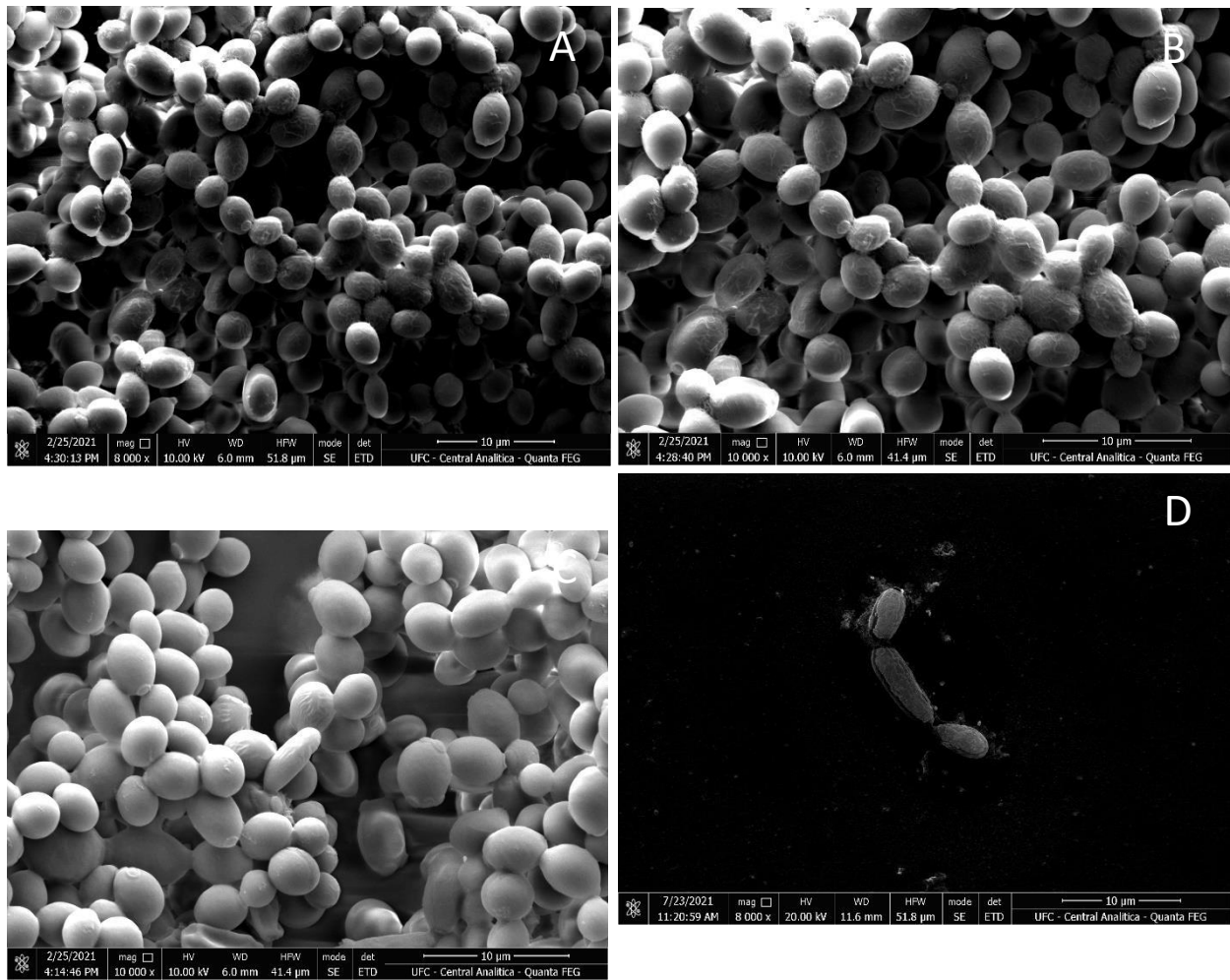


**Figure 5.** Scanning Electron Microscopy (SEM) images showing alterations on preformed biofilm of *C. parapsilosis* cells after incubation with *Mo-CBP<sub>3</sub>-Pepl*. **(A)** The surface of biofilm control cells is covered by well-defined and organized structures. **(B)** Biofilm cells exposed to NYS, showing few alterations in the cell surface. **(C)** *Mo-CBP<sub>3</sub>-Pepl*-treated cells, showing some alterations in cell membrane, such as scars and cell wall damage. **(D)** Biofilm cells incubated with *Mo-CBP<sub>3</sub>-Pepl* in contact with NYS, leading to strong alterations in the shape of the cells, deformation, cell wall damage and leakage of internal content.

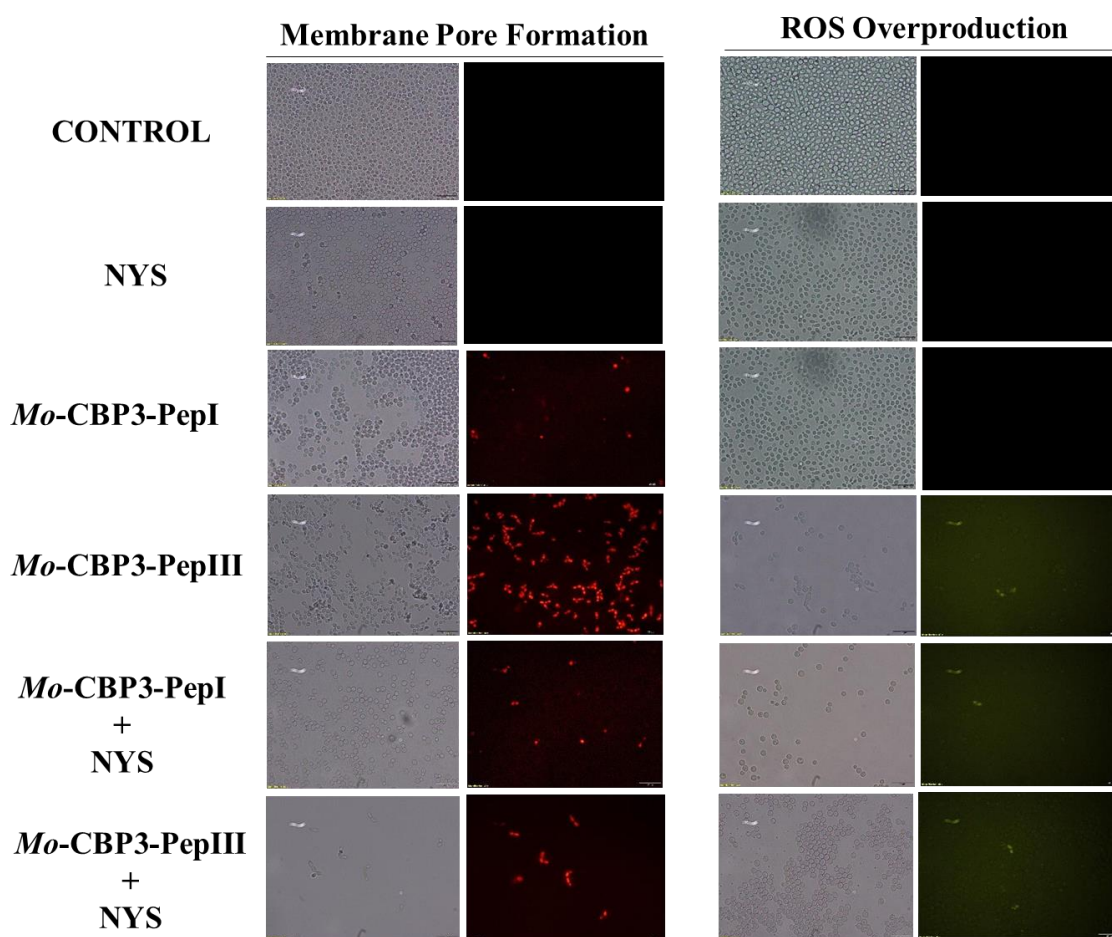


**Figure 6.** Fluorescence images showing membrane pore formation and ROS overproduction on inhibition of the biofilm of *C. albicans* cells. Control solution of DMSO-NaCl, treated with *Mo*-CBP3-PepI and *Mo*-CBP3-PepIII at  $50 \mu\text{g mL}^{-1}$  and synergistic activity of both peptides with NYS. Membrane pore formation was measured by propidium iodide uptake assay and ROS overproduction was detected using 2', 7' dichlorofluorescein diacetate (DCFH-DA).

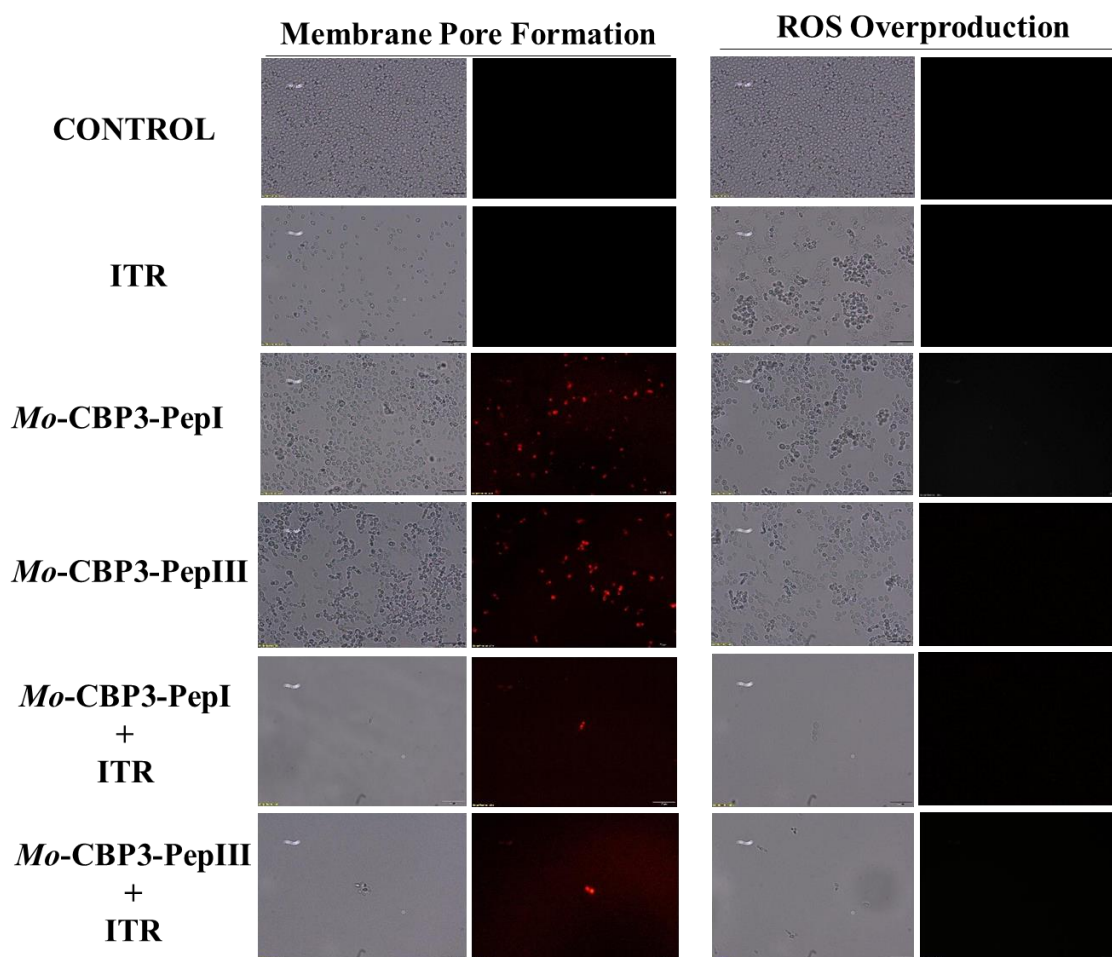


**Figure 7.** Fluorescence images showing membrane pore formation and ROS overproduction on inhibition of the biofilm of *C. parapsilosis* cells. Control solution of DMSO-NaCl, treated with *Mo*-CBP3-PepI and *Mo*-CBP3-PepIII at  $50 \mu\text{g mL}^{-1}$  and synergistic activity of both peptides with ITR. Membrane pore formation was measured by propidium iodide uptake assay and ROS overproduction was detected using 2', 7' dichlorofluorescein diacetate (DCFH-DA).

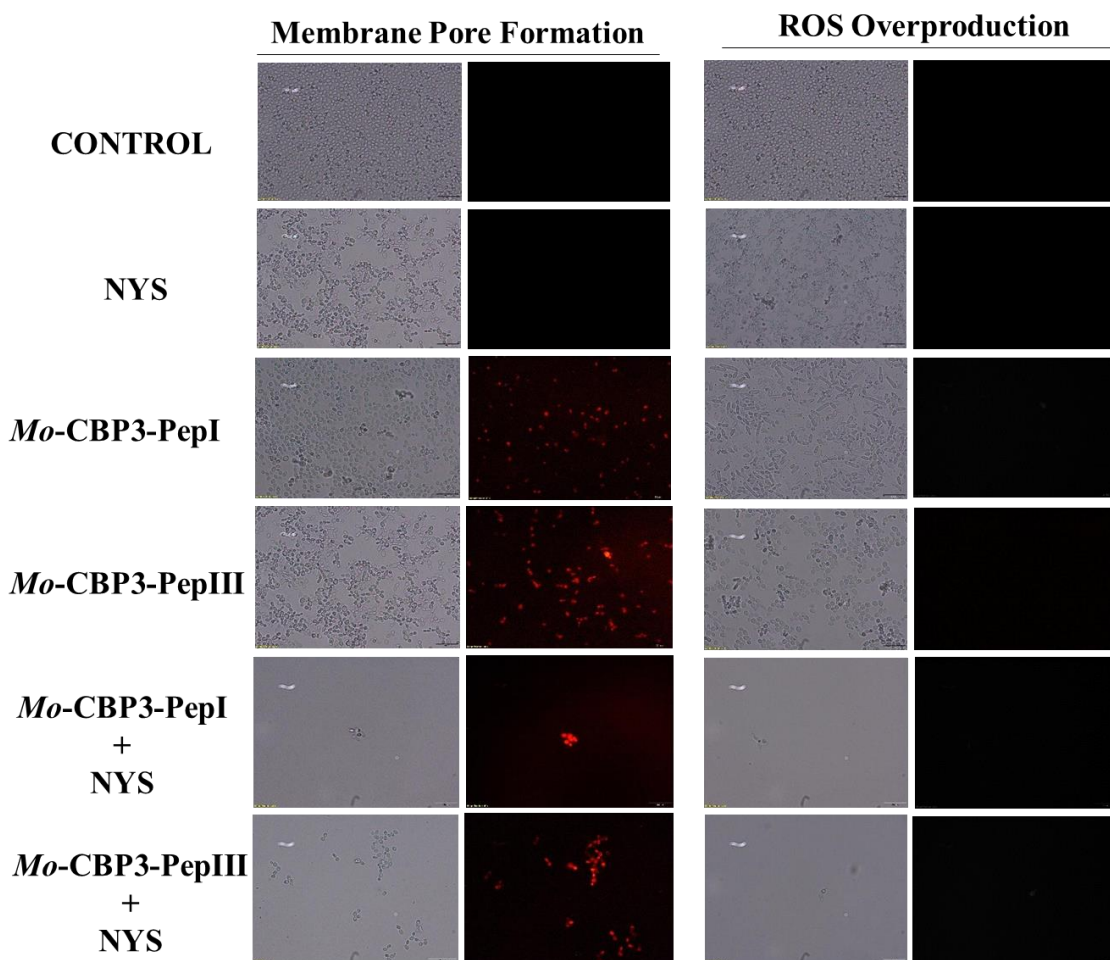


**Figure 8.** Fluorescence images showing membrane pore formation and ROS overproduction on inhibition of the biofilm of *C. parapsilosis* cells. Control solution of DMSO-NaCl, treated with *Mo*-CBP3-PepI and *Mo*-CBP3-PepIII at  $50 \mu\text{g mL}^{-1}$  and synergistic activity of both peptides with NYS. Membrane pore formation was measured by propidium iodide uptake assay and ROS overproduction was detected using 2', 7' dichlorofluorescein diacetate (DCFH-DA).

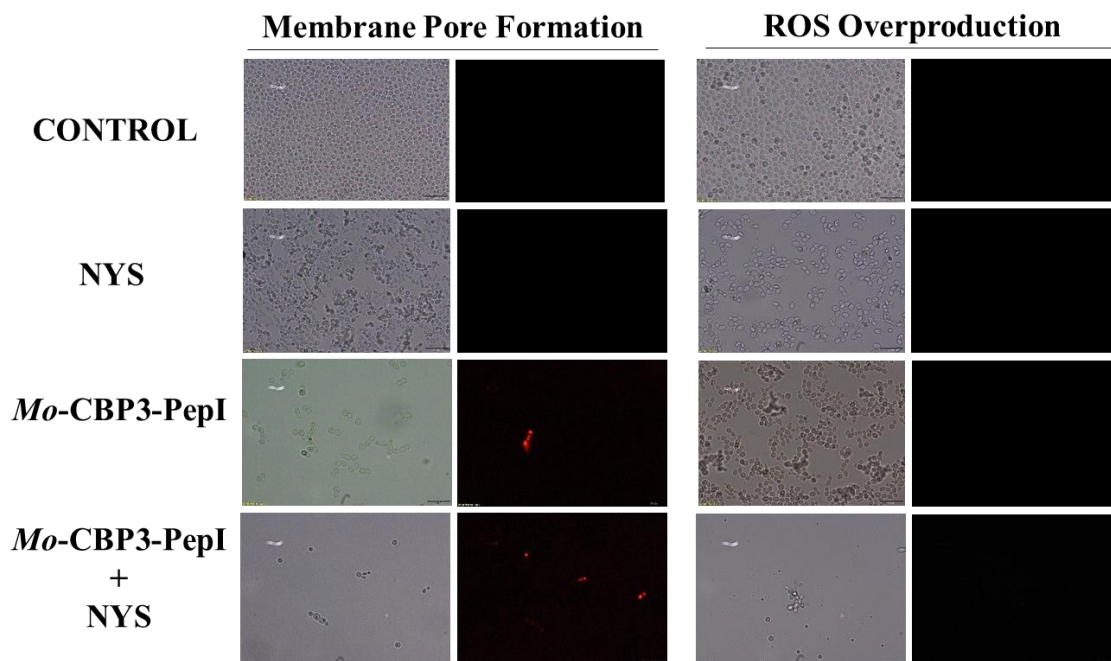


**Figure 9.** Fluorescence images showing membrane pore formation and ROS overproduction on degradation of the biofilm of *C. albicans* cells. Control solution of DMSO-NaCl, treated with *Mo*-CBP3-PepI at  $50 \mu\text{g mL}^{-1}$  and synergistic activity with NYS. Membrane pore formation was measured by propidium iodide uptake assay and ROS overproduction was detected using 2', 7' dichlorofluorescein diacetate (DCFH-DA).



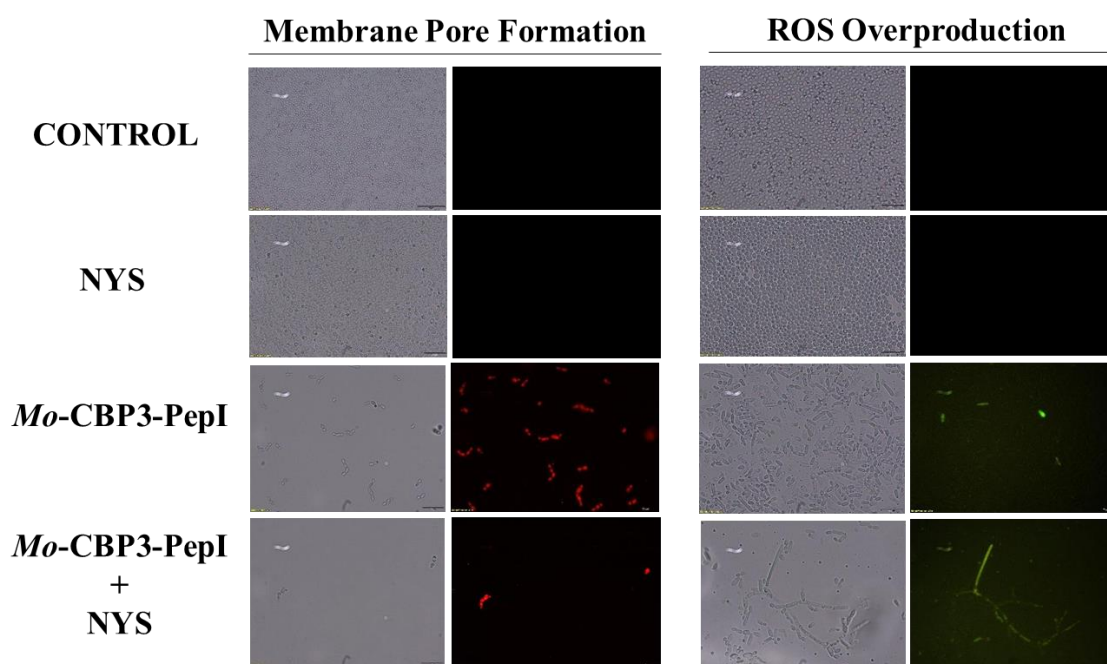
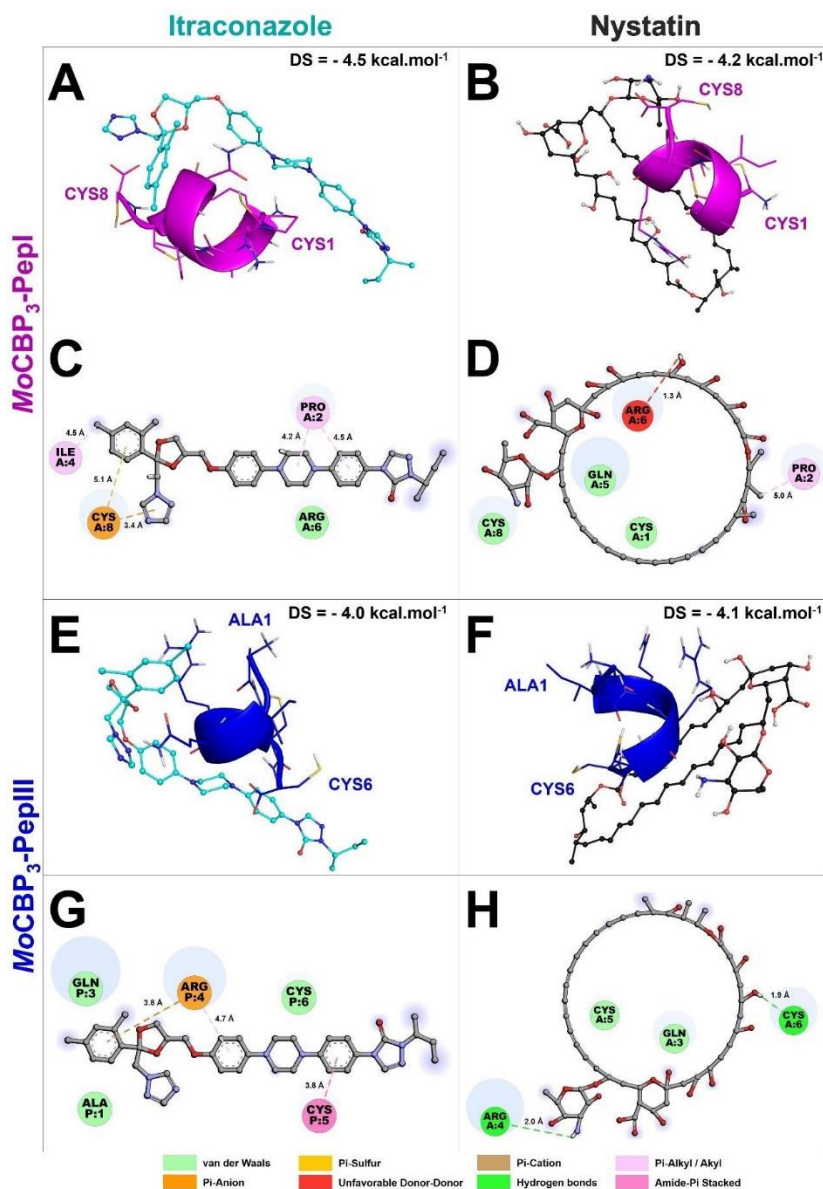


**Figure 10.** Fluorescence images showing membrane pore formation and ROS overproduction on degradation of the biofilm of *C. parapsilosis* cells. Control solution of DMSO-NaCl, treated with *Mo*-CBP<sub>3</sub>-PepI at 50  $\mu\text{g mL}^{-1}$  and synergistic activity with NYS. Membrane pore formation was measured by propidium iodide uptake assay and ROS overproduction was detected using 2', 7' dichlorofluorescein diacetate (DCFH-DA).



**Supplementary Figure 1.** Molecular docking revealed that *Mo*-CBP<sub>3</sub>-Pepl and *Mo*-CBP<sub>3</sub>-PeplIII interacting with ITR and NYS. *Mo*-CBP<sub>3</sub>-Pepl is represented in pink (A and B) and *Mo*-CBP<sub>3</sub>-PeplIII in blue (E and F). C, D, G and H show the binding sites of *Mo*-CBP<sub>3</sub>-Pepl and *Mo*-CBP<sub>3</sub>-PeplIII with ITR and NYS.



**Table 1.** Hemolytic activity of *Mo*-CBP<sub>3</sub>-PepI and *Mo*-CBP<sub>3</sub>-PepIII, antifungal drugs, and combined solution toward human red blood cells

Peptides/Combinations	% Hemolysis		
	Type-A Blood	Type-B Blood	Type-O Blood
0.1% Triton X-100	100	100	100
DMSO-NaCl Solution	0	0	0
NYS (1000 µg mL <sup>-1</sup> )	100	100	100
ITR (1000 µg mL <sup>-1</sup> )	75	68	58
<i>Mo</i> -CBP <sub>3</sub> -PepI (50 µg mL <sup>-1</sup> )	0	0	0
<i>Mo</i> -CBP <sub>3</sub> -PepIII (50 µg mL <sup>-1</sup> )	0	0	0
<i>Mo</i> -CBP <sub>3</sub> -PepI (50 µg mL <sup>-1</sup> ) + NYS (1000 µg mL <sup>-1</sup> )	14	23	2
<i>Mo</i> -CBP <sub>3</sub> -PepI (50 µg mL <sup>-1</sup> ) + ITR (1000 µg mL <sup>-1</sup> )	0	4	8
<i>Mo</i> -CBP <sub>3</sub> -PepIII (50 µg mL <sup>-1</sup> ) + NYS (1000 µg mL <sup>-1</sup> )	45	30	18
<i>Mo</i> -CBP <sub>3</sub> -PepIII (50 µg mL <sup>-1</sup> ) + ITR (1000 µg mL <sup>-1</sup> )	50	15	2

## 6. CONCLUSÃO

Os resultados obtidos mostram o potencial de peptídeos sintéticos bioinspirados em proteínas anteriormente identificadas contra biofilmes de microrganismos resistentes. Os peptídeos *Mo*-CBP3-PepI, *Mo*-CBP3-Pep3, PepGAT e PepKAA possuem atividade contra biofilmes de *C. albicans*, *C. krusei* e *C. parapsilosis* atuando tanto na inibição da formação do biofilme como na redução da biomassa de biofilmes pré-formados. Foi constatado que os mecanismos pelos quais os peptídeos desempenham sua atividade se dá por meio da formação de poros na membrana e indução da superprodução de espécies reativas de oxigênio, desestabilizando a membrana celular e causando extravasamento do conteúdo citoplasmático. Ademais, os resultados mostram que tais peptídeos podem ser capazes de se ligar a estruturas presentes na parede celular desestabilizando-a, bem como possuir alvos intracelulares específicos, levando as células à morte.

Os resultados obtidos com os ensaios de sinergismo sugerem que essas novas moléculas podem melhorar a atividade de antifúngicos já utilizados no tratamento de pacientes acometidos bem como reduzir a toxicidade de drogas comuns como nistatina e itraconazol. É válido salientar que os peptídeos não possuem efeitos tóxicos para as células do hospedeiro e não possuem atividade hemolítica contra eritrócitos humanos.

Desta forma, pode-se concluir que *Mo*-CBP3-PepI, *Mo*-CBP3-Pep3, PepGAT e PepKAA são peptídeos promissores no combate a biofilmes microbianos de interesse clínico bem como podem atuar como adjuvantes às drogas já utilizadas, melhorando sua atividade farmacológica e, sobretudo, contribuem na superação aos mecanismos de resistência microbiana.

## REFERÊNCIAS

- AKBARI, R. et al. Action mechanism of melittin-derived antimicrobial peptides, MDP1 and MDP2, de novo designed against multidrug resistant bacteria. **Amino acids**, v. 50, n. 9, p. 1231-1243, 2018.
- ALONSO, B. et al. Production of biofilm by *Staphylococcus aureus*: Association with infective endocarditis?. **Enfermedades Infecciosas y Microbiología Clínica**, 2021.
- AMARAL, Jackson L. et al. Computational approach, scanning electron and fluorescence microscopies revealed insights into the action mechanisms of anticandidal peptide Mo-CBP3-PepIII. **Life Sciences**, v. 281, p. 119775, 2021.
- ARMSTRONG, A. E. et al. Cell-free DNA next-generation sequencing successfully detects infectious pathogens in pediatric oncology and hematopoietic stem cell transplant patients at risk for invasive fungal disease. **Pediatric Blood & Cancer**, v. 66, n. 7, p. e27734, 2019.
- BARREIRO, C. et al. Worldwide Clinical Demand for Antibiotics: Is It a Real Countdown?. **Antimicrobial Therapies**, p. 3-15, 2021.
- BARTELL, J. A. et al. Evolutionary highways to persistent bacterial infection. **Nature communications**, v. 10, n. 1, p. 1-13, 2019.
- BATISTA, A. B. et al. New insights into the structure and mode of action of Mo-CBP 3, an antifungal chitin-binding protein of *Moringa oleifera* seeds. *PloS one*, [s.l.], v. 9, n. 10, p.e111427, 2014.
- BEHZADI, P. et al. Metallo- $\beta$ -lactamases: A review. **Molecular Biology Reports**, v. 47, n. 8, p. 6281-6294, 2020.
- BHATNAGAR, K. et al.. The mutational landscape of quinolone resistance in *Escherichia coli*. **PloS One**, v. 14, n. 11, p. e0224650, 2019.
- BOGDANOVA, L. R. et al. Spectroscopic, zeta potential and molecular dynamics studies of the interaction of antimicrobial peptides with model bacterial membrane. **Spectrochimica Acta Part A: Molecular and Biomolecular Spectroscopy**, v. 242, p. 118785, 2020.
- BOPARAI, J. et al. Mini review on antimicrobial peptides, sources, mechanism and recent applications. **Protein and Peptide Letters**, v. 27, n. 1, p. 4-16, 2020.

CAPECCHI, A. et al. Machine learning designs non-hemolytic antimicrobial peptides. **Chemical Science**, v. 12, n. 26, p. 9221-9232, 2021.

CHAN, B. M. J. et al. A brief history of penicillin. **Dalhousie Medical Journal**, v. 47, n. 1, 2020.

CORRÊA, J. A. F. et al. Fundamentals on the molecular mechanism of action of antimicrobial peptides. **Materialia**, v. 8, p. 100494, 2019.

DODDS, D. R. Antibiotic resistance: A current epilogue. **Biochemical pharmacology**, v. 134, p. 139-146, 2017.

DHINGRA, S. et al. Microbial resistance movements: an overview of global public health threats posed by antimicrobial resistance, and how best to counter. **Frontiers in Public Health**, v. 8, p. 531, 2020.

GHAI, I.; et al. Understanding antibiotic resistance via outer membrane permeability. **Infection and drug resistance**, v. 11, p. 523, 2018.

GIFONI, J. M. et al. A novel chitin-binding protein from *Moringa oleifera* seed with potential for plant disease control. *Peptide Science*, [s.l.], v. 98, n. 4, p. 406-415, 2012.

GUO, Y. et al. Prevalence and therapies of antibiotic-resistance in *Staphylococcus aureus*. **Frontiers in cellular and infection microbiology**, v. 10, p. 107, 2020.

GUCWA, K. et al. Antifungal activity and synergism with azoles of polish propolis. **Pathogens**, v. 7, n. 2, p. 56, 2018.

HASAN, T. H. et al. Mechanisms of antibiotics resistance in bacteria. **Sys Rev Pharm**, v. 11, n. 6, p. 817-823, 2020.

HEALEY, K. R. et al. Limited ERG11 mutations identified in isolates of *Candida auris* directly contribute to reduced azole susceptibility. **Antimicrobial agents and chemotherapy**, v. 62, n. 10, p. e01427-18, 2018.

HILLER, C. X. et al. Antibiotic microbial resistance (AMR) removal efficiencies by conventional and advanced wastewater treatment processes: A review. **Science of the Total Environment**, v. 685, p. 596-608, 2019.

KAVANAUGH, J. S. et al. Identification of extracellular DNA-binding proteins in the biofilm matrix. **MBio**, v. 10, n. 3, p. e01137-19, 2019.

- KHATOON, Z. et al. Bacterial biofilm formation on implantable devices and approaches to its treatment and prevention. **Heliyon**, v. 4, n. 12, p. e01067, 2018.
- KEANE, S. et al. Systematic review on the first line treatment of amphotericin B in critically ill adults with candidemia or invasive candidiasis. **Expert Review of Anti-infective Therapy**, v. 16, n. 11, p. 839-847, 2018.
- KLÜMPER, U. et al. Selection for antimicrobial resistance is reduced when embedded in a natural microbial community. **The ISME journal**, v. 13, n. 12, p. 2927-2937, 2019.
- KUMAR, V. et al. B3Pdb: an archive of blood–brain barrier-penetrating peptides. **Brain Structure and Function**, v. 226, n. 8, p. 2489-2495, 2021.
- KURMOO, Y. et al. Real time monitoring of biofilm formation on coated medical devices for the reduction and interception of bacterial infections. **Biomaterials Science**, v. 8, n. 5, p. 1464-1477, 2020.
- LAUXEN, A. I. et al. Mechanism of Resistance Development in *E. coli* against TCAT, a Trimethoprim-Based Photoswitchable Antibiotic. **Pharmaceuticals**, v. 14, n. 5, p. 392, 2021.
- LEE, J. et al. Antimicrobial peptide HPA3NT3-A2 effectively inhibits biofilm formation in mice infected with drug-resistant bacteria. **Biomaterials Science**, v. 7, n. 12, p. 5068-5083, 2019.
- LERMINIAUX, N. A. et al. Horizontal transfer of antibiotic resistance genes in clinical environments. **Canadian journal of microbiology**, v. 65, n. 1, p. 34-44, 2019.
- LI, J. et al. Synergism between Host Defense Peptides and Antibiotics Against Bacterial Infections. *Current Topics in Medicinal Chemistry*, [s.l.], v.20, n. 14, p. 1238–1263, 2020
- LIMA, Patrícia G. et al. Synthetic peptides against *Trichophyton mentagrophytes* and *T. rubrum*: Mechanisms of action and efficiency compared to griseofulvin and itraconazole. **Life Sciences**, v. 265, p. 118803, 2021.
- LIMA, P. G. et al. Synthetic antimicrobial peptides: Characteristics, design, and potential as alternative molecules to overcome microbial resistance. **Life Sciences**, v. 278, p. 119647, 2021.
- LIU, N. et al. Emerging new targets for the treatment of resistant fungal infections. **Journal of medicinal chemistry**, v. 61, n. 13, p. 5484-5511, 2018.
- MAGANA, M. et al. The value of antimicrobial peptides in the age of resistance. **The Lancet Infectious Diseases**, v. 20, n. 9, p. e216-e230, 2020

- MCINNES, R. S. et al. Horizontal transfer of antibiotic resistance genes in the human gut microbiome. **Current opinion in microbiology**, v. 53, p. 35-43, 2020.
- MORAVEJ, H. et al. Antimicrobial peptides: features, action, and their resistance mechanisms in bacteria. **Microbial Drug Resistance**, v. 24, n. 6, p. 747-767, 2018.
- MOTTA, J. et al. Gastrointestinal biofilms in health and disease. **Nature Reviews Gastroenterology & Hepatology**, v. 18, n. 5, p. 314-334, 2021.
- NETO, J. X. S. et al. A chitin-binding protein purified from *Moringa oleifera* seeds presents anticandidal activity by increasing cell membrane permeability and reactive oxygen species production. **Frontiers in microbiology**, [s.l.], v. 8, p. 980, 2017.
- NETT, J. E. et al. Contributions of the biofilm matrix to *Candida* pathogenesis. **Journal of Fungi**, v. 6, n. 1, p. 21, 2020.
- OLIVEIRA, J. T. A et al. Mo-CBP3-PepI, Mo-CBP3-PepII, and Mo-CBP3-PepIII are synthetic antimicrobial peptides active against human pathogens by stimulating ROS generation and increasing plasma membrane permeability. **Biochimie**, v. 157, p. 10-21, 2019.
- PANG, Z. et al. Antibiotic resistance in *Pseudomonas aeruginosa*: mechanisms and alternative therapeutic strategies. **Biotechnology advances**, v. 37, n. 1, p. 177-192, 2019.
- PAPPAS, P. G. et al. Invasive candidiasis. **Nature Reviews Disease Primers**, v. 4, n. 1, p. 1-20, 2018.
- PATRA, S. et al. Chemotherapeutic efficacy of curcumin and resveratrol against cancer: Chemoprevention, chemoprotection, drug synergism and clinical pharmacokinetics. In: **Seminars in cancer biology**. Academic Press, 2021. p. 310-320.
- PERFECT, J. R. The antifungal pipeline: a reality check. *Nature reviews Drug discovery*, v. 16, n. 9, p. 603, 2017.
- PRISTOV, K. E. et al. Resistance of *Candida* to azoles and echinocandins worldwide. **Clinical Microbiology and Infection**, v. 25, n. 7, p. 792-798, 2019.
- POURNAJAF, A. et al. Integron types, antimicrobial resistance genes, virulence gene profile, alginate production and biofilm formation in Iranian cystic fibrosis *Pseudomonas aeruginosa* isolates. **Infez Med**, v. 26, n. 3, p. 226-36, 2018.

RAMSTEDT, M. et al. Can multi-species biofilms defeat antimicrobial surfaces on medical devices?. **Current Opinion in Biomedical Engineering**, p. 100370, 2022.

REVIE, N. M. et al. Antifungal drug resistance: evolution, mechanisms and impact. **Current opinion in microbiology**, v. 45, p. 70-76, 2018.

RIBEIRO DA CUNHA, B. et al. Antibiotic discovery: where have we come from, where do we go?. **Antibiotics**, v. 8, n. 2, p. 45, 2019.

RODRIGUES, M. L. Fungal diseases as neglected pathogens: A wake-up call to public health officials. In: **Advances in Clinical Immunology, Medical Microbiology, COVID-19, and Big Data**. Jenny Stanford Publishing, 2021. p. 399-411.

RUSS, D. et al. Escape mutations circumvent a tradeoff between resistance to a beta-lactam and resistance to a beta-lactamase inhibitor. **Nature communications**, v. 11, n. 1, p. 1-9, 2020.

SALEHI, M. et al. Opportunistic fungal infections in the epidemic area of COVID-19: a clinical and diagnostic perspective from Iran. **Mycopathologia**, v. 185, n. 4, p. 607-611, 2020.

STEKEL, D. First report of antimicrobial resistance pre-dates penicillin. **Nature**, v. 562, n. 7726, 2018.

STROLLO, S. et al. Epidemiology of hospitalizations associated with invasive candidiasis, United States, 2002–2012. *Emerging infectious diseases*, [s.l.], v. 23, n. 1, p. 7, 2017.

SOUZA, P. F. N. et al. Synthetic antimicrobial peptides: From choice of the best sequences to action mechanisms. **Biochimie**, v. 175, p. 132-145, 2020.

TAN, P. F. et al. Design, optimization, and nanotechnology of antimicrobial peptides: From exploration to applications. **Nano Today**, v. 39, p. 101229, 2021.

TAYLOR, P. et al. Antibiotic use on crops in low and middle-income countries based on recommendations made by agricultural advisors. **CABI Agriculture and Bioscience**, v. 1, n. 1, p. 1-14, 2020.

VAN DAELE, R. et al. Antifungal drugs: what brings the future?. **Medical mycology**, v. 57, n. Supplement\_3, p. S328-S343, 2019.

VESTBY, L. K. et al. Bacterial biofilm and its role in the pathogenesis of disease. **Antibiotics**, v. 9, n. 2, p. 59, 2020.

VILLASMIL, M. L. et al. An Erg11 lanosterol 14- $\alpha$ -demethylase-Arv1 complex is required for *Candida albicans* virulence. **Plos one**, v. 15, n. 7, p. e0235746, 2020.

WU, X. et al. Inflammatory immune response in rabbits with *Staphylococcus aureus* biofilm-associated sinusitis. In: **International Forum of Allergy & Rhinology**. 2018. p. 1226-1232.

XI, Y. et al. Dual corona vesicles with intrinsic antibacterial and enhanced antibiotic delivery capabilities for effective treatment of biofilm-induced periodontitis. **ACS nano**, v. 13, n. 12, p. 13645-13657, 2019.

YELIN, I.; KISHONY, Roy. Antibiotic resistance. **Cell**, v. 172, n. 5, p. 1136-1136. e1, 2018.



## APÊNDICE A - ARTIGO CIENTÍFICO 3

Artigo publicado na revista Life Sciences – Fator de impacto: 5.037

Acesso disponível em: (<https://doi.org/10.1016/j.lfs.2020.118803>)



Contents lists available at [ScienceDirect](#)

Life Sciences

journal homepage: [www.elsevier.com/locate/lifescie](http://www.elsevier.com/locate/lifescie)



### Synthetic peptides against *Trichophyton mentagrophytes* and *T. rubrum*: Mechanisms of action and efficiency compared to griseofulvin and itraconazole

Patrícia G. Lima, Pedro F.N. Souza<sup>\*</sup>, Cleverton D.T. Freitas, Leandro P. Bezerra, Nilton A. S. Neto, Ayrles F.B. Silva, Jose T.A. Oliveira, Daniele O.B. Sousa<sup>\*</sup>

Department of Biochemistry and Molecular Biology, Federal University of Ceará, Fortaleza, Ceará CEP 60.440-554, Brazil

#### ARTICLE INFO

##### Keywords:

Synthetic antifungal peptides  
Dermatophytes  
Synthetic peptides  
Griseofulvin  
Itraconazole

#### ABSTRACT

**Aims:** According to the WHO, 20–25% of people worldwide are affected by skin infections caused by dermatophytes, such as those of the *Trichophyton* genus. Additionally, several dermatophytes have developed resistance to drugs such as griseofulvin and itraconazole. This study tested 28 albumins-derived antimicrobial peptides (AMPs) as alternative antidermatophytic molecules.

**Main methods:** Membrane pore formation assays, tests to detect overproduction of ROS, scanning electron microscopy (SEM) and fluorescence microscopy (FM) were carried out to provide insight into the mechanisms of antidermatophytic action.

**Key findings:** All AMPs (at 50 µg mL<sup>-1</sup>) tested reduced the mycelial growth of *T. mentagrophytes* and *T. rubrum* by up to 95%. In contrast, using a concentration 20-fold higher, griseofulvin only inhibited *T. mentagrophytes* by 35%, while itraconazole was not active against both dermatophytes. Scanning electron and fluorescence microscopies revealed that the six AMPs caused severe damage to hyphal morphology by inducing cell wall rupture, hyphal content leakage, and death. Peptides also induced membrane pore formation and oxidative stress by overproduction of ROS. Based on the stronger activity of peptides than the commercial drugs and the mechanism of action, all six peptides have the potential to be either employed as models to develop new antidermatophytic drugs or as adjuvants to existing ones.

**Significance:** The synthetic peptides are more efficient than conventional drug to treat infection caused by dermatophytes being potential molecules to develop new drugs.

## APÊNDICE B – ARTIGO CIENTÍFICO 4

Artigo publicado na revista Journal of Biomolecular Structures and Dynamics


– Fator de impacto: 3.31

Acesso disponível em: (<https://doi.org/10.1080/07391102.2020.1871415>)

JOURNAL OF BIOMOLECULAR STRUCTURE AND DYNAMICS  
<https://doi.org/10.1080/07391102.2020.1871415>



### ACE2-derived peptides interact with the RBD domain of SARS-CoV-2 spike glycoprotein, disrupting the interaction with the human ACE2 receptor

Pedro F. N. Souza<sup>a</sup> , Jackson L. Amaral<sup>a,b</sup>, Leandro P. Bezerra<sup>a</sup>, Francisco E. S. Lopes<sup>c</sup>, Valder N. Freire<sup>b</sup>, Jose T. A. Oliveira<sup>a</sup> and Cleverson D. T. Freitas<sup>a</sup>

<sup>a</sup>Department of Biochemistry and Molecular Biology, Federal University of Ceará, Fortaleza, Brazil; <sup>b</sup>Department of Physics, Federal University of Ceará, Fortaleza, Brazil; <sup>c</sup>Center for Permanent Education in Health Care, CEATS/School of Public Health of Ceará-ESP-CE, Fortaleza, Brazil

Communicated by Ramaswamy H. Sarma

#### ABSTRACT

Vaccines could be the solution to the current SARS-CoV-2 outbreak. However, some studies have shown that the immunological memory only lasts three months. Thus, it is imperative to develop pharmacological treatments to cope with COVID-19. Here, the *in silico* approach by molecular docking, dynamic simulations and quantum biochemistry revealed that ACE2-derived peptides strongly interact with the SARS-CoV-2 RBD domain of spike glycoprotein (S-RBD). ACE2-Dev-Pepl, ACE2-Dev-PeplI, ACE2-Dev-PeplII and ACE2-Dev-PeplIV complexed with S-RBD provoked alterations in the 3D structure of S-RBD, leading to disruption of the correct interaction with the ACE2 receptor, a pivotal step for SARS-CoV-2 infection. This wrong interaction between S-RBD and ACE2 could inhibit the entry of SARS-CoV-2 in cells, and thus virus replication and the establishment of COVID-19 disease. Therefore, we suggest that ACE2-derived peptides can interfere with recognition of ACE2 in human cells by SARS-CoV-2 *in vivo*. Bioinformatic prediction showed that these peptides have no toxicity or allergenic potential. By using ACE2-derived peptides against SARS-CoV-2, this study points to opportunities for further *in vivo* research on these peptides, seeking to discover new drugs and entirely new perspectives to treat COVID-19.

#### ARTICLE HISTORY

Received 13 October 2020  
 Accepted 29 December 2020

#### KEYWORDS

SARS-CoV-2 RBD; COVID-19; ACE2 receptor; ACE2-derived peptides

## ANEXO A – ARTIGO CIENTÍFICO 5

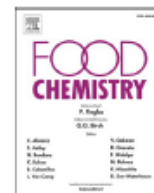
Artigo publicado na revista Food Chemistry – Fator de impacto: 7.514

Acesso disponível em: (<https://doi.org/10.1016/j.foodchem.2021.131410>)

ELSEVIER

Contents lists available at ScienceDirect

Food Chemistry

journal homepage: [www.elsevier.com/locate/foodchem](http://www.elsevier.com/locate/foodchem)

## Latex peptidases produce peptides capable of delaying fungal growth in bread

Deborah C. Freitas<sup>a</sup>, Rafael A. Zambelli<sup>b,\*</sup>, Márcio V. Ramos<sup>a</sup>, João P.B. Oliveira<sup>a</sup>, Pedro F. N. Souza<sup>a</sup>, Glauber B.M. Santos<sup>b</sup>, Celso S. Nagano<sup>c</sup>, Leandro P. Bezerra<sup>a</sup>, Ayrles F.B. Silva<sup>a</sup>, Jefferson S. Oliveira<sup>d</sup>, Cleverton D.T. Freitas<sup>a,\*</sup>

<sup>a</sup> Departamento de Bioquímica e Biologia Molecular, Universidade Federal do Ceará, Centro de Ciências, Campus do Pici, Fortaleza, Ceará CEP 60440-900, Brasil

<sup>b</sup> Departamento de Engenharia de Alimentos, Universidade Federal do Ceará, Fortaleza, CE, Brasil

<sup>c</sup> Departamento de Engenharia de Pesca, Universidade Federal do Ceará, Fortaleza, CE, Brasil

<sup>d</sup> Laboratório de Bioquímica de Plantas Laticíferas (LABPL), Universidade Federal do Delta do Parnaíba – UFDPAr, CEP 64.202-020 Parnaíba, Piauí, Brasil

## ARTICLE INFO

## Keywords:

Antimicrobial peptides  
*Calotropis procera*  
*Carica papaya*  
*Cryptostegia grandiflora*  
 Gluten peptides  
*Penicillium*

## ABSTRACT

Antimicrobial peptides (AMPs) have been reported to be promising alternatives to chemical preservatives. Thus, this study aimed to characterise AMPs generated from the hydrolysis of wheat gluten proteins using latex peptidases of *Calotropis procera*, *Cryptostegia grandiflora*, and *Carica papaya*. The three hydrolysates (obtained after 16 h at 37 °C, using a 1:25 enzyme: substrate ratio) inhibited the growth of *Aspergillus niger*, *A. chevalieri*, *Trichoderma reesei*, *Fythium oligandrum*, *Penicillium* sp., and *Lasiodiplodia* sp. by 60–90%, and delayed fungal growth on bread by 3 days when used at 0.3 g/kg. Moreover, the specific volume and expansion factor of bread were not affected by the hydrolysates. Of 28 peptides identified, four were synthesised and exhibited activity against *Penicillium* sp. Fluorescence and scanning electron microscopy suggested that the peptides damaged the fungal plasma membrane. Bioinformatics analysis showed that no peptide was toxic and that the antigenic ones had cleavage sites for trypsin or pepsin.